QSAR Studies on Thiazolidines: A Biologically Privileged Scaffold

Yenamandra S. Prabhakar (✉) · V. Raja Solomon · Manish K. Gupta ·
S. B. Katti (✉)

Medicinal and Process Chemistry Division, Central Drug Research Institute,
Lucknow-226 001, India
yenpra@yahoo.com, setu_katti@yahoo.com

Abstract A large number of drugs and biologically relevant molecules contain hetero-cyclic systems. Often the presence of hetero atoms or groupings imparts preferential specificities in their biological responses. Amongst the heterocyclic systems, thiazolidine is a biologically important scaffold known to be associated with several biological activities. Some of the prominent biological responses attributed to this skeleton are antiviral,

antibacterial, antifungal, antihistaminic, hypoglycemic, anti-inflammatory activities. This diversity in the biological response profiles of thiazolidine has attracted the attention of many researchers to explore this skeleton to its multiple potential against several activities. Many of these synthetic and biological explorations have been subsequently analyzed in detailed quantitative structure-activity relationship (QSAR) studies to correlate the respective structural features and physicochemical properties with the activities to identify the important structural components in deciding their activity behavior. In this, drugs or any biologically active molecules may be viewed as structural frames consisting of strategically positioned functional groups that will interact effectively with the complementary groups/sites of the receptor. With this in focus, the present article reviews the QSAR studies of diverse biological activities of the thiazolidines published during the past decade.

Keywords Thiazolidines · QSAR · Molecular modeling

Abbreviations

AF	*Aspergillus fumigatus*
AIDS	acquired immune deficiency syndrome
ANN	artificial neural network
AR	aldose reductase
ATPase	adenosin tri-phosphatase
BPN	back propagation neural networks
CA	*Candida albicans*
cAMP	cyclic-adenosine mono phosphate
CN	*Cryptococcus neoformans*
CODESSA	comprehensive descriptors for structural and statistical analysis
CoMFA	comparative molecular field analysis
CoMSIA	comparative molecular similarity analysis
COX	cyclooxygenase
CPE	carrageenan mice paw edema
CP-MLR	combinatorial protocol in multiple linear regression
E/L	enzyme ligand interaction
FA	factor analysis
G/PLS	genetic partial least squares
GAGs	glycosaminoglycans
GFA	genetic function approximation
HBTU	2-(1H-benzotrizo-1-yl)-1,1,3,3-tetramethyluraniumhexafluorophospate
HIV	human immunodeficiency virus
MEDV	molecular electronegativity distance vector
MFA	molecular field analysis
MLR	multiple linear regression
MMPs	metalloproteinases
MOE	molecular operating environment
MOPAC	molecular orbital partial atomic charge
MSA	molecular shape analysis
NNRTIs	non-nucleoside reverse transcriptase inhibitors
NO	nitric oxide
NPY5R	neuropeptide Y5 receptor
NRTIs	nucleoside reverse transcriptase inhibitors

NSAIDs   non-steroidal anti-inflammatory drugs
OA   octopamine agonists
PCR   principle components regression
PLS   partial least square
PPARs   peroxisome proliferator-activated receptors
QSAR   quantitative structure-activity relationship
RSM   receptor surface model
RT   reverse transcriptase
TM   *Tricophyton mentagrophyte*
TxA2   Thromboxane A2
TZDs   thiazolidinediones
VSMP   variable selection and modeling method based on prediction

1
Introduction

The quantitative structure activity relationship (QSAR) study envisages establishment of a mathematical/functional relationship between the chosen activity and selected properties of the congeneric series of compounds. In the early years of QSAR, most of the explorations revolved around the numerical expressions and presentation of the correlations and/or patterns from regression, discriminant and clustering approaches. With advancements in computer hardware performance and software, the graphical expression and visual presentation of modeling results have taken long-strides along with the mathematical/functional relationships. These strategies have been effectively put to use particularly in the area of rational drug design. This is evident from a large number of original research publications and review articles published in the literature [1–3]. Against this backdrop the present article highlights the QSAR and molecular modeling explorations carried out on thiazolidine heterocyclic systems. In chemical parlance the term thiazolidine refers to a five-membered ring system containing sulfur and nitrogen; the numbering system is as shown in Fig. 1.

In small-molecule heterocyclic compounds, thiazolidine is a recognized scaffold for potential drugs and drug candidates. Anticonvulsant, sedative, antidepressant, anti-inflammatory, antihypertensive, antihistaminic and antiarthritic activities are a few among many other biological responses shown by this scaffold (Table 1) [4].
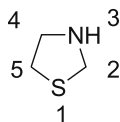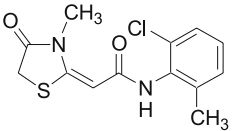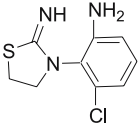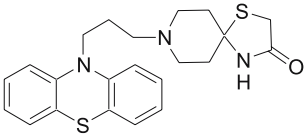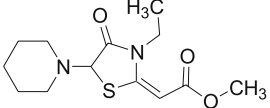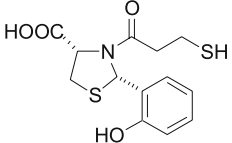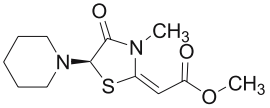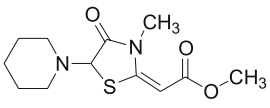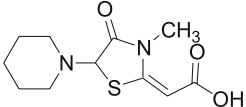

Fig. 1 Structure and numbering of Thiazolidine

Table 1 Diverse biological responses of thiazolidine derivatives [4]
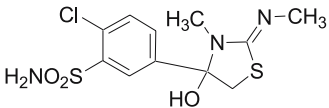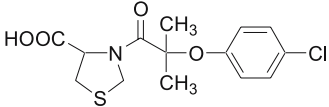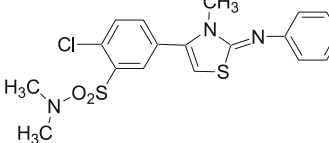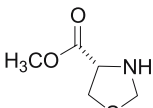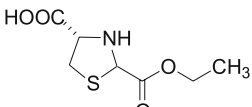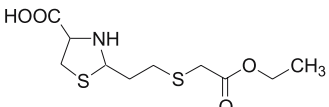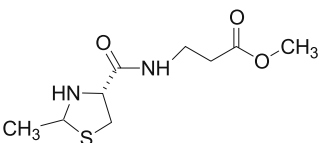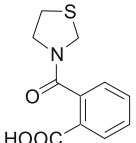
No.	Names[a]	Chemical structure	Use
1	Ralitoline[b]		Anticonvulsant
2	Timiridine esilate[b]		Antidepressant
3	Spiclomazine[b]		Psychotropic
4	Piprozolin		Choleretic
5	Rentiapril[c]		Antihypertensive (ACE inhibitor)
6	Dexetozoline[b]		Antihypertensive
7	Etozolin[b]		Antihypertensive, Diuretic
8	Ozolinone[c]		Diuretic

[a] Names not protected under a registered trademark
[b] WHO recommended non-proprietary names
[c] WHO unprotected non-proprietary names
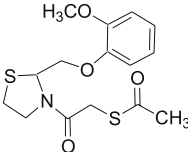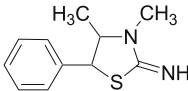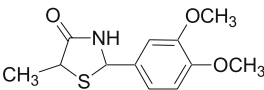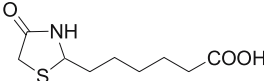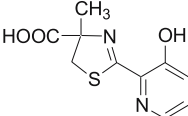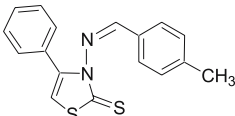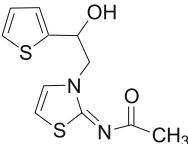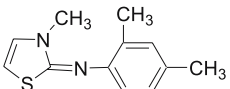
Table 1 (continued)

No.	Names [a]	Chemical structure	Use
9	Tizolemide [b]		Diuretic
10	Timofibrate [b]		Antihyperlipidemic
11	Metibride [b]		Antihyperlipidemic
12	Carbolidine		Mucolytic
13	Telmesteine [b]		Mucolytic
14	Letosteine [c]		Mucolytic
15	Alonacic [b]		Mucolytic
16	Neosteine [c]		Mucolytic

[a] Names not protected under a registered trademark
[b] WHO recommended non-proprietary names
[c] WHO unprotected non-proprietary names

Table 1 (continued)
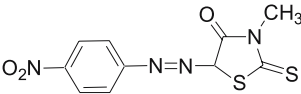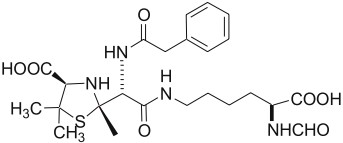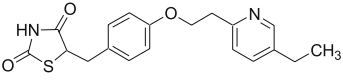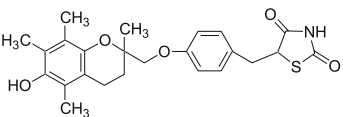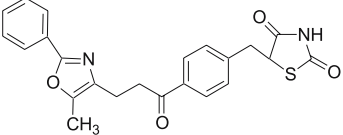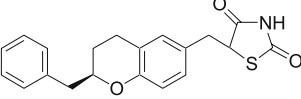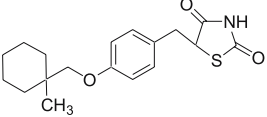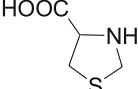
No.	Names[a]	Chemical structure	Use
17	Guaisteine[b]		Antitussive
18	Thiadrine		Antitussive, Anti-asthmatic
19	Mezolidon		Antiulcer agent
20	Thiazolidomycin		Antibiotic for several streptomyces species
21	Ferrithiocin		Promotes antibacterial activity of cephalosporins
22	Fezatione		Antifungal, Antitrichophytic
23	Antazonite[c]		Parasticide, Anthelmintic
24	Cyamiazole		Acaricide, Ectoparasiticde

[a] Names not protected under a registered trademark
[b] WHO recommended non-proprietary names
[c] WHO unprotected non-proprietary names

Table 1 (continued)
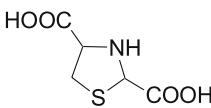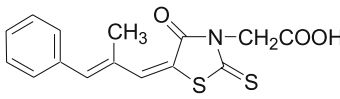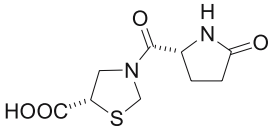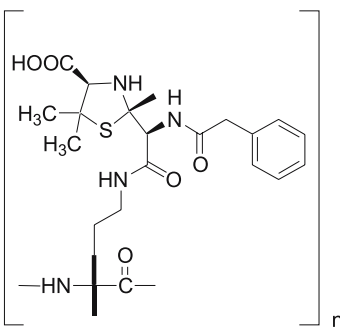
No.	Names[a]	Chemical structure	Use
25	Nitrodan[c]		Anthelmintic (veterinary)
26	Libecilide[b]		Anti-allergic (inhibits penicillin induced antibodies)
27	Pioglitazone[b]		Oral hypoglycemic agents
28	Troglitazone[b]		Oral hypoglycemic agents
29	Draglitazone[b]		Oral hypoglycemic agents
30	Englitazone[b]		Oral hypoglycemic agents
31	Ciglitazone[b]		Oral hypoglycemic agents
32	Timonacic[b]		Hepatoprotectant Antineoplastic

[a] Names not protected under a registered trademark
[b] WHO recommended non-proprietary names
[c] WHO unprotected non-proprietary names

Table 1 (continued)

No.	Names[a]	Chemical structure	Use
33	Tidiacic[b]		Treatment of liver disorders
34	Epatrestat[b]		Aldose reductase inhibitor
35	Pidotimod[b]		Immunomodulator
36	Benpenolisin[b]		Diagnostic aid (penicillin sensitive)

[a] Names not protected under a registered trademark
[b] WHO recommended non-proprietary names
[c] WHO unprotected non-proprietary names

Furthermore, the avenues of simple chemical transformations in the generation of a diverse variety of pendants on the thiazolidine scaffold has fascinated medicinal chemists and led to exploration of the wealth of biological information involved in these processes. Therefore, a conscious effort is made in the chemistry part of the present review to cull out select modifications of the thiazolidine skeleton namely thiazolidine-4-carboxylic acids and 4-thiazolidinones from the vast array of thiazolidines.

2
Chemistry

2.1
Thiazolidine

The parent compound thiazolidine can be obtained in high yield as hydrochloride by the reaction of cysteamine hydrochloride with aqueous formaldehyde at ambient temperature (Scheme 1) [5].
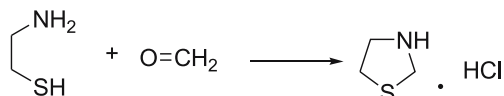
Scheme 1   General synthesis of thiazolidine

By logical extension of the scheme one can generate substituted thiazolidine and its homologs by the reaction of appropriate carbonyl compounds with suitable α-aminothiols (Scheme 2) [6].
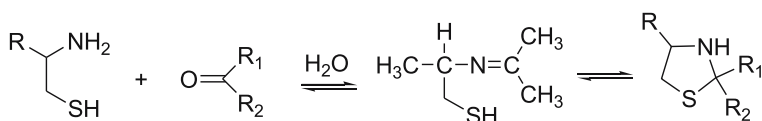
Scheme 2

Furthermore, many thiazolidines are in equilibrium with its acyclic thiol form alternately in aqueous media, with the β-mercaptoalkylamine and the carbonyl compound from which they were formed. The position of the equilibrium depends on the nature of the ring substituents (Scheme 2) [7]. Thiazolidines with unsubstituted ring nitrogen (N3) are readily hydrolyzed by boiling in aqueous acidic or basic solution and the hydrolysis is completed in the presence of a compound which reacts with either of the cleavage products. The presence of substituents on the nitrogen atom (N3) stabilizes the thiazolidine ring. Under strong acidic or basic conditions or at high temperature, 1,3-thiazolidines undergo epimerization followed by decomposition to the aldehyde and aminothiol [8]. Simple oxidative transformations of the thiazolidine skeleton lead to a number of scaffolds namely, N-oxidies, 2- or 3-thiazolines, and thiazoles. Oxidation can also occur at the sulfur atom (S1), to afford sulfoxide or sulfone derivatives [7]. Thus, thiazolidine is amenable to chemo selective reactions leading to different structural entities (Fig. 2).
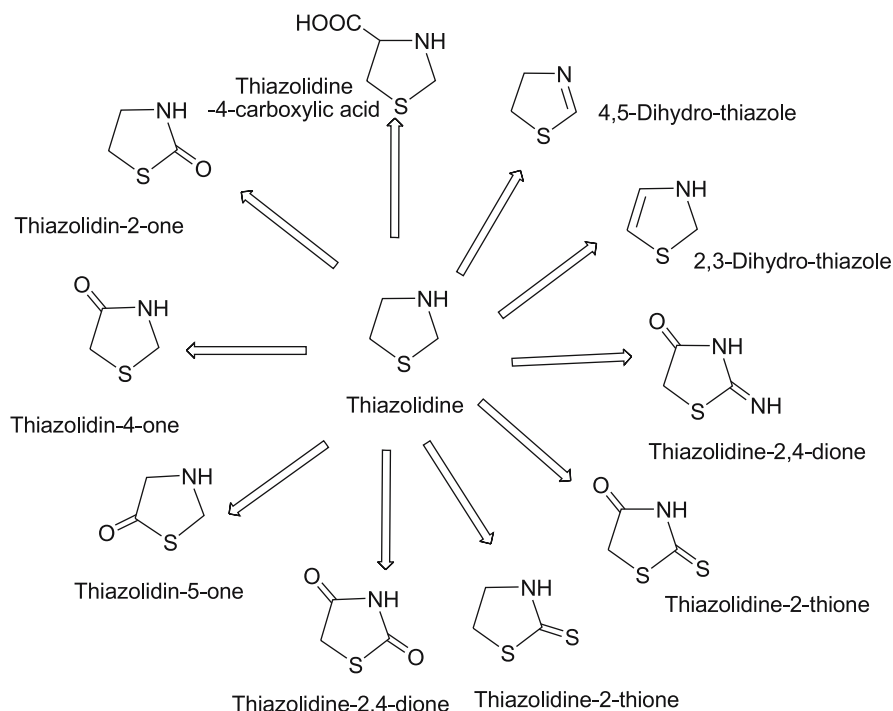
Fig. 2 Some representative chemical transformations of thiazolidine

2.2
Thiazolidine-4-carboxylic Acids

Discovery of thiazolidine-4-carboxylic acids was made accidentally by Birch
and Harris [9] during a study of the effect of formaldehyde on the titra-
tion curves of amino acids. Later, Schubert [10] explained the formation
of thiazolidine-4-carboxylic acid by condensation of cysteine and formalde-
hyde followed by intramolecular cyclization. Accordingly, a large num-
ber of thiazolidine-4-carboxylic acids can be synthesized by condensation
of aldehydes and ketones with cysteine and/or pencillamine as shown
in Scheme 3.
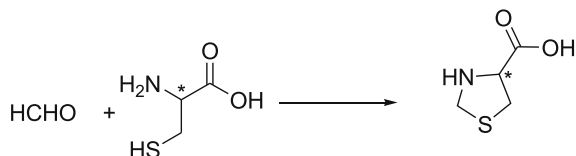
Scheme 3 General synthesis of thiazolidine-4-carboxylic acid
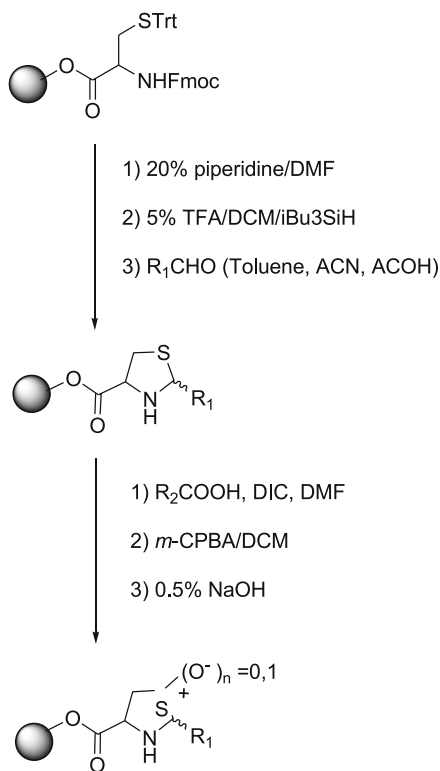
Scheme 4 A solid-phase synthetic protocol of thiazolidine derivatives [13]

Although cyclization can take place in many ways, according to Kallen [11] the most preferred pathway involves imine formation followed by intramolecular cyclization. During the course of cyclization a new chiral center at C-2 is created thereby giving rise to a diastereomeric mixture namely 2R, 4R and 2S, 4R. An interesting situation arises when the reactant aldehyde is also chiral. The stereochemistry at the newly formed center is controlled by the stereochemistry of the aldehyde [12]. In view of the biological importance of thiazolidine, Patek et al. reported a solid-phase synthesis protocol (Scheme 4) [13]. This enables the synthesis of compound libraries for quick lead optimization.

2.3
Properties of Thiazolidine-4-carboxylic Acids

The unsubstituted thiazolidine-4-carboxylic acid, i.e. thioproline, is remarkably stable towards both alkali as well as acid while the 2-substituted thiazolidine-4-caroxylic acids are unstable under similar conditions [14].

However, the N3-substituted thiazolidines are stable in solution because the substituent group prevents the ring opening. The parent compounds are generally solids and exhibit poor solubility in different solvents whereas N3-substitution increases solubility in most of the organic solvents. The ring heteroatoms (S1 and N3), C-2 and the C4-pendant carboxylic group are amenable to further chemical transformation in generating libraries of compounds.

2.4
Thiazolidin-4-ones

Several protocols for the synthesis of thiazolidin-4-ones are available in the literature [15–23]. Essentially they are three component reactions involving an amine, a carbonyl compound, and a mercapto acid. The process can be either a one-pot three-component condensation or a two-step process as shown in Scheme 5. The reaction has been suggested to proceed via imine formation followed by the attack of the sulfur nucleophile on the imine carbon. The last step involves intramolecular cyclization with the elimination of water to give thiazolidin-4-ones. This step appears to be critical for obtaining high yields. Therefore, variations have been affected in this step to facilitate removal of water. Most commonly used protocols employ azeotropic distillation, molecular sieves, and use of other desiccants like anhydrous zinc chloride [24], sodium sulfate [25], or magnesium sulfate [26]. These protocols require prolonged heating at 70–80 °C for 17–20 h and give moderate to good yields.
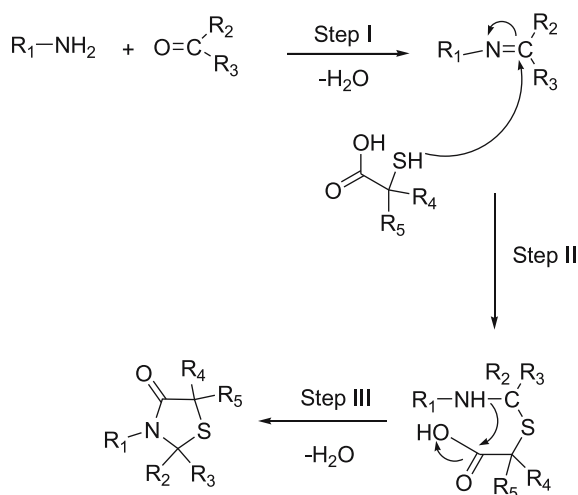
Scheme 5 A synthesis of thiazolidine-4-one derivatives

More recently, an improved protocol has been reported wherein N,N''-dicyclohexylcarbodiimide (DCC) or 2-(1H-benzotrizo-1-yl)-1,1,3,3-tetra-methyluraniumhexafluorophospate (HBTU) (Scheme 6) is used as a dehydrating agent to accelerate the intramolecular cyclization resulting in faster reaction and improved yields [27, 28]. The DCC/HBTU-mediated protocol has the advantage of mild reaction conditions, a very short reaction time, and product formation in almost quantitative yields. More importantly, yields of the thiazolidinones are independent of the nature of the reactants. This modification is compatible with a solid-phase combinatorial approach to generate a library of compounds.

Recently, Holmes et al. reported the solution and polymer-supported synthesis of 4-thiazolidinones and 4-metathiaznones derived from amino acids (Scheme 7) [29]. A three-component condensation of an amino ester or resin-bound amino acid (glycine, alanine, β-alanine, phenylalanine, and valine),
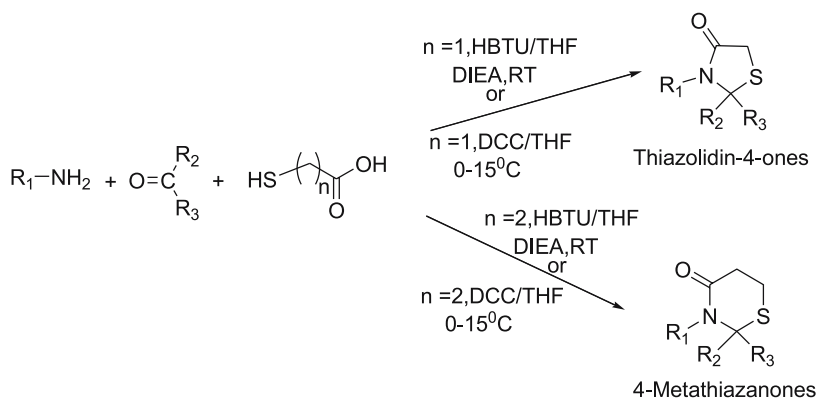
Scheme 6 Synthesis of thiazolidine-4-one derivatives in DCC/HBTU protocol [27, 28]
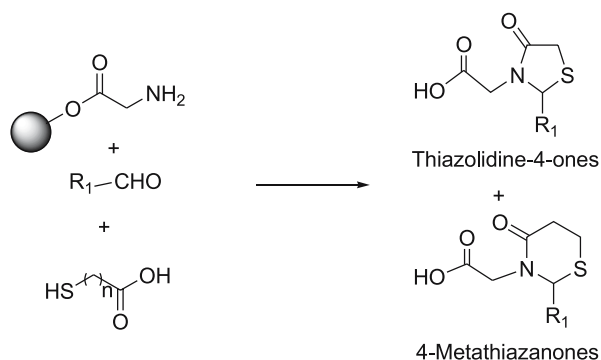
Scheme 7 A solid-phase synthesis of thiazolidin-4-ones derivatives [29]
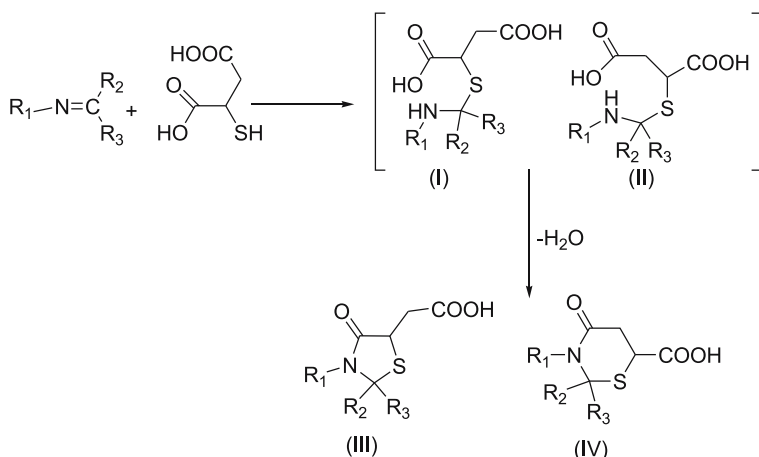
Scheme 8

an aldehyde (benzaldehyde, *o*-tolualdehyde, *m*-tolualdehyde, *p*-tolualdehyde, and 3-pyridine carboxaldehyde), and an α-mercapto carboxylic acid led to the formation of five- and six-membered heterocycles. In amino acids, the carboxylic acid function served as an anchor group for attachment to the site of support. The condensation of this support bound amine with several aldehydes and mercapto acetic acids in a one-pot reaction for 2 h at 70 °C with removal of water has afforded the desired products. For successful completion of the reaction, they employed 15 to 25 equiv. of reagent solution relative to resin loading.

A special situation arises when mercaptosuccinic acid is used as a mercapto component. Both the carboxyl functions are prone to nucleophilic attack by the imine nitrogen and give rise to five- (I) as well as six-membered (II) cyclic structures. Subsequently, Poop et al. showed by X-ray crystal structure analysis that a five-membered (III) cyclic structure is preferred over the six-membered (IV) cyclic structures (Scheme 8) [30].

2.5
Properties of Thiazolidine-4-ones

The N3-unsubstituted thiazolidinones are usually solids and often melt with decomposition, but substitution at this position lowers the melting point. The thiazolidinones that do not carry N3-aryl or higher alkyl substitution are partially soluble in water and can be recrystallized from water. Thiazolidinones undergo a limited number of chemical transformations as shown in Scheme 9. The methylene carbon atom at the 5-position of thiazolidinone possesses nucleophilic activity and can attack an electrophilic center. Most frequently the reaction occurs in the presence of
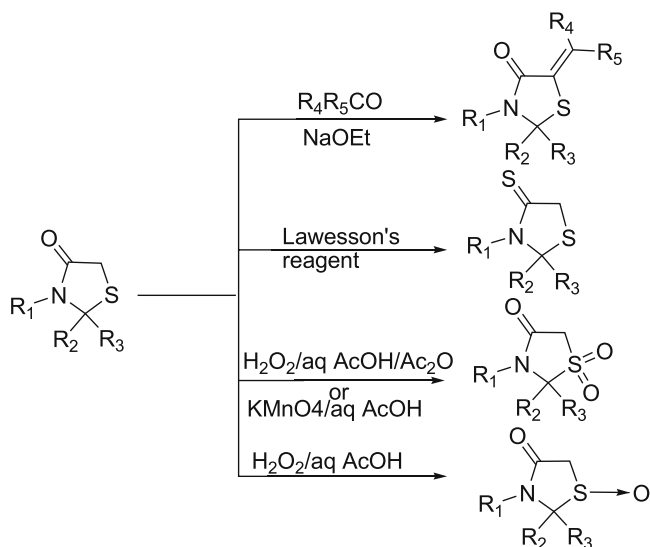
Scheme 9 Different chemical transformations of thiazolidin-4-ones

a base and the anion of the 4-thiazolidinone attacking species as shown in Scheme 9 [31, 32].

The carbonyl group of 4-thiazolidinone is highly unreactive. But in a few cases it undergoes certain reactions for example 4-thiazolidinone on treatment with Lawesson's reagent gives corresponding 4-thione derivatives in almost quantitative yields [33]. Oxidation of 2,3-disubstituted-4-thiazolidinone with hydrogen peroxide in acetic anhydride and acetic acid [34] or by potassium permanganate in aqueous acetic acid solution [35] results in the corresponding sulfones. On the other hand, the oxidation with hydrogen peroxide in aqueous acetic acid solution gives the corresponding sulfoxide [36]. A more detailed account of the chemistry and biological activities of thiazolidine-4-carboxylic acids can be found in earlier reviews [37–40].

The diverse biological activities exhibited by the thiazolidines can be broadly classified into those affecting the host biology including the metabolic disorders and those affecting the parasite function in the host. The former activity profile relates mostly to the inflammatory, ulceration, allergy, and blood coagulation processes and to the metabolic disorders such as obesity, diabetes, and associated pathological manifestations. The latter category of activities is mostly concerned with the human immunodeficiency virus (HIV) and fungi. Apart from these some QSAR reports on the insecticidal activity of thiazolidines have also been included to widen the scope of this article.

3
QSAR and Modeling Studies

QSAR and modeling studies comprise of two basic components. The first one corresponds to the measurements (parameterization) of the chosen object in numeric or boolean form and the other one addresses the development of relational expressions between or among the measurements made on the objects. The reviewed studies have used different physicochemical, quantum chemical, topological, and topographical descriptors from various sources such as Hansch and Leo's monograph [41], Molecular Orbital Partial Atomic Charge (MOPAC) [42], ChemDraw's property/descriptor database [43], Comprehensive Descriptors for Structural and Statistical Analysis (CODESSA) [44, 45], Molecular Electronegativity Distance Vector (MEDV-13) [46], and DRAGON [47] etc for the parameterization of the chemical structure. The 2D-QSAR results presented in the review have been brought out using different statistical procedures and programs namely, simple Multiple Linear Regression (MLR), Principle Components in multiple linear Regression (PCR), Partial Least Square (PLS) [48], Genetic Function Approximation (GFA) [49], Genetic Partial Least Squares (G/PLS) [50], Combinatorial Protocol in Multiple Linear Regression (CP-MLR) [51], Variable Selection and Modeling method based on Prediction (VSMP) [52], Artificial Neural Network (ANN) [53–55], discriminant and cluster analysis.

The 3D-QSAR results explained in this article have come from the application of Comparative Molecular Field Analysis (CoMFA) [56], Comparative Molecular Similarity Analysis (CoMSIA) [57], Molecular Shape Analysis (MSA) [58, 59], Molecular Field Analysis (MFA) [60], and steric and electrostatic field interactions in Receptor Surface Model (RSM) [61, 62] techniques to the datasets. Apart from these, results of some interesting pharmacophore identification [63, 64], virtual screening [65, 66], docking [67, 68] and X-ray crystallographic studies have been discussed to give the complete picture of "virtual to wet chemistry". All these 3D studies have been carried out using various commercial software packages namely Insight II [69], SYBYL [70], MOE [71]. All these packages use "built-in" statistical techniques for the assessment of significance of the developed models. They are similar to one or more statistical procedures of 2D-QSAR. Most of the 2D and 3D results presented in this review have been validated through various techniques such as leave one out, leave many out, and external test sets. However, to maintain uniformity and conciseness, only limited statistical measures of the goodness-of-fit of regression equations have been presented. In all regression equations, n is the number of compounds in the dataset, r is the correlation coefficient, Q^2 is cross-validated r^2 from the leave-one/many out procedure, s is the standard error of the estimate, and F is the F-ratio between the variances of calculated and observed activities. The values given in the parentheses of the regression equation are the standard errors (with-

out arithmetic sign) or 95% confidence limits (with ± arithmetic sign) of the regression coefficients. A mention is made about the nature of each QSAR study/methodology along with the results. The contributing or modeling descriptors for each case have been identified and discussed along with the modeling equations. In the succeeding sections of this article QSAR studies on the diverse biological responses elicited by the various compounds anchored via the thiazolidine skeleton system have been described. Hereafter, "thiazolidine" has been used to broadly address all nitrogen-sulfur containing five-membered heterocyclic systems with different oxidation states. However, care has been taken to specify the name of the chemical congener(s) under each investigation.

3.1
Anti-inflammatory Agents

3.1.1
Cyclooxygenase Inhibitors

Thiazolyl and benzothiazolyl derivatives are known for their anti-inflammatory, analgesic, and antipyretic activities [72–77], for example Meloxicam (Fig. 3) is a known non-steroidal anti-inflammatory agent with a thiazolyl

2-[4-(thiazole-2-yl) phenyl]propionic acid
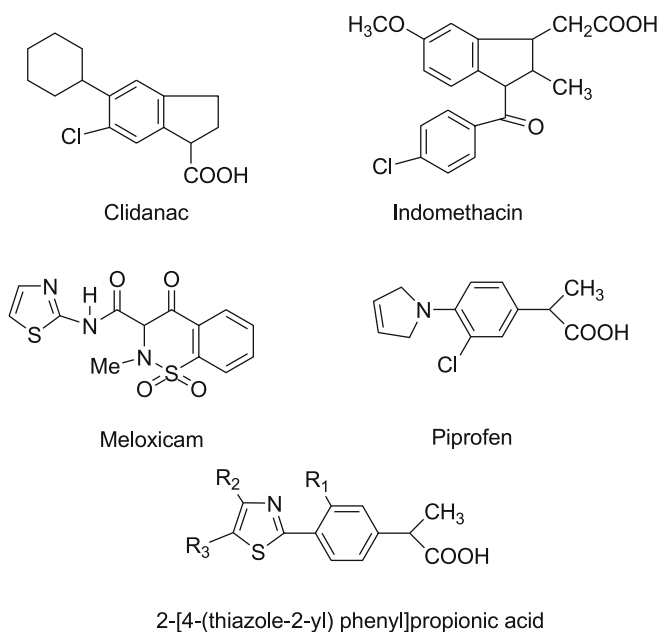
Fig. 3 General structure of 2-[4-(thiazole-2-yl) phenyl]propionic acid derived cyclooxygenase (COX) inhibitors and some of its seed structures

moiety as part of its scaffold [78]. These non-steroidal anti-inflammatory agents are known to act through the inhibition of cyclooxygenase (COX) involved in the arachidonic acid pathway. In this contest, the development of 2-[4-(thiazole-2-yl) phenyl]propionic acid derivatives (Fig. 3, Table 2) as anti-inflammatory agents has its roots in the sub-structural units of indomethacin, clidanac, and piprofen (Fig. 3) [79, 80].

Naito and co-workers investigated the COX inhibitory activity of these 2-[4-(thiazole-2-yl) phenyl]propionic acid derivatives (Fig. 3, Table 2) in terms of different physicochemical and structural descriptors of the substituent positions (R_1, R_2 and R_3) [80]. The following equations show the correlation of the activity with these descriptors in different groups of compound.

$$pI_{50} = 1.08(0.50)\pi(R_1) + 1.18(0.97)\sigma_1(R_1) + 5.64$$
$$n = 11, \quad r = 0.89, \quad s = 0.28, \quad F = 15.81 \tag{1}$$

$$pI_{50} = -4.10(2.75)\sigma_R(R_2) - 0.72(0.28)\Delta L(R_2)$$
$$+ 0.43(0.39)\pi(R_2) + 5.81$$
$$n = 15, \quad r = 0.91, \quad s = 0.46, \quad F = 17.90 \tag{2}$$

$$pI_{50} = 1.03(0.42)\pi(R_1) - 4.48(1.64)\sigma_R(R_2)$$
$$- 0.86(0.13)\Delta L(R_2) + 0.44(0.27)\pi(R_{2,3})$$
$$- 0.40(0.26)\Delta L(R_3) - 1.48(0.52)I(\text{iso}) + 6.11$$
$$n = 45, \quad r = 0.95, \quad s = 0.38, \quad F = 53.97 . \tag{3}$$

Equation 1 correlated the activity of these compounds in terms of their R_1 substituent (Table 2; compounds 1–11). This has suggested that higher hydrophobicity and electron-withdrawing properties of the R_1 substituent would lead to better activity [80]. Equation 2 has presented the requirements of the R_2 substituent (Table 2, compounds 1, 12–25) in terms of the STERIMOL length parameter (ΔL) [81]. It has suggested that electron releasing and hydrophobic substituents with a small length would be conducive at the R_2 position for better inhibitory activity. Equation 3 is a collective model of all the compounds together (Table 2) and represents the influence of R_1, R_2 and R_3 substituents on the activity. In this, $\pi(R_{2,3})$ and $I(\text{iso})$ represent the sum of the hydrophobic effects of R_2 and R_3 substituents and an indicator variable defined to account for the *iso*-propyl group at the R_2 position of the compounds, respectively. The negative regression coefficient of $I(\text{iso})$ in this equation has led to the suggestion that the steric restriction at the receptor site for the compounds carrying α-branched alkyl groups are R_2 substituents. The larger negative coefficient of the ΔL term of R_2 (compared to that of R_3) has further confirmed this effect. In summary, this study has indicated that the activity prefers hydrophobic substituents for R_1, R_2, and R_3 positions of these compounds (Fig. 3). It has also suggested that electron-withdrawing

Table 2 COX inhibitory activity of 2-[4-(thiazole-2-yl)phenyl]propionic acid derivatives (Fig. 3) [80]

No.	R_1	R_2	R_3	pI_{50} [b] obsd	cald [c]
1	H	H	H	5.56	6.04
2	F	H	H	6.60	6.51
3	Cl	H	H	6.70	6.81
4	Br	H	H	7.00	6.78
5	CF_3	H	H	6.52	6.58
6	Me	H	H	5.70	6.16
7	OMe	H	H	5.28	5.60
8	SMe	H	H	6.52	6.32
9	OH	H	H	6.22	6.18
10	NO_2	H	H	5.54	5.61
11	NH_2	H	H	6.00	6.02
12	H	Me	H	6.14	6.17
13	H	Et	H	5.52	5.28
14	H	i-Pr	H	4.79	4.16
15	H	Bu	H	3.98	4.13
16	H	acetyl	H	3.98	3.33
17	H	Ph	H	4.44	4.14
18	H	vinyl	H	5.68	5.45
19	H	allyl	H	4.89	4.63
20	H	CH_2OH	H	4.80	4.55
21	H	CH_2OMe	H	4.52	4.29
22	H	$CONH_2$	H	3.12	3.75
23	H	CONHMe	H	2.99	3.08
24	H	$CONMe_2$	H	3.04	3.13
25	H	CF_3	H	5.09	5.01
26	H	H	Me	5.26	5.86
27	H	H	Et	5.49	5.68
28	H	Me	Me	6.00	5.92
29	H	Et	Me	4.99	4.98
30 [a]	H	CH_2CH_2	CH_2	6.15	4.82
31 [a]	H	CH_2CH_2	CH_2CH_2	6.15	4.72
32	F	Me	H	7.00	6.64
33	F	Et	H	5.92	5.75
34	F	i-Pr	H	4.47	4.63
35	F	Bu	H	4.29	4.60
36	F	H	Me	6.52	4.33
37	F	H	Et	6.05	6.15

[a] Compounds are not included in regression analysis study
[b] Cyclooxysenase inhibitory activity
[c] Calculated activity by Eq. 3

Table 2 (continued)

No.	R_1	R_2	R_3	pI_{50} [b] obsd	cald [c]
38	F	Me	Me	6.70	6.39
39	F	Et	Me	5.30	5.45
40	Cl	Me	H	7.00	6.94
41	Cl	Et	H	6.15	6.05
42	Cl	i-Pr	H	4.47	4.93
43	Cl	Bu	H	4.21	4.90
44	Cl	H	Me	7.22	6.63
45	Cl	H	Et	6.70	6.45
46	Cl	Me	Me	6.10	6.69
47	Cl	Et	Me	5.92	5.75

[a] Compounds are not included in regression analysis study
[b] Cyclooxysenase inhibitory activity
[c] Calculated activity by Eq. 3

groups are favorable for R_1 and electron-rich groups are favorable for R_2. In addition to these, steric restrictions have been found to operate in the case of R_2 and R_3 groups.

Both COX-1 and COX-2 enzymes in the arachidonic acid pathway are known to play a role in the inflammatory process. However, the selective inhibition of COX-2 leads to the reduction of the inflammation without any risk of ulceration and bleeding of the stomach or intestinal tract, a side effect commonly associated with most of the non-selective anti-inflammatory drugs. This has made COX-2 an attractive target for many researchers to investigate the structural requirements of its inhibitors. In pursuit of this goal Liu et al. carried out a QSAR study on the COX-2 inhibitory activity of indomethacin (Fig. 3), SC-58125, NS-398 (Fig. 4) together with some thiazolone and oxazolone derivatives (Fig. 4, Table 3) with the MEDV-13 (molecular electronegativity distance vector based on 13 atomic types) descriptors [82]. These descriptors represent the electrotopological state of the molecules [83, 84]. In this study good predictive models (Eq. 4) have been obtained for the COX-2 inhibitory activity of these compounds in terms of the MEDV-13 descriptors.

$$pIC_{50} = 0.089(0.013)x_1 + 0.126(0.029)x_7 + 0.175(0.028)x_{29}$$
$$+ 0.706(0.178)x_{52} + 5.944$$
$$n = 21, \quad r = 0.925, \quad Q^2 = 0.783, \quad s = 0.283, \quad F = 23.62 . \tag{4}$$

In this equation x_1, x_7, x_{29}, and x_{52} are part of MEDV-13 descriptors of the compounds. However, no interpretation has been provided, in terms of prop-
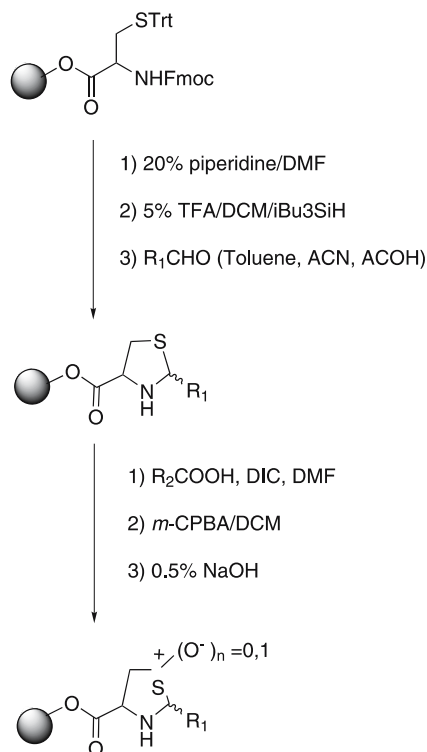
Fig. 4 Structures of SC-58125, NS-398, thiazolones and oxazolones associated with cyclooxygenase-2 (COX-2) inhibitory activity

erties of participating descriptors, to diagnose the inhibitory behavior of the compounds.

In a different study, Vigorita et al. used the docking experiments to analyze and understand the configuration preferences of the optical isomers of 3,3′-(1,2-ethanediyl)-bis[2-(3,4-dimethoxyphenyl)-4-thiazolidinones] (Fig. 5) in relation to the available structures of COX-1 and COX-2 enzymes [85].

These compounds have two equivalent chiral centers (C-2 and C-2′) (Fig. 5). They have been pharmacologically evaluated as a racemic mixture (2R, 2′R/2S, 2′S) and as meso isomers (2R, 2′S). In the docking experiments the differences between the interaction modes of *RR*, *SS*, and *RS* isomers have been analyzed using the ligand internal energies and enzyme/ligand (E/L) interaction energies of the respective isomers with the available structures of COX-1 and COX-2 enzymes (Fig. 6, Table 4) [85].

This study has suggested the features of COX catalytic sites vis-à-vis the interaction modes of *RR*, *SS*, and *RS* enantiomers of 3,3′-(1,2-ethanediyl)-bis[2-(3,4-dimethoxyphenyl)-4-thiazolidinones] with the active sites of the enzyme [85]. A comparison of the E/L interaction energy of these enan-

Table 3 Molecular descriptors and COX-2 inhibitory activities of thiazolone and oxa-zolone derivatives (Fig. 4) [84]

No.	X	R_1	R_2	R_3	x_1	x_7	x_{29}	x_{52}	pIC$_{50}$[a] obsd	cald[b]
1	NMe	t-Bu	H	$NHC(=NH)NH_2$	15.73	– 8.87	3.22	0	4.09	3.98
2	O	t-Bu	H	NHOEt	15.20	0	1.12	0	4.10	4.78
3	S	t-Bu	H	NHCN	14.71	0	2.65	– 0.76	4.26	4.55
4	O	t-Bu	H	OH	14.73	0	– 1.51	0	4.47	4.36
5	O	t-Bu	H	NHO-allyl	15.33	0	0.69	0	4.59	4.69
6	S	t-Bu	H	$NHC(=NH)NH_2$	14.87	0	3.51	– 0.78	4.68	4.67
7	S	t-Bu	H	NMeOMe	16.86	– 8.20	7.67	0	4.74	4.74
8	S	t-Bu	Me	$NHC(=NH)NH_2$	16.28	0	4.61	– 0.79	4.92	4.73
9	O	t-Bu	H	$NHC(=NH)NH_2$		0	– 1.28	1.18	5.29	5.23
10	S	t-Bu	H	OH	14.73	0	2.21	0	5.33	5.00
11	S	t-Bu	H	NHOEt	14.87	0	6.44	0	5.49	5.70
12	S	t-Bu	H	NHO-allyl	15.35	0	5.90	0	5.57	5.59
13	S	t-Pr	H	$NHC(=NH)NH_2$	15.48	0	3.39	– 0.76	5.74	5.56
14	S	t-Bu	H	Sme	4.89	0	7.83	0	5.74	5.92
15	S	t-Bu	H	NHOMe	15.57	0	6.12	0	5.77	5.64
16	S	t-Bu	H	SH	15.33	0	5.33	0	5.82	5.54
17	S	t-Bu	H	NHOH	14.96	0	5.07	0	5.82	5.49
18	S	i-Pr	H	NHOMe	14.92	0	5.99	0	6.24	6.53
19	Indomethacin				0.13	– 2.31	0.13	0	0.13	5.64
20	SC-58125				0	– 0.18	5.15	0	5.15	6.66
21	NS-398				0	0.01	0.00	0	0.00	6.10

[a] COX-2 inhibitory activity
[b] Eq. 4
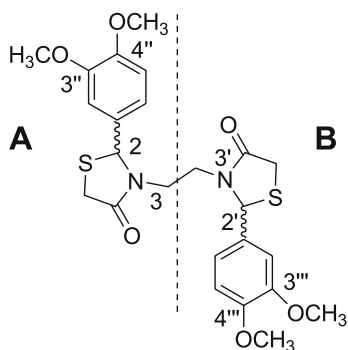
Fig. 5 3,3′-(1,2-ethanediyl)-bis[2-(3,4-dimethoxyphenyl)-4-thiazolidinones]. (Reprinted with permission from [85] Copyright 2003 Elsevier Ltd.)
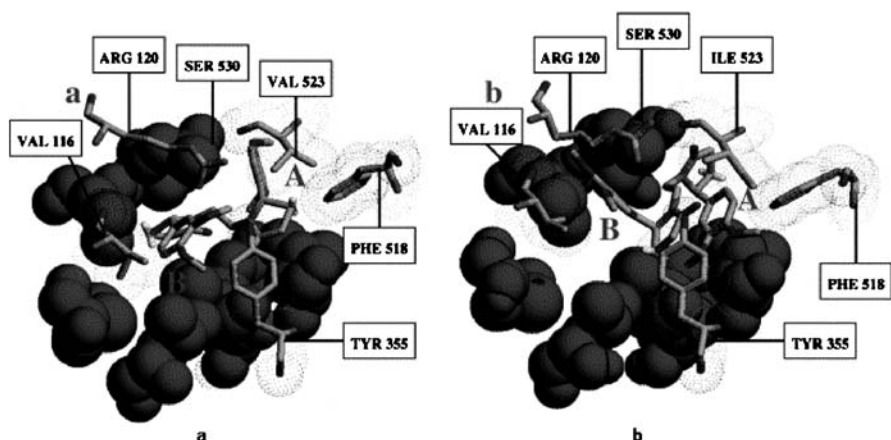
Fig. 6 Entrance view of the *SS* isomer of 3,3'-(1,2-ethanediyl)-bis[2-(3,4-dimethoxyphenyl)-4-thiazolidinones] into the COX-2 (**a**) and COX-1 (**b**) binding sites. In this **A** and **B** refer to thiazolidinone moieties as shown in Fig. 5. The steric effect of the non-conserved residue at position 523 (valine in **a** and isolucine in **b**) is reported to be crucial for the distinctive recognition of this compound between COX-1 and COX-2 isoenzymes. (Reprinted with permission from [85]. Copyright 2003 Elsevier Ltd.)

Table 4 Geometrical descriptors[a], E/L (enzyme/ligand) interaction and ligand internal energies [85]

Isomer	Isozyme	N – C – C – N dihedral angle (°)	Ar/Ar distance (Å)	Enzyme/ligand interaction energy (kcal/mol)	Ligand internal energy (kcal/mol)
RR	COX-1	– 163.15	5.706	3.73	41.88
	COX-2	– 77.01	4.478	– 3.31	10.66
SS	COX-1	– 134.85	6.124[b]	14.74	53.01
	COX-2	– 154.59	7.443	– 47.15	12.06
RS	COX-1	– 83.80	7.824	– 37.93	25.62
	COX-2	59.37	4.603	– 46.88	28.93

[a] Global minimum conformations within the enzyme clefts
[b] Folded conformation with the phenyl of moiety "A" in close proximity to the thiazolidinone of moiety "B" (see Fig. 5)

tiomers has indicated that the *SS* isomer has the highest affinity for the COX-2 (Table 4). Further, the internal energy of the *SS* isomer has been reported to be more favorable for binding into the COX-2 catalytic site than into COX-1 (Table 4). It has been shown that the *SS* enantiomer has the capability to deeply penetrate into the catalytic site of the COX-2 (Fig. 6a) by assuming

an extended conformation. It has also highlighted the ligand's electrostatic and van der Waals (VdW) interactions with several residues (Arg120, Val116, Ser530, and Tyr385) of the enzyme's binding site. However, in the case of the COX-1, it has been reported that the ligand has to undergo an unfavorable folding (dihedral angle of N – C – C – N is – 134.85°) for binding to the COX-1 site (Fig. 6b). Also, in this situation, one of the thiazolidinone moieties (moiety "A" in Fig. 5) of the ligand has been reported to be in the proximity of a hydrophobic pocket delimited by residues Ile523, Tyr355, and Phe518. All these findings have prompted Vigorita et al. to suggest the favorability of *SS* enantiomers for binding to the COX-2 catalytic site [85].

3.1.2
Nitric Oxide Synthase Inhibitors

Thiazolidines are also known to interfere in the inflammatory process through nitric oxide (NO) and glycosaminoglycans (GAGs) pathways [86, 87]. During the inflammation process, the increased activity of matrix metalloproteinases (MMPs) causes the release of GAGs, followed by the cleavage of collagen and proteoglycans, the primary components of the cartilage. Also, in a feed-back mechanism, the NO, from the NO synthases, determines the inhibition of GAGs and stimulation of chondrocyte production and thereby the levels of MMPs [88–90]. Against this background Panico et al. quantitatively analyzed some 4-alkyl/aryl-2-(N-substituted aminoalkylamido) thiazoles (Fig. 7, Table 5) for their effect on NO production and GAGs release [87].

For these compounds (Table 5) the following equations have been developed to explain their NO and GAGs inhibitory activity.

$$\text{NOinh} = -196.156(94.346)q_{NR1} + 4.742(1.377)pKa - 57.001$$

$$n = 9, \quad r = 0.850, \quad s = 5.383, \quad F = 7.83 \tag{5}$$

$$\text{GAG} = 0.035(0.013)P + 3.381(0.734)pKa - 19.241$$

$$n = 9, \quad r = 0.883, \quad s = 2.508, \quad F = 10.68 . \tag{6}$$

These equations led to the suggestion that the *pKa* is the major descriptor for deciding the NO and GAG inhibitory activities of the compounds under investigation. As the R_1 substituent in these compounds is primarily responsible

Fig. 7 General structure of 4-alkyl/aryl-2-(N-substituted aminoalkylamido) thiazoles associated with nitric oxide (NO) and glycosaminoglycans (GAGs) release inhibition

Table 5 4-Alkyl/aryl-2-amido thiazoles in modeling the nitric oxide (NO) and glycosaminoglycans (GAGs) release inhibitory activity (Fig. 7) [87]

No.	R	n	$N(R_1)_2$
1	Ph	1	NMe_2
2	Ph-OMe	1	Pyrrolidine
3	Ph-OMe	1	Piperidine
4	CH_2COOEt	1	Piperidine
5	H	2	Pyrrolidine
6	Ph	2	Pyrrolidine
7	Ph-pOMe	2	NMe_2
8	Ph-pOMe	2	Pyrrolidine
9	CH_2COOEt	2	Morpholine

for the basicity, the pyrrolidine moiety has been suggested as the most preferred group for this position for improved activity. Apart from the pKa, the charge at NR_1 (qNR_1) and the parachor (P) of the molecules have been found to influence the activities [87].

A different series of 4-alkyl/aryl-2-(N-substituted aminoalkylamido) thiazoles (Fig. 8, Table 6) were analyzed by Litina et al. for their anti-inflammatory activity in terms of the inhibition of carrageenan mice paw edema (%CPE) [90]. In this study the activity (%CPE) was correlated with several physicochemical and indicator parameters of these compounds (Table 6) [91].

$$\log(\%CPE) = 0.078(0.054)c\log D_{7.4} - 0.017(0.013)c\log D_{7.4}^2$$
$$+ 0.029(0.008)SURF + 0.060$$
$$n = 16, \quad r = 0.711, \quad s = 0.107, \quad F = 4.09 \tag{7}$$

(compounds excluded: 11–15 and 22–26)

$$\log(\%CPE) = 0.107(0.031)c\log D_{7.4} - 0.027(0.007)c\log D_{7.4}^2$$
$$+ 0.043(0.005)SURF - 0.681$$
$$n = 13, \quad r = 0.945, \quad s = 0.052, \quad F = 24.95 \tag{8}$$

(compounds excluded: 1, 6, and 13 11–15 and 22–26)
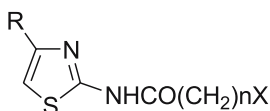
Fig. 8 General structure of 4-alkyl/aryl-2-(N-substituted aminoalkylamido) thiazoles associated with carrageenan induced mice paw edema inhibitory activity

Table 6 Physicochemical properties and carrageenan mice paw edema (%CPE) inhibitory activity of 4-alkyl/aryl-2-amido thiazoles (Fig. 8) [91]

No	R	X	n	RM	c log	$Pc\log D_{7.4}$	SURF	pKa	log %CPE[a] obsd	cald[b]
1	H	NMe$_2$	1	−0.54	0.31	0.13	53.5	7.11	1.45	1.64
2	H	cN(CH$_2$)$_4$NMe	1	−0.12	1.10	0.9	56.8	7.17	1.85	1.84
3	Me	NMe$_2$	1	−0.57	0.81	0.63	50.5	7.11	1.58	1.55
4	Me	NEt$_2$	1	−0.53	1.71	0.81	47.2	8.24	1.37	1.42
5	Ph	NMe$_2$	1	−0.27	2.41	2.24	52.3	7.09	1.72	1.68
6	Ph	cNC$_4$H$_8$	1	−0.14	3.29	2.40	58.8	8.22	1.69	1.95
7	p-OMePh	NMe$_2$	1	−0.26	2.43	2.42	49.7	5.55	1.54	1.56
8	p-OMePh	cNC$_4$H$_8$	1	−0.16	3.30	3.23	56.8	6.68	1.74	1.83
9	p-OMePh	cNC$_5$H$_{10}$	1	−0.03	3.86	3.86	53.6	5.73	1.73	1.64
10	p-Cl-Ph	cNC$_5$H$_{10}$	1	−0.3	4.56	4.56	57.1	4.33	1.67	1.70
11	CH$_2$OCOEt	NMe$_2$	1	−0.60	0.66	0.29	52.3	7.09	1.65	1.60
12	CH$_2$OCOEt	NEt$_2$	1	−0.51	1.56	0.64	49.4	8.22	1.73	1.51
13	CH$_2$OCOEt	cNC$_4$H$_8$	1	−0.45	1.54	0.27	58.8	8.22	1.55	1.88
14	CH$_2$OCOEt	cNC$_5$H$_{10}$	1	−0.54	2.09	1.49	55.7	7.25	1.78	1.82
15	CH$_2$OCOEt	cN(CH$_2$)$_4$O	1	−0.59	0.82	0.40	57.4	5.17	1.69	1.83
16	H	cNC$_4$H$_8$	2	0.14	1.38	−0.87	60.3	9.65	1.81	1.81
17	Ph	cNC$_4$H$_8$	2	−0.26	3.00	0.55	56.8	9.85	1.84	1.82

[a] Log of percent inhibition of carrageenan-induced edema, log %CPE, in mice
[b] Eq. 8

Table 6 (continued)

No	R	X	n	RM	c log	$Pc\log D_{7.4}$	SURF	pKa	log %CPE[a] obsd	cald[b]
18	p-OMePh	NMe_2	2	0.13	2.66	2.45	48.5	7.18	1.73	1.51
19	p-OMePh	cNC_4H_8	2	0.26	3.50	2.7	54.6	8.31	1.75	1.76
20	p-OMePh	cNC_5H_{10}	2	− 0.53	4.06	3.78	52.3	7.36	1.60	1.59
21	p-OMePh	$cN(CH_2)_4O$	2	− 0.34	2.79	2.7	53.6	6.80	1.74	1.72
22	CH_2OCOEt	NMe_2	2	− 0.2	0.89	− 0.72	50.7	8.72	1.72	1.42
23	CH_2OCOEt	NEt_2	2	− 0.16	1.87	− 0.76	48.3	9.85	1.81	1.31
24	CH_2OCOEt	cNC_4H_8	2	− 0.03	1.73	− 1.13	56.8	9.85	1.54	1.61
25	CH_2OCOEt	cNC_5H_{10}	2	− 0.17	2.29	0.40	54.1	8.88	1.63	1.69
26	CH_2OCOEt	$cN(CH_2)_4O$	2	− 0.54	1.02	0.13	55.6	6.80	1.77	1.73

[a] Log of percent inhibition of carrageenan-induced edema, log %CPE, in mice
[b] Eq. 8

In deriving these equations several compounds have been excluded as outliers. The parabolic relation in $c \log D_{7.4}$ has suggested 1.98 as the optimum hydrophobicity for easy transportation and rapid delivery to the target biomacromolecule. The positive regression coefficient of the parameter surface tension ($SURF$) has been interpreted as the anti-inflammatory activity of the test compound increases linearly with the increase in its surface tension. On the basis of the above results it has been concluded that the pharmacokinetic properties of these compounds play a key role in their anti-inflammatory activity. These findings have been found to be in good agreement with previously reported results concerning other non-steroidal anti-inflammatory drugs (NSAIDs) [92].

3.1.3
Adenosine Receptor Antagonists

Thiazoles and related analogues have been indicated to influence the inflammatory processes through their antagonistic activity at the adenosine receptors [93–95]. Among the various adenosine receptors, the subtypes A_1 and A_3 have been indicated in inflammation, asthma [96, 97], glaucoma [98], myocardial and cerebral ischemia [99–102]. A systematic template search of quinazolines, isoquinolines and other prototypes has resulted in the induction of the thiazole class as adenosine A_3 receptor antagonists (Fig. 9) [93].

These findings prompted Jung et al. to explore several thiazole and thiadiazole derivatives as potent human adenosine A_3 receptor antagonists (Fig. 9, Table 7) [95]. Using principal component factor analysis (FA) and genetic function approximation (GFA) techniques, Bhattacharya et al. quantitatively analyzed the adenosine A_3 receptor antagonistic activity of these compounds (Fig. 9, Table 7) with the quantum chemical descriptors (Wang–Ford charges from the AM1 method), hydrophobicity ($\log P$) and some indicator parameters [103]. In this study, Eq. 9 has emerged from the factor analysis and
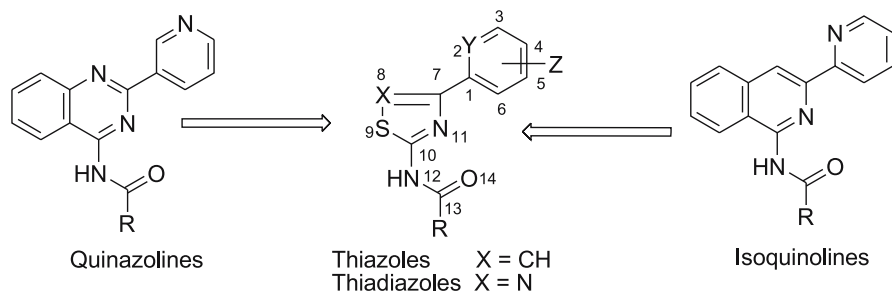
Fig. 9 General structure of thiazole and thiadiazole class of adenosine A_1 and A_3 receptor antagonists and their quinazoline, isoquinoline seed structures

Table 7 Thiazole and thiadiazole analogues in modeling the adenosine A_3 receptor antagonistic activity (Fig. 9) [103–105]

	X	Z	R	pKi [a] obsd	cald [b]	cald [c]	cald [d]
1. (LUF5417)	N	H	4-OMePh	7.09	–	–	7.31
2	CH	H	Me	7.74	8.03	7.89	7.65
3	CH	H	(Me$_3$C)O	5.29	5.22	5.22	5.59
4	CH	H	NCCH$_2$	6.69	7.13	6.50	7.88
5	CH	4-Cl	Me	7.29	7.04	7.48	7.31
6	CH	4-Cl	PhCH$_2$	7.00	6.74	7.07	6.55 [e]
7	CH	4-MeO	Me	8.52	8.42	8.24	7.88
8	CH	3-MeO	Me	8.39	8.42	8.39	7.89
9	CH	2MeO	Me	7.09	7.00	7.06	7.47
10	CH	4-MeO	Me	6.28	6.73	6.35	5.93
11	CH	4-MeO	Et	8.62	7.88	8.26	8.09
12	CH	4-MeO	Pr	8.11	8.04	8.28	8.00
13	CH	4-MeO	*i*-Pr	7.79	7.39	7.80	7.43
14	CH	4-MeO	NCCH$_2$	7.61	8.18	7.57	8.17
15	CH	4-MeO	*t*-Bu	7.50	7.20	7.67	7.62
16	CH	4-MeO	(Me$_3$C)O	5.49	5.50	5.61	6.06 [e]
17	CH	4-MeO	Ph	7.54	7.29	7.62	6.83 [e]
18	CH	4-MeO	PhCH$_2$	7.85	7.43	7.85	6.96 [e]
19	CH	4-MeO	PhCH$_2$CH$_2$	7.54	7.08	7.51	7.36
20	CH	4-MeO	*p*-MeOPhCH$_2$	5.94	7.16	5.97	7.24
21	CH	4-MeO	*p*-MeOPhCH$_2$CH$_2$	7.54	6.88	7.49	7.89
22	CH	4-MeO	Ph$_2$CH	6.28	6.97	6.29	6.13
23	CH	4-MeO	Ph$_2$CHCH$_2$	6.40	6.41	6.40	6.58
24	CH	4-MeO	2-Furan	7.50	7.68	7.40	6.63
25	CH	4-MeO	Thiophene-2-CH$_2$	7.49	7.24	7.47	6.45 [e]
26	CH	4-MeO	2-Thiophene	7.16	7.28	7.38	6.67
27				6.43			6.81
28	N	H	CH$_3$	8.64	8.92	8.62	8.57 [e]
29	N	H	PhCH$_2$	7.10	7.51	6.92	6.99
30	N	4-MeO	Me	9.10	8.88	9.08	8.78
31	N	4-MeO	PhCH$_2$	7.62	7.52	7.59	7.66
32	N	4-MeO	Et	8.95	8.82	9.10	8.60

[a] Adenosine A_3 receptor antagonistic activity
[b] Eq. 10, compounds 1 and 27 are not in the regression [103]
[c] Eq. 14, compounds 1 and 27 are not in the regression [104]
[d] Eq. 15 [105]
[e] Test set compound

Eqs. 10 and 11 have emerged from the GFA technique.

$$pKi = -3.951(2.415)q_2 - 2.623(2.136)q_5 + 2.441(1.489)q_7$$
$$- 0.275(0.261)\log P - 1.498(0.763)I_{OBu_t}$$
$$+ 0.895(0.614)I_{MeEt} + 4.030$$
$$n = 30, \quad r = 0.893, \quad Q^2 = 0.689, \quad s = 0.483, \quad F = 15.0 \tag{9}$$

$$pKi = -1.940(2.072)q_2 - 11.413(3.878)q_8 - 13.611(5.005)q_9$$
$$- 0.038(0.029)(\log P)^2 - 1.556(0.722)I_{OBu_t} + 3:083$$
$$n = 30, \quad r = 0.902, \quad Q^2 = 0.753, \quad s = 0.452, \quad F = 21.0 \tag{10}$$

$$pKi = -1.932(2.150)q_2 - 1.413(4.012)q_8 - 13.741(5.189)q_9$$
$$- 0.311(0.260)\log P - 1.518(0.747)I_{OBu_t} + 3.686$$
$$n = 30, \quad r = 0.896, \quad Q^2 = 0.739, \quad s = 0.465, \quad F = 19.6. \tag{11}$$

The equation from factor analysis (Eq. 9) has explained the activity in terms of $\log P$, I_{MeEt}, (an indicator parameter defined for the presence of the methyl or ethyl substituent at the R position), I_{OBu_t} (an indicator parameter defined for the presence of the *tert*-butyloxy group at the R position) and Wang–Ford charges (q_2, q_5, and q_7) of atoms C2, C5, and C7. This has suggested that less hydrophobic compounds with methyl or ethyl and without the *tert*-butyloxy group at the R position would be favorable for the adenosine A_3 receptor antagonistic activity [103]. The GFA technique has resulted in equations with improved statistics (Eqs. 10 and 11). These equations have suggested that less hydrophobic compounds without a *tert*-butyloxy group at the R position would be better for the binding affinity at the receptor. Moreover, the Wang–Ford charges at atoms C2, X8, and S9 have been identified as contributing ones to modulate the binding affinity of these compounds. In this the Wang–Ford charges of X8 and S9 are from part of the thiazole/thiadiazole nucleus and signify their role in deciding the activity of these compounds.

The adenosine A_3 receptor antagonistic activity of these compounds have been further analyzed [104] in 3D-QSAR using molecular shape analysis (MSA) and molecular field analysis (MFA) techniques in Cerius2 (version 4.8) software [50]. In this, Jurs atomic charge descriptors were used for the MSA study and H^+ point charges and CH_3 derived steric fields were used for the MFA study. In this 3D-QSAR study, MSA resulted in Eqs. 12 and 13 and MFA led to Eq. 14.

$$pC = 0.140(0.052)JursPPSA_3 + 61.920(20.616)Jurs\ RNCG$$
$$- 1.024(0.766)JursRPCS - 0.006(0.004)JursSASA$$
$$+ 0.006(0.004)Energy + 1.645(1.022)Fo - 8.735$$
$$n = 30, \quad r = 0.901, \quad Q^2 = 0.705, \quad s = 0.215, \quad F = 16.6 \tag{12}$$

$$pC = 0.130(0.048)\text{JursPPSA}_3 + 61.291(20.009)\text{Jurs RNCG}$$
$$- 1.056(0.749)\text{JursRPCS} + 0.007(0.004)\text{Energy}$$
$$+ 1.701(0.988)Fo - 0.001(0.000)\text{PMI}_{mag} - 10.180$$
$$n = 30, \quad r = 0.907, \quad Q^2 = 0.700, \quad s = 0.203, \quad F = 17.8 \tag{13}$$

$$pC = -0.050\text{H}^+/283 - 0.028\text{H}^+/366 - 0.031\text{H}^+/427$$
$$- 0.019\text{H}^+/448 - 0.054\text{H}^+/466 - 0.052\text{H}^+/534$$
$$- 0.030\text{H}^+/608 - 0.021\text{H}^+/618 - 0.020\text{H}^+/687$$
$$+ 0.033\text{H}^+/757 - 0.010\text{CH}_3/417 - 0.052\text{CH}_3/474$$
$$+ 0.025\text{CH}_3/529 - 0.022\text{CH}_3/756 + 5.59$$
$$n = 30, \quad r = 0.990, \quad Q^2 = 0.716, \quad s = 0.500. \tag{14}$$

The equations from MSA (Eqs. 12 and 13) have explained the activity in terms of atomic charge weighted positive surface area (JursPPSA$_3$), the charge of the most negative atom divided by the total negative charge (JursRNCG), total molecular solvent-accessible surface area (JursSASA), relative positive charge surface area (JursRPCS), conformational energy of the molecules (Energy), partial moment of inertia, energy of the most stable conformer (PMI$_{mag}$), and the ratio of common overlap steric volume to the volume of individual molecules (*Fo*). On the basis of the 3D-QSAR equation from the MFA the authors could explain the 96.1% variance in the activity with cross-validated r^2 as 0.716. In this equation, the numbers suffixed to H$^+$/ and CH$_3$/, respectively, notify the significant polar and steric grid locations involved in modeling the adenosine A$_3$ receptor antagonists. From these studies they have concluded the importance of Jurs descriptors and the interaction energies of various molecular field grid locations in modeling the activity of these analogues [104].

Borghini et al. [105] have also carried out a QSAR study on the adenosine A$_3$ receptor antagonistic activity of these compounds (Fig. 9, Table 7) with the CODESSA descriptors. For this study, 26 compounds were taken in the training set for the model development and six compounds were placed in the test set to verify the developed model. This study resulted in the following correlation (Eq. 15) for the adenosine A$_3$ receptor antagonistic activity of the compounds in terms of electrostatic descriptors namely "HACA-2/TMSA" (ratio of total charge weighted hydrogen-acceptor charged surface area and total molecular surface area), MPCS (minimum partial charge on the S atom), "WNSA-3" (total surface weighted partial negative surface area), and RNH (number of H atoms at the position *R*).

$$pKi = 17296(260)\text{HACA-2/TMSA} + 22.73(4.44)\text{RNH}$$
$$+ 46.56(10.83)\text{MPCS} - 0.382(0.009)\text{WNSA-3} - 6.17$$
$$n = 26, \quad r = 0.840, \quad Q^2 = 0.548, \quad s = 0.559, \quad F = 12.23. \tag{15}$$

Table 8 Thiazole and thiadiazole analogues in modeling the adenosine A_1 receptor antagonistic activity (Fig. 9) [105]

No.	X	Y	R	pKi[a] obsd	cald[b]
1	CH	CH	4-OMePh	7.12	
2	N	CH	4-OMePh	7.49	7.50
3	CH	N	Ph	5.77	5.68
4	CH	N	4-ClPh	6.70	6.32
5	CH	N	4-IPh	5.62	6.20
6	CH	N	4-MePh	5.80	5.94
7	CH	N	4-OMePh	5.49	5.96[c]
8	CH	N	3,4-diClPh	5.80	6.15[c]
9	CH	N	3-ClPh	5.77	5.58
10	CH	N	4-NO$_2$Ph	5.82	6.00
11	CH	N	4-OCH(Me)$_2$Ph	5.24	5.54
12	CH	N	Cyclopentyl	6.04	5.47
13	N	CH	Ph	7.51	7.47
14	N	CH	4-ClPh	7.39	7.90[c]
15	N	CH	4- MePh	7.52	7.39
16	N	CH	4-OHPh	8.14	8.30
17	N	CH	4-OCH2CO$_2$Ph	7.00	7.12
18	N	CH	Cyclohexyl	5.85	6.79
19	N	CH	(*trans*) 4-OMe-cyclohexyl	7.49	6.77
20	N	CH	(*cis*) 4-OMe-cyclohexyl	6.96	6.81
21	N	CH	(*trans*) 4-OH-cyclohexyl	7.70	7.27[c]
22	N	CH	(*cis*) 4-OH-cyclohexyl	7.38	7.15
23	N	CH	NHPh	6.00	5.96
24	CH	N	NHPh	6.03	5.66[c]
25	CH	CH	Ph	7.41	7.52
26	CH	CH	3-ClPh	7.07	7.31
27	CH	CH	4-BrPh	7.48	7.18[c]
28	CH	CH	4-ClPh	7.74	7.52
29	CH	CH	4-NO$_2$Ph	7.66	7.11
30	CH	CH	4- MePh	7.44	7.32
31	CH	CH	4-C(Me)$_3$Ph	5.87	6.51
32	CH	CH	4-CF$_3$Ph	6.78	6.78
33	CH	CH	3,4-diClPh	7.23	7.30
34	CH	CH	2,4-diClPh	7.24	7.17

[a] Adenosine A_1 receptor antagonistic activity
[b] Eq. 16 [105]
[c] Test set compound

This equation also suggested the importance of polarity/partial charges on the heteroatoms of the thiazole moiety for adenosine A_3 receptor antagonistic activity. On this basis, it has been suggested that thiadiazoles capable of accepting hydrogen bonds and carrying a small non-polar alkyl substituent at the position R, would be better for binding to the adenosine A_3 receptor [105].

With the CODESSA descriptors, Borghini et al. [105] also carried out a QSAR study on the adenosine A_1 receptor antagonistic activity of another series of thiazoles/thiadiazoles (Fig. 9) [93, 94]. In this, 27 compounds were included for training the model and seven compounds were used for testing the model (Fig. 9, Table 8). The following three descriptor model in terms of MPCN (minimum partial charge on the N atom), ZXS/ZXR (ZX Shadow/ZX Rectangle), and PP/D^2 (polarity parameter/square distance) has been derived to explain the affinity of these compounds to the adenosine A_1 receptor.

$$pKi = 155.1(17.38)\text{MPCN} + 3.86(0.99)\text{ZXS/ZXR}$$
$$+ 2.12(1.11)\text{PP}/D^2 + 17.28$$
$$n = 27, \quad r = 0.901, \quad Q^2 = 0.742, \quad s = 0.382, \quad F = 33.15. \quad (16)$$

In Eq. 15, the coefficient of ZXS/ZXR has suggested a preference for an aromatic substituent for the R group. The positive regression coefficients of MPCN and PP/D^2 are in favor of an increase in the partial charge and polarity in the compounds for better activity. This has prompted us to suggest that thiadiazole derivatives with aromatic substituents would enhance the affinity of the compounds for the adenosine A_1 receptor.

3.1.4
Histamine (H_1) Antagonists

Thiazolidines are known to show their action on histamine receptors. The geometrical similarity between 2-aryl-3-[3-(*N*,*N*-dimethylamino)propyl]-1,3-thiazolidin-4-ones and different histamine (H_1) antagonists such as bamipine, clemastine, cyproheptadine, triprolidine, promathazine, chlorpheniramine, and carbinoxamine (Fig. 10) [106, 107] prompted Diurno et al. to evaluate these compounds for antihistaminic activity [108]. Singh and coworkers have investigated the QSAR of the antihistaminic (H_1) activity of 2,3-disubstituted thiazolidin-4-ones (Table 9) with the hydrophobicity (π), molar refractivity (MR), Hammett's sigma (σ) constant, dipole moment (μ), and Swain and Lupton's polarity (F) and resonance (R) constants of the substituent groups [109]. In this study the antihistaminic (H_1) activity of these compounds has been found to be best explained by $\sum$F and π_4 descriptor-
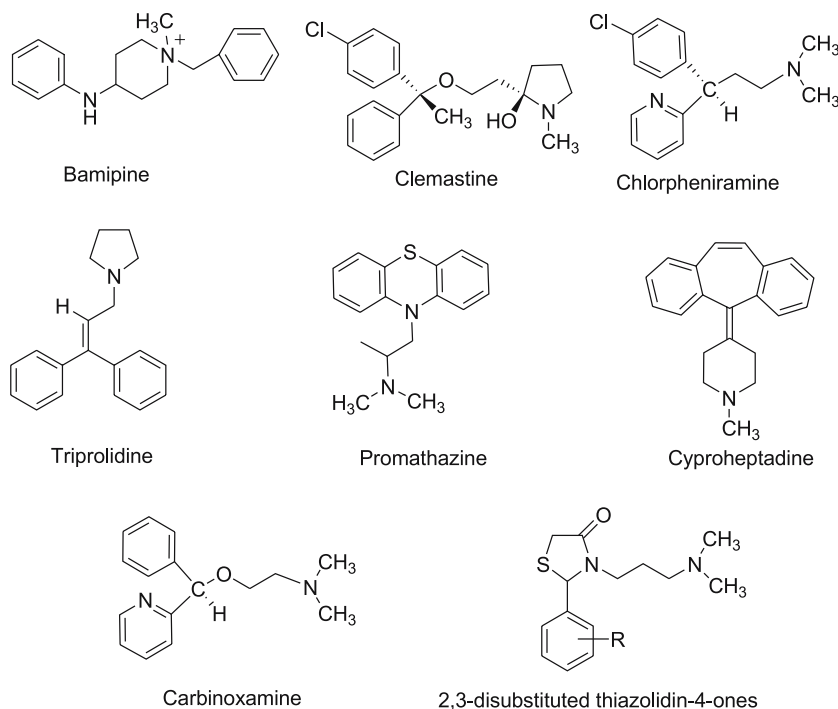
Fig. 10 Selected histamine (H_1) antagonists and 2,3-disubstituted thiazolidin-4-ones embedded with some of their structural features

combinations of R substituent groups (Eq. 17) [109].

$$pA_2 = -2.753(0.715) \sum F + 0.907(0.297)\pi_4 + 7.267$$
$$n = 15, \quad r = 0.832, \quad s = 0.672, \quad F = 13.54 \tag{17}$$

$$pA_2 = -2.573(0.346) \sum F + 1.019(\pm0.148)\pi_4 + 7.412$$
$$n = 13, \quad r = 0.961, \quad s = 0.320, \quad F = 60.70 . \tag{18}$$

In deriving Eq. 18, compounds 3 and 6 (Table 9) have been excluded as they were found to be outliers in the study. From this, they concluded that the hydrophobic substituent at the 4-position of the phenyl ring and cumulative negative polar effects of all the substituents in the phenyl group are advantageous for antihistaminic activity [109].

Agrawal et al. have studied the anti-histaminic activity of these 2,3-di-substituted thiazolidin-4-one analogues (Table 9) with graph theoretical indices and discovered the following equation for the activity in terms of the rooted Wiener index (Ww), rooted Szeged index (Szw), molecular redundancy index (MRI), and an indicator variable Ip_1 (for the p-alkyl of the aryl

Table 9 Physicochemical properties and anti-histaminic activity of 2,3-disubstituted thiazolidin-4-ones derivatives (Fig. 10) [109]

No.	R	$\sum F$	π_4	pA_2 [a] obsd	cald [b]
1	H	0.00	0.00	7.4	7.4
2	4-F	0.43	0.14	7.1	6.5
3	4-Cl	0.41	0.71	5.6	7.1
4	4-Br	0.44	0.86	7.4	7.2
5	4-Me	− 0.04	0.56	8.3	8.1
6	4-OMe	0.26	− 0.02	5.0	6.7
7	4-NO$_2$	0.67	− 0.28	5.2	5.4
8	4-NH$_2$	0.02	− 1.23	6.0	6.1
9	4-iPr	− 0.05	1.53	8.7	9.1
10	3-F	0.43	0.00	6.4	6.3
11	3-Cl	0.41	0.00	6.2	6.4
12	3-Br	0.44	0.00	6.4	6.3
13	3-Me	− 0.04	0.00	7.7	7.5
14	3-OMe	0.26	0.00	6.4	6.7
15	3-NO$_2$	0.67	0.00	5.4	5.7

[a] 50% inhibition of histamine (H_1) activity in isolated guinea pig ileum (relative to mepyramine)
[b] Eq. 18

moiety) [110].

$$pA_2 = 99.776MRI + 0.989Szw - 1.414Ww + 0.859Ip_1 - 34.882$$
$$n = 11, \quad r = 0.980, \quad s = 0.228, \quad F = 37.13 . \tag{19}$$

However, in deriving this equation four compounds (Table 9, compounds 3, 6, 7, and 15) have been excluded from the study. Between these two studies, the model (Eq. 18) proposed by Singh et al. [109] is far superior when compared to the later one (Eq. 19) [110].

In another interesting study, considering the importance of asparagine, aspartic acid, threonine, and lysine in the binding of agonists/antagonists to the histamine (H_1) receptor, Brzezinska and co-workers [111, 112] have quantitatively investigated the antihistaminic (H_1) activity of substituted thiazoles and benzthiazole derivatives [113–115] (Fig. 11, Table 10) using the log P and reverse and normal phase thin layer chromatographic (TLC) parameters (Rm values) generated through impregnating the TLC plates with these selected amino acids. The idea behind impregnating the TLC plates with amino acids was to assess their contribution in the binding affinities at the receptor site and in turn use them in modeling the activity of the compounds. Accordingly,

Table 10 Thiazole and benzthiazole derivatives in modeling the anti-histaminic activity (Fig. 11) [111, 112]

No.	R	n	pA_2[a] obsd	cald[b]	cald[c]
1	H	–	4.44	4.10	4.53
2	3-Me	–	4.00	4.18	3.83
3	3-F	–	4.53	4.79	4.62
4	3-Cl	–	4.82	5.02	4.78
5	3-Br	–	4.65	5.20	4.92
6	3-OMe	–	4.14	4.13	4.37
7	H	–	5.88	5.72	5.87
8	3-F	–	6.15	6.22	5.69
9	3-Cl	–	6.38	5.96	6.04
10	4-F	–	5.99	5.74	5.78
11	4-Br	–	5.87	6.01	6.19
12	H	–	5.98	5.78	6.10
13	Me	3	5.70	5.56	5.92
14	H	2	5.82	5.74	5.46
15	Me	2	5.60	5.25	5.60
16	$-CH_2$-Ph-4-Me	3	5.99	6.32	6.23
17	$-C_2H_4$-Ph-4-Me	2	6.08	6.14	6.12
18	$-CH_2$-Ph	2	5.77	5.90	5.74

[a] 50% inhibition of histamine (H_1) antagonist activity (isolated guinea pig ileum) relative to temelastine
[b] Eq. 20 [111]
[c] Eq. 21 [112]
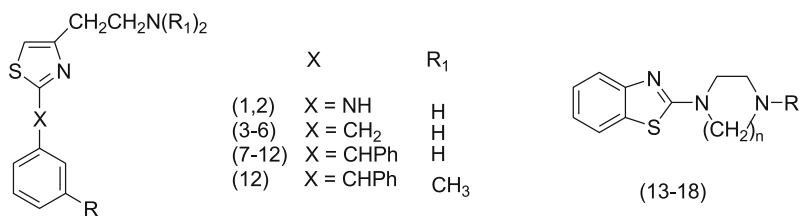
Fig. 11 Structures of thiazole and benzthiazole derivatives

the Rm values of the compounds have been measured under different chromatographic environments [111, 112]. Following are the representative QSAR equations of the antihistaminic (H_1) activity in the reverse and normal phase

TLC studies, respectively, of these compounds.

reverse phase TLC model

$$pA_2 = -1.27(0.23)S2/C + 9.59(2.60)C\text{-}S6 + 0.63(0.09)\log P + 3.96$$
$$n = 18, \quad r = 0.94, \quad s = 0.289, \quad F = 35.11 \tag{20}$$

normal phase TLC model

$$pA_2 = 1.16(0.34)S4 + 0.16(0.03)S7/C + 0.54(0.07)\log P + 4.16$$
$$n = 18, \quad r = 0.95, \quad s = 0.254, \quad F = 47.04. \tag{21}$$

The terms S2, S4, S6, S7, and C represent, respectively, the chromatographic environment(s) formed by combinations of asparagine, lysine, asparagine + lysine, asparagine + aspartic acid + threonine and/or control (without amino acids). In these equations S2/C, S4, C-S6, and S7/C refer to the Rm values (independent descriptors) of corresponding chromatographic environments (impregnation) reflected in modeling the antihistaminic (H_1) activity. These studies have highlighted the importance of overall hydrophobicity of the compounds in deciding the activity. They have also quantified the interaction of selected amino acids with the compounds. It further suggested that the normal phase TLC parameters modeled the activity better than the reverse phase TLC parameters. This study has opened up a novel way for generating the receptor-directed interaction information in terms of amino acids for modeling the antihistaminic (H_1) activity of these compounds. One can adapt to this kind of procedure for the study of other receptors also.

3.1.5
H^+K^+-ATPase Inhibitors

Thiazolidines have been reported to be a core scaffold for antiulcer compounds. La Mattina et al. have evaluated a series of 128 compounds belonging to 4-substituted-2-guanidino thiazoles (Fig. 12) against gastric hydrogen-potassium stimulated adenosine triphosphatase (H^+K^+-ATPase), a therapeutic target of anti-ulcer drugs [116].

Goel and Madan [117] investigated the SAR of the antiulcer activity of these compounds with Wiener's topological index (Wiener number of chemical graph, W(G)) [118] and the first-order molecular connectivity index ($^1\chi$) [119] using a typical classification procedure. In the case of Wiener's

R1= substituted guanidine group
R2= H, Me,-CHO
R3= aryl, pyrrol, indole
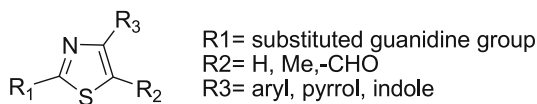
Fig. 12 General structure of 4,5-substituted-2-guanidinothiazoles associated with H^+K^+-ATPase inhibitory activity

topological index, the compounds have been correctly classified into active and inactive groups to the order of 89%. A Wiener index value in the range of 391 to 540 was observed to be associated with the active analogues. In the case of the molecular connectivity index the overall accuracy of prediction has been reported to be 88%; and, the activity that has been found to be associated with the $^1\chi$ values is the range of 5.75 to 7.20 [117]. This approach is very handy and quick for the screening of large databases.

Borges and Takahata studied the QSAR of a different series of 4-indolyl, 2-guanidinothiazole derivatives (Fig. 13; Table 11) for their H^+K^+-ATPase inhibitory activity using 94 quantum chemical descriptors generated for this purpose [120].

They adopted partial least square (PLS), principal component regression (PCR), and back propagation neural network (BPN) methods for the derivation of the regression models. Among these approaches, the activity has been found to be best explained in the PLS analysis with five latent variables. In terms of the whole molecular structure, this has led to the suggestion that the energies of the highest occupied molecular orbitals – 9, – 8, – 7, – 5, – 3, – 2, and – 1 ($\in_{HOMO-9}$, $\in_{HOMO-8}$, $\in_{HOMO-7}$, $\in_{HOMO-5}$, $\in_{HOMO-3}$, $\in_{HOMO-2}$, $\in_{HOMO-1}$) the dipole moments along the x- and z-axis (μ_x, μ_z) and quadrupole moments yy, zz, and xz (Quad$_{yy}$, Quad$_{zz}$, and Quad$_{xz}$) are important contributors to model the activity. In terms of individual atomic centers of these analogues, the study has identified the electron densities F_3^T, F_6^T, F_4^H, F_9^H, F_4^L, F_6^L, F_7^L, F_8^L F_{11}^T, F_{13}^H, F_{14}^H, F_{12}^L, F_{13}^L, F_{14}^L, and F_{15}^L and the charges Q_2, Q_3, Q_5, Q_6, Q_{12}, and Q_{18} (the subscript numbers correspond to the atom identification number as shown in Fig. 13; the super scripts T, H, and L represent Total, HOMO, and LUMO, respectively) as important to explain the activity of the analogues. This study has explained the activity in terms of a detailed electronic profile of the compounds. However, these results are far more sophisticated and at the same time too complex to comprehend when compared to that of Goel and Madan's investigations involving Wiener's and Chi indices [117].
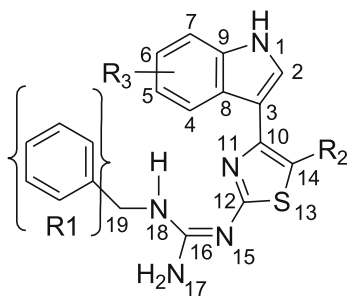
Fig. 13 General structure of 4-indolyl-2-guanidinothiazoles associated with H^+K^+-ATPase inhibitory activity

Table 11 4-Indolyl, 2-guanidinothiazole derivatives in modeling the H^+K^+-ATPase inhibitory activity (Fig. 13) [120]

No.	R_1	R_2	R_3	IC_{50}[a] obsd	Predicted[b] PLS	PCR	BPN
1	H	H	H	9.0	6.0	3.3	8.4
2	C_7H_7	H	H	1.5	1.3	3.2	1.2
3	H	Me	H	7.6	7.9	2.2	7.6
4	H	H	5-OMe	19.0	16.2	4.4	7.2
5	C_7H_7	H	5-OMe	4.3	3.5	3.7	6.4
6	H	H	5-OC_7H_7	1.2	1.3	3.9	1.4
7	C_7H_7	H	5-OC_7H_7	1.8	1.7	3.6	0.61
8	H	H	2-Me	9.0	10.6	3.1	5.2
9	C_7H_7	H	2-Me	1.7	2.2	2.90	1.1
10	H	Me	2-Me, 5-Cl	0.6	0.47	0.97	2.8
11	C_7H_7	Me	2-Me, 5-Cl	1.1	0.74	0.61	0.89
12	C_7H_7	H	4-Me	3.3	3.7	0.87	0.27
13	H	H	5-Me	1.8	2.3	2.9	2.9
14	C_7H_7	H	5-Me	0.94	1.1	2.9	0.57
15	C_7H_7	H	6-Me	1.6	1.5	3.5	2.2
16	H	H	7-Me	7.6	6.7	3.6	6.7
17	C_7H_7	H	7-Me	1.0	1.4	3.4	2.2
18	H	H	5-Cl	1.8	1.5	2.3	1.9
19	C_7H_7	H	5-Cl	0.7	0.87	0.98	0.31
20	H	Me	5-Cl	0.59	0.81	0.8	2.1
21	C_7H_7	Me	5-Cl	0.7	0.63	0.88	0.77
22	H	H	5-Br	0.96	1.1	2.6	1.0
23	C_7H_7	H	5-Br	0.7	0.52	2.3	1.1
24	H	H	5-F	7.4	9.2	4.1	9.9
25	C_7H_7	H	5-F	2.7	3.3	3.9	3.2
26	H	H	5-CO_2Me	6.7	5.3	2.4	0.37
27	C_7H_7	H	5-CO_2Me	3.1	3.4	2.1	4.2
28	C_7H_7	H	5-NHCOEt	23.8	21.7	5.9	4.0

[a] H^+K^+-ATPase inhibitory activity
[b] Predicted activity by leave one out procedure

3.1.6
Antiepileptic Agents

Thiazolidines/thiazoles in fusion with other aromatic systems are also potential bioactive scaffolds. Riluzole (Fig. 14)—a benzothiazole analogue—is known to intervene in epilepsy, a cerebral disorder of the central nervous system, via a glutamatergic mechanism [121]. The anticonvulsant activity of riluzole has been attributed to its direct action on the voltage-dependent

Table 12 Physicochemical properties and anticonvulsant activity of benzothiazolamine derivatives (Fig. 14) [123]

No	X	45SUBST	π	MR	$-\log IC_{50}$ [a] obsd	cald [b]
1	6-OCF$_3$ (Riluzole)	0	1.04	0.79	5.39	4.82
2	H	0	0.00	0.10	4.59	4.53
3	6-SMe	0	0.61	1.38	4.80	4.13
4	6-Me	0	0.56	0.56	3.82	4.54
5	6-CHMe$_2$	0	1.53	1.50	5.17	4.68
6	6-COOH	0	$-$ 0.32	0.69	3.88	$-$
7	6-SO$_2$Me	0	$-$ 1.63	1.35	3.30	3.22
8	6-Cl	0	0.71	0.60	5.17	4.57
9	6-OMe	0	$-$ 0.02	0.79	3.30	3.74
10	6-COPh	0	1.05	3.03	3.30	3.96
11	6-SO$_2$NH$_2$	0	$-$ 1.82	1.23	3.30	3.14
12	6-Br	0	0.86	0.89	4.85	4.50
13	6-NO$_2$	0	$-$ 0.28	0.74	3.66	4.23
14	6-CF$_3$	0	0.88	0.50	5.31	5.04
15	6-F	0	0.14	0.09	3.30	4.30
16	6-OH	0	$-$ 0.67	0.28	3.30	3.47
17	6-NH$_2$	0	$-$ 1.23	0.54	3.30	2.99
18	5-OMe	1	$-$ 0.02	0.79	3.30	3.14
19	5-Me	1	0.56	0.56	3.30	3.70
20	5-CF$_3$	1	0.88	0.50	4.00	4.02
21	5-COPh	1	1.05	3.03	3.30	3.06
22	4-OMe	1	$-$ 0.02	0.79	3.30	2.90
23	4-Me	1	0.56	0.56	3.82	3.63
24	4-Cl	1	0.71	0.60	4.58	3.68
25	4-CF$_3$	1	0.88	0.50	3.86	4.10
26	4-Ph	1	1.96	2.54	5.04	$-$
27	4-Me,5-F	1	0.70	0.66	3.30	3.55
28	4,5-(CHCH)$_2$	1	1.30	1.75	3.30	3.49
29	4,6-F$_2$	1	0.28	0.18	3.30	3.17
30	4,6-Cl$_2$	1	1.42	1.21	3.30	3.67
31	4,6-Me$_2$	1	1.12	1.13	3.30	3.59
32	5,6-Me$_2$	1	0.99	1.13	3.30	3.56

[a] Sodium flux (NaFl) inhibition
[b] Eq. 22

sodium channels [122]. Hays et al. have investigated the QSAR of the anticonvulsant activity of substituted 2-benzothiazolamines (Fig. 14, Table 12) with hydrophobicity (π), molar refractivity (MR), Hammett's sigma (σ) and Swain and Lupton's polarity ($\mathcal{F}$) and resonance ($\mathcal{R}$) constants and an indicator parameter (45SUBST) describing the importance of the 4 and/or 5
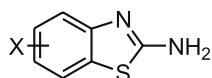
Fig. 14 General structure of benzothiazolamines associated with anticonvulsant activity

substituents [123]. This study has resulted in the following equation to explain the variation in the anticonvulsant activity of these analogues.

$$- \log \mathrm{IC}_{50} = 0.57(0.12)\pi - 0.90(0.19)45\mathrm{SUBST}$$
$$- 0.45(0.14)\mathrm{MR} + 0.92(0.38)\mathcal{R} + 4.57$$
$$n = 30, \quad r = 0.794, \quad s = 0.480, \quad F = 10.80 \, . \tag{22}$$

On this basis it has been suggested that an increase in lipophilicity (π), decrease in size (MR), increase in resonance effect ($\mathcal{R}$), and the absence of 4 or 5 substitution of the benzothiazolamine ring system would be favorable for anticonvulsant activity. This has been presented as an example of QSAR in fused systems. In the literature more study reports are available where the thiazole moiety existed as part of the fused ring systems [77].

3.2
Metabolic Disorders

3.2.1
β_3-receptor Agonists

Thiazoles have been investigated as a potential drug scaffold in the treatment of metabolic disorders such as obesity, diabetes, cataracts, and thrombosis. They have been reported to be associated with the β_3 agonist activity (a subtype of β-adrenergic receptor) through the activation of adenyl cyclase [124, 125]. This receptor has been implicated in obesity, a condition of abnormal body weight resulting from the accumulation of extra adipose tissue due to a state of positive energy balance characterized by diminished energy expenditure when compared to the energy intake [126]. A systematic exploration involving several imidazolindinone (**a**), imidazolone (**b**), indoline (**c**), and thiazole (**d,e**) derivatives in the stimulation of adenyl cyclase revealed the advantage of the thiazole derivatives (**e**) over the rest of compounds as β_3 agonists (Fig. 15) [124, 125, 127, 128].

In this context, Hanumantharao et al. [129] have carried out a QSAR analysis of the β_3 agonist activity of the thiazole derivatives (**e**) with the molecular descriptors generated from the MOE programme [71]. This has resulted in QSAR models (Eq. 23 and 24) of these compounds in terms of hydrophobicity of VdW surface areas with different polarities ($S \log P$, $S \log P_{\mathrm{VSA0}}$ and $S \log P_{\mathrm{VSA8}}$), electrostatic potential energy (E_{ele}), and zero-order connectivity

Table 13 Physicochemical/electronic properties and β_3-agonist activity of thiazole derivatives (comp. **e**, Fig. 15) [129]

No.	n	R	E_{ele}	Slog P	Slog P_{VSA0}	Slog P_{VSA8}	pEC$_{50}$ [a] obsd	cald [b]	Cald [c]
1	0	C$_8$H$_{17}$	−0.04	6.87	43.40	119.68	−1.00	−0.92	−0.86
2	0	CH$_3$CONH(CH$_2$)$_5$	−0.04	4.89	61.41	63.07	−1.70	−1.42	−1.78
3	0	C$_2$H$_4$Ph	−0.05	5.75	43.40	6.47	−1.52	−1.69	−1.46
4	0	CH$_2$-naphthyl	−0.04	6.71	43.40	6.47	−0.70	−0.67	−0.65
5	0	2-benzofuranyl	−0.04	6.38	43.40	6.47	−0.96	−0.88	−0.75
6	0	3-indolyl	−0.04	6.12	43.40	6.47	−0.69	−0.81	−0.86
7	0	3-pyridinyl	−0.04	5.03	43.40	6.47	−1.60	−1.26	−1.44
8	0	2-pyridinyl	−0.04	5.03	43.40	6.47	−1.34	−1.41	−1.52
9	0	3,4,diF-Ph	−0.04	5.91	43.40	6.47	−0.85	−0.91	−1.01
10	0	PhcC$_6$H$_{11}$	−0.04	7.76	43.40	81.94	−0.08	−0.22	−0.23
11	0	Ph-tBu	−0.04	6.93	43.40	6.47	−0.38	−0.40	−0.40
12	0	4-OH-Ph	−0.04	5.34	68.78	6.47	−1.65	−1.91	−1.34
13	0	4-AcNH-Ph	−0.05	5.59	43.40	6.47	−1.65	−1.54	−1.71
14	0	4F-PhCH$_2$	−0.04	5.70	43.40	6.47	−0.79	−0.96	−1.13
15	1	C$_8$H$_{17}$	−0.04	6.58	61.41	138.55	−0.99	−1.10	−0.99
16	1	CH$_2$-naphthyl	−0.04	6.22	61.41	6.47	−1.08	−0.90	−0.86

[a] β_3-agonist activity
[b] Eq. 23
[c] Eq. 24
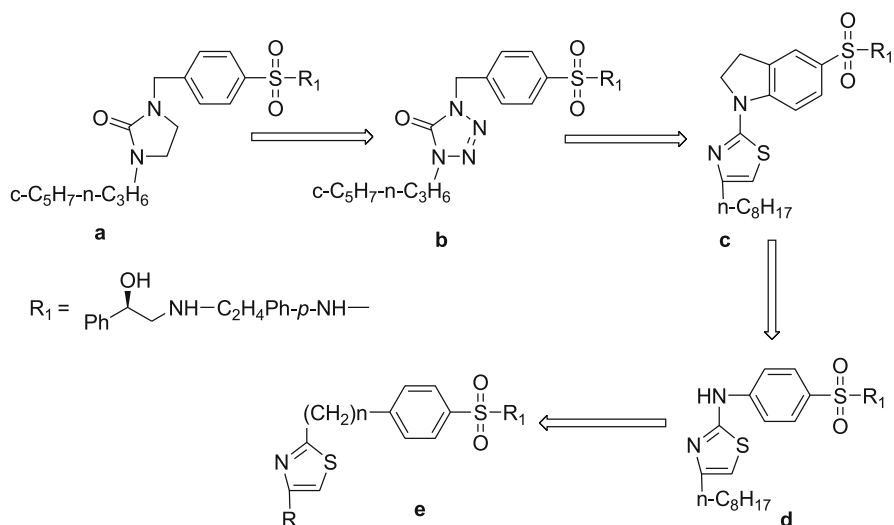
Fig. 15 Development of thiazoles (**d, e**) as β-adrenergic receptor (β_3) agonists from their predecessors (**a–c**)

index (chi0) (Table 13).

$$
\begin{aligned}
p\text{EC}_{50} = {} & 0.266(0.039)\text{chi0} + 88.998(14.954)E_{\text{ele}} \\
& - 0.030(0.006)S\log P_{\text{VSA0}} - 3.880 \\
& n = 16, \quad r = 0.936, \quad Q^2 = 0.712, \quad s = 0.191, \quad F = 28.30
\end{aligned} \tag{23}
$$

$$
\begin{aligned}
p\text{EC}_{50} = {} & 45.869(15.591)E_{\text{ele}} + 0.558(0.071)S\log P \\
& - 0.003(0.001)S\log P_{\text{VSA8}} - 2.526 \\
& n = 16, \quad r = 0.930, \quad Q^2 = 0.798, \quad s = 0.200, \quad F = 25.36 \,.
\end{aligned} \tag{24}
$$

These equations have led them to suggest that molecules with a high electro-static potential energy and that are lipophilic in nature would be favorable for β_3-agonist activity.

3.2.2
Neuropeptide Y5 Receptor Antagonists

Other then the β_3 adrenergic receptor agonistic activity, some thiazole deriva-tives have been reported to show antiobesity activity through the neuro-peptide Y5 receptor (NPY5R) [130, 131]. The antagonists of the NPY5 recep-tor (NPY5R) are known to decrease the food intake in animal models [132]. A virtual screening of a large database with the pharmacophore model (Fig. 16) developed from the hydrophobic and topological similarity of three

seed structures (compounds **a–c**, Fig. 16) has paved the way for the discovery of some thiazoles as NPY5R antagonists [130, 133–135].

From this virtual screening, 31 compounds (compound **e**, Fig. 16) have been identified to show the activity at $IC_{50} < 10\,\mu M$. Among these a thiazole analogue, 2-(3-benzonitrile)amino-5-benzoyl-thiazole (compound **f**, Fig. 16), has been found to be the most active compound with an IC_{50} of 40 nM for the mouse Y5 receptor and even showed activity in a mice feeding model at
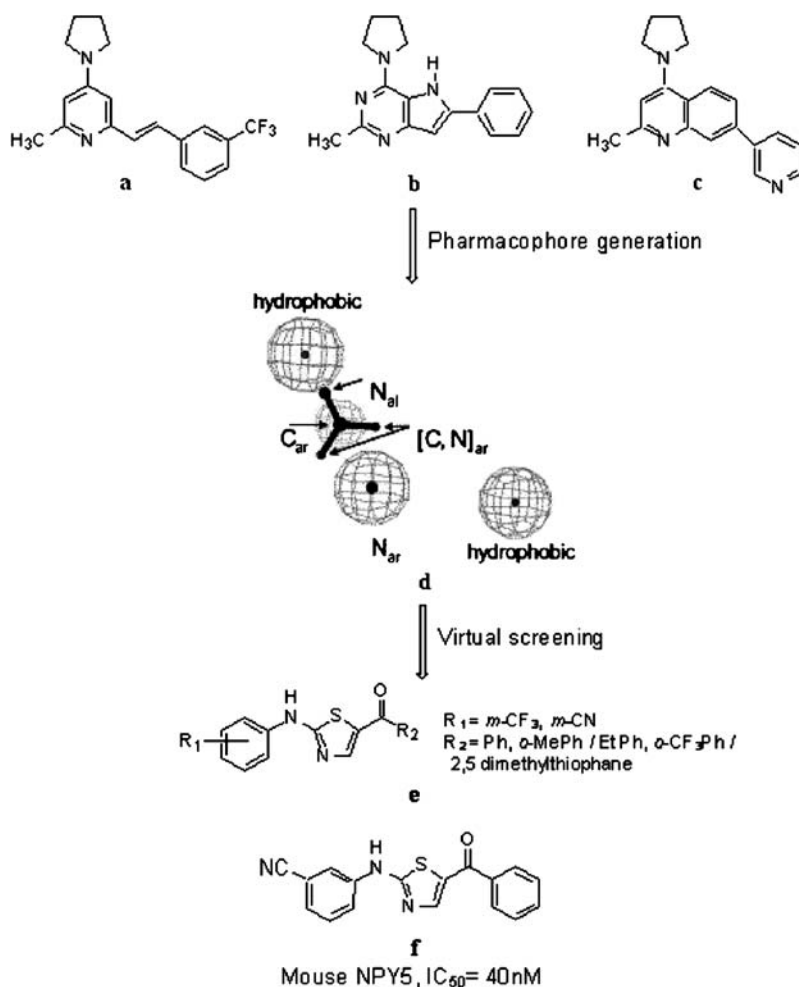
Fig. 16 Strategy adopted in the identification of thiazoles (**e**) as potential NPY5 receptor antagonists from the virtual screening of 3D-pharmacophore (**d**) (Reprinted with permission from [130]. Copyright 2005 Elsevier Ltd.) developed from three dissimilar seed structures (compounds **a–c**). From of this strategy compound **f** has been identified and found to show mouse NPY5 receptor inhibition (IC_{50}) at 40 nM

10 mg/kg via intra peritoneal root [130]. The consensus between the pharma-cophore patterns of the compounds **f** and **a** have been highlighted in Fig. 17. In a further SAR study, Guba et al. discovered that electron-withdrawing sub-stituents on aryl moieties would be better for the activity. The position of choice for the substituent groups on the aryl moieties (at 2- and 5- of the thiazole), have been found to be *meta* and *ortho*, respectively [130].

In continuation of the search for more active ligands for the NPY5 receptor, Nettekoven, Guba and co-workers [131] observed that thiazole **g** derivatives showed 10 times more affinity than that of thiazole **h** derivatives for the mouse receptor (Fig. 18). This difference in the activity profile of the thiazole isomers **g** and **h** has been explained through the conformational analysis of core scaffolds (Fig. 18).

The thiazole isomers **g** and **h** differed in their minimum energy conforma-tions (Fig. 18) due to different torsional angles between the carbonyl function and the heterocycle system. In the thiazole **g** isomer a favorable short distance interaction between the carbonyl oxygen and the thiazole sulfur ($C = O - S$ type of interaction), below the sum of the van der Waals radii (< 3.3 Å), has led to an energetically highly preferred conformation. This has found sup-port from Iwaoka et al. [136] simulation studies on comparable molecular systems. However, in the thiazole **h** isomer the repulsive interaction between the carbonyl oxygen and the thiazole nitrogen has resulted in a high energy bent conformation. The potential energy difference between these conformer states has been found to be of the order of 10 to 7 kJ/mol. This is taken as the reason for the 10-fold increment in the activity profile of the thiazole **g** iso-
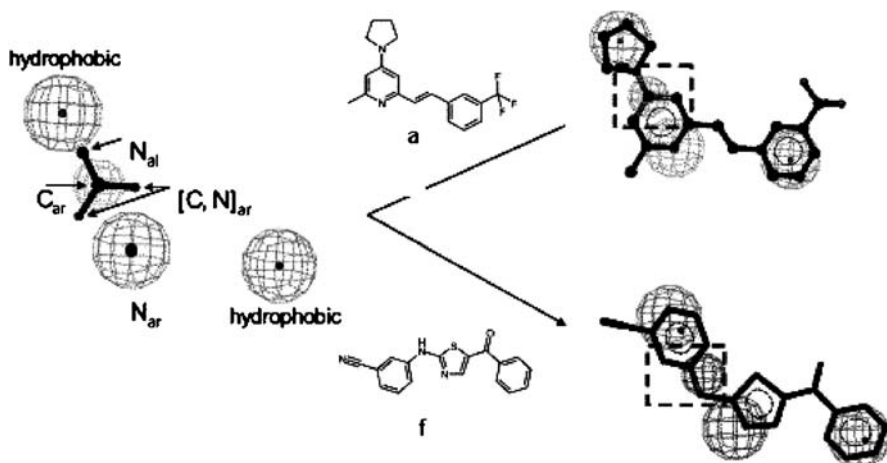
Fig. 17 Mapping of the 3D pharmacophore hypothesis onto compounds **a** and **f** (Fig. 16). The trigonal substitution pattern around C_{ar} is allowed to rotate yielding a novel scaffold in the 3D virtual screening campaign (the match is highlighted by the *dashed rectangle*). (Reprinted with permission from [130]. Copyright 2005 Elsevier Ltd.)
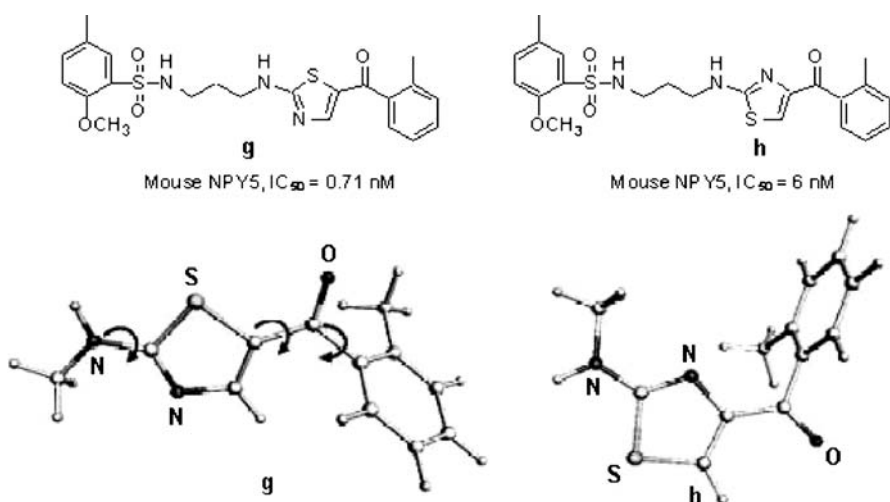
Fig. 18 Conformations corresponding to the minimum energies for the thiazole isomers **g** and **h**. The *arrows* represent the torsional angles sampled in both isomers. (Reprinted with permission from [131]. Copyright 2005 Elsevier Ltd.)

mer when compared to that of isomer **h**. This study has clearly demonstrated a successful structure-activity investigation involving a lead identification from the virtual screening of totally unrelated seed compounds followed by modification of the generated lead through SAR and conformational studies that finally emerged with far more active compounds compared to the initial leads.

3.2.3
PPAR Agonists

In addition to their affinity to β-adrenergic and neuropeptide Y5 receptors, thiazolidines are also known to act on peroxisome proliferator-activated receptors (PPARs). In the biological system PPARs regulate the expression of genes involved in the fatty acid and carbohydrate metabolism and in adipocyte differentiation [137]. Among the PPARs, the PPARγ subtype has received wide attention as its agonists specifically promote insulin action and glucose utilization in the peripheral tissues. Thiazolidinediones (TZDs) are among the early chemical classes reported as the agonists of PPARγ with high affinity [138, 139]. The SAR studies with the TZD analogues have suggested that an acidic head group with a central spacer group followed by a linear lipophilic tail are the primary structural requirements of PPARγ agonists. The desired linker fragment between the head group (2,4-thiazolidinedione) and the central spacer group has been suggested to be the methylene moiety. Any deviation in the linker fragment length and α,β-unsaturation in

thiazolidinediones have been reported to reduce the PPARγ activity. For the lipophilic tail a variety of aryl and heteroaryl groups such as, pyridyl (**a**), oxazoyl (**b, c**), benzoxazoyls (**d**) have been found to be tolerated with the activity [138, 139, 141–143]. Different alkyl ether, alkyl ketones (**c**), olefin and some cyclic moieties have been investigated as linkers between the central spacer group and the lipophilic tail (Fig. 19). The PPARγ agonistic response of these compounds has been found to tolerate all these structural variations [140, 144].

The TDZs contain a chiral center at C-5 of the heterocyclic head group. The binding assays have indicated that the (*S*)-enantiomer of the TZD binds to the PPARγ with high affinity [145]. However, under physiological conditions it has been observed to undergo racemization [146]. These studies have provided gross structural requirements of TDZ and related ligands for the PPARγ agonistic activity. The X-ray studies of the co-crystals of TDZ analogues with different PPARs have indicated that PPARγ's ligand-binding domain (LBD) has an overall similarity with other nuclear receptors [147].

In these X-ray studies, it has been observed that the TDZ moiety binds in helices 3, 4, and 10 and to the activating function-2 by making hydrogen bonds with groups in the side chains of His-449, Tyr-473, His-323, and Ser-289. In the Y-shaped cavity, the agonist's lipophilic tail group has been found to occupy the downward position of "Y" by interacting with amino acid residues Met-348, Ile-341, and Ile-281 (Fig. 20) [148, 149]. Also, Yanagisawa and co-workers molecular modelling studies with the oximes having 5-
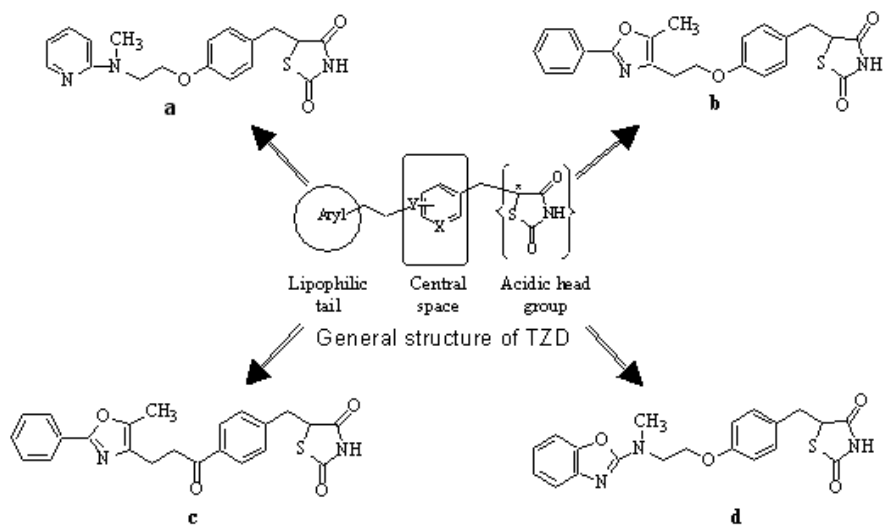
Fig. 19 Primary structural requirements of thiazolidinediones (TZDs) for PPARγ agonistic activity
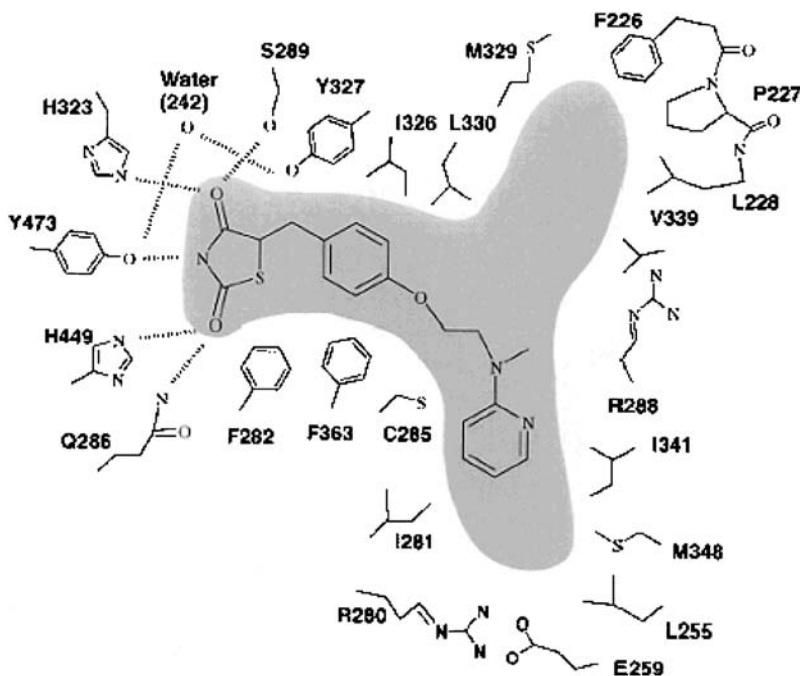
Fig. 20 Ligand (Rosiglitazone)-enzyme (PPARγ) crystal structure where the ligand is shown in the binding domain of PPARγ (Reprinted with permission from [151]. Copyright 2001 Elsevier Science Inc.)

benzyl-2,4-thiazolidinedione moieties (Fig. 21) [150] as agonists of the PPARs has shown that they occupy a similar binding domain of PPARγ [151]. All these studies have led to the suggestion that the PPARγ LBD comprises of 13 α-helices and a small four-stranded β-sheet. The helices 3, 7, and 10 have been found to form a Y-shaped cavity to accommodate the ligand scaffolds (Fig. 20).

More recent studies have confirmed that dual activation of PPARγ and PPARα subtypes would be beneficial for treating type-2 diabetes [139]. In this connection KRP-297, a TZD derivative has been found to express in vitro as well as in vivo affinity for both the PPARα and PPARγ subtypes [152]. In light of this, Desai and co-workers have investigated the PPARα/γ dual agonistic activity of a series of TZD and oxazolidinedione derivatives (comp. **a**, Fig. 22, Table 14) to assess their antidiabetic activity [153, 154].

Subsequently, Khanna et al. carried out the CoMFA and docking studies of these TZDs and oxazolidinediones in conjunction with their PPARα/γ dual activity [155]. The common CoMFA model featuring the PPARα and PPARγ binding sites has been found to best explain the affinities of these ligands for the receptors (number of significant components = 6; cross-validated

Table 14 Thiazolidinedione and oxazolidinedione derivatives in modeling (CoMFA) PPAR-α, γ and dual (d) binding affinity (comp. **a**, Fig. 22) [155]

No.	X	R_1	pIC_{50} [a] (α) obsd	perd	(γ) obsd	perd	(d) obsd	perd
1	S	OPh	7.55	7.47	7.24	7.37	14.79	14.79
2 [b]	S	OPh	7.33	–	7.12	–	14.45	
3 [c]	S	OPh	5.30	5.11	6.71	6.78	12.01	12.01
4	S	OPh-4-CH(Me)$_2$	5.68	5.76	6.77	6.72	12.45	12.45
5	S	OPhC(Me)$_3$	5.0	5.03	6.47	6.49	11.47	11.47
6	S	OPh-4-CH$_2$CH(Me)$_2$	5.0	5.05	6.54	6.50	11.54	11.54
7	S	OPh-4-cC$_5$H$_9$	5.70	–	6.48	–	12.18	–
8	S	OPh-Ph	5.0	5.07	6.65	6.54	11.65	11.65
9	S	OPh-4Cl	7.0	–	7.14	–	14.14	–
10	S	OPh-4F	7.55	7.25	7.11	7.15	14.66	14.66
11	S	OPh-4OMe	5.59	5.42	6.52	6.75	12.11	12.11
12	S	OPh-4OH	6.02	6.43	7.52	7.22	13.54	13.54
13	S	OPh-3,4-di-Cl$_2$	7.17	–	7.19	–	14.36	–
14	S	OPh-3-Me,4-Cl	6.79	6.92	7.25	7.13	14.04	14.04
15	S	OPh-3-Me,4-F	6.95	7.06	7.11	7.22	14.06	14.06
16	S	OcC$_6$H$_{11}$	5.85	6.10	7.43	7.27	13.28	13.28
17	S	OcC$_7$H$_{13}$	6.68	6.93	7.07	7.18	13.75	13.75
18	S	OcC$_5$H$_9$	7.38	7.09	7.20	7.26	14.58	14.58
19	S	COPh	7.05	7.04	7.72	7.66	14.77	14.77
20	S	COPh-4Cl	5.0	–	6.84	–	11.84	–
21	S	3-benzoisoxazyl	7.43	7.57	7.52	7.56	14.95	14.95
22	S	COcC$_6$H$_{11}$	6.92	6.93	7.19	7.10	14.11	14.11
23	S	CH = cC$_6$H$_{10}$	7.21	7.13	6.82	6.94	14.03	14.03
24	S	CH$_2$cC$_6$H$_{11}$	7.34	7.31	7.23	7.14	14.57	14.57
25	S	cC$_6$H$_{11}$	5.30	–	6.47	–	11.77	–
26	O	cC$_6$H$_{11}$	6.54	6.36	6.31	6.17	12.85	12.85
27	O	Ph	5.57	5.78	6.35	6.38	11.92	11.92
28	O	cC$_7$H$_{13}$	6.21	6.35	6.19	6.12	12.40	12.40
29	O	cC$_5$H$_9$	6.20	–	5.97	–	12.17	–
30	O	4-cyclohexanone	4.82	4.67	5.94	5.86	10.76	10.76
31	O	4-cyclohexanol	4.82	4.85	6.74	6.88	11.56	11.56
32	O	1,1-difluoro-4-cyclohexane	6.23	6.01	6.27	6.35	12.50	12.50
33	O	1,1-dimethyl-4-cyclohexane	5.48	5.33	5.75	5.80	11.23	11.23
34	O	4-tetrahydro-pyran	5.54	5.72	6.12	6.18	11.66	11.66

[a] PPAR α/γ and dual (d) binding affinities
[b] Without propyl group
[c] $O - (CH_2)_4 - O$ in place of $O - (CH_2)_3 - O$
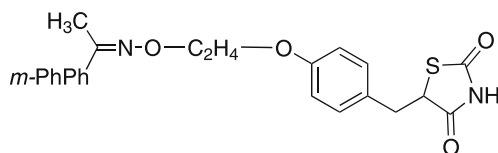
Fig. 21 2,4-thiazolidinedione carrying an oxime moiety as a PPARγ agonist
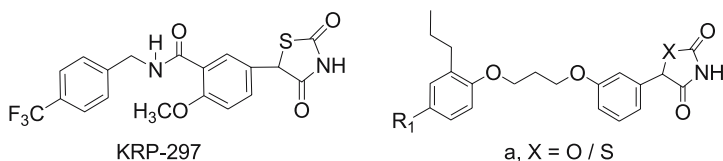
Fig. 22 Structures of KRP-297 and thiazolidinedione/oxazolidinedione derivatives associated with PPARα/γ dual agonistic activity

r^2 (r^2_{cv}) = 0.782; non cross-validated r^2 (r^2_{ncv}) = 0.985). In this, the steric and electrostatic field contributions have been found to be 0.535 and 0.465 parts respectively (comp. **a,** Fig. 22 Table 14). Apart from this, for these compounds by making use of the protein sequences of PPARγ and PPARα molecular docking studies have also been carried out in FlexX. An earlier X-ray study of PPARα and PPARγ has suggested a common Y-shaped binding pocket for both the receptors with a difference in their amino acid content that is His323 in PPARα being replaced by Tyr314 in PPARγ [156]. Against this background, it has been observed that in both the receptors, the compounds (ligands) have been found to assume a U-shape and bind to the enzyme through forming strong hydrogen bonds by involving the ligand's acidic fragment (thiazolidinedione moiety) and a set of residues (Tyr314, Tyr464, His440, and Ser280 in PPARα, and His323, Tyr473, His449, and Ser289 in PPARγ) in the active site. In light of this, the variations in the binding affinities of these compounds for the PPARα/γ-receptors have been explained by using these differences. These studies exemplify the scope of the design of ligands from targeting "a single receptor" to "multiple receptors".

3.2.4
Aldose Reductase Inhibitors

Some typical structural templates embedded with the thiazolidine frame have been reported as potent inhibitors of *aldose reductase* (AR), an enzyme in the polyol pathway responsible for the conversion of glucose to sorbitol. In this, the accumulation of sorbitol has been attributed to causing cataracts, neuropathy, and retinopathy in diabetic cases [157, 158]. The planar hydrophobic (aromatic) regions and propensity to charge transfer interactions have been
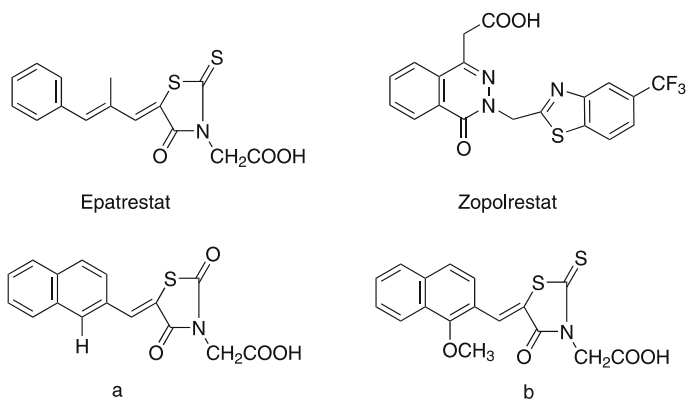
Fig. 23 Structures of epatrestat, zopolrestat, 2,4-dioxo-5-(naphthylmethylene)-3-thiazol-idineacetic acid (**a**) and its 2-thioxo analogue (**b**) as *Aldose Reductase* inhibitors

identified as some known structural requirements of the AR inhibitors [159]. Considering these features together with epatrestat (Fig. 23), a potent inhibitor of AR with a thiazolidine frame as part of its scaffold, Fresneau et al. have come up with new compounds, 2,4-dioxo-5-(naphthylmethylene)-3-thiazolidineacetic acid (compound **a**, Fig. 23) and its 2-thioxo analogue (compound **b**, Fig. 23) as AR inhibitors [160].

In a pursuit to understand the binding modes of these inhibitors with AR, a molecular modeling study has been carried out with compounds (**a**) and (**b**) and these results have been compared with the crystal structure of the complex of AR and Zopolrestat, a known AR inhibitor (Fig. 23) [160, 161]. This study has specifically identified three sites of interaction on the enzyme; site 1, an anionic pocket to accommodate a negative charge, such as a carboxylic group at the OH of Tyr48; site 2, a hydrophobic binding pocket with amino acids Trp111, Leu300, and Trp219 to accommodate aromatic moieties; and site 3 a hydrogen bonding site with SH of Cys298. This has led to the suggestion that a strong interaction at the identified sites would lead to better inhibitory activity for the compounds [160]. This study has illustrated an example of discovering novel compounds starting from the existing drugs and high active compounds.

3.2.5
Thromboxane A2 Receptor Antagonists

The emergence of thiazolidine derivatives as a structure class for platelet aggregation inhibitory activity has its roots in a marine natural product, D-cysteinolic acid (**a**) [162, 163]. The medicinal chemistry and modeling strategies have navigated D-cysteinolic acid (**a**) through various modifications to culminate in the thiazolidine analogues with different activity profiles (Fig. 24).

Among these compounds, D-cysteinolic acid (**a**) has exhibited mild platelet aggregation inhibitory activity and 2-(4-hydoxy-3-methoxyphenyl)-thiazolidine (**b**), a synthetically transformed compound of this natural product, has displayed an elevated activity, thus ushering thiazolidines into this pharmacological domain [162, 163]. In this, the elevated activity may have resulted from the restriction in the spatial disposition of nitrogen and sulfur when compared to (**a**). Also this has clearly shown the necessity of mutual proximity of these heteroatoms in the molecular skeleton for the activity. From Fig. 24, compounds **c** (3-benzoyl-2-(4-hydroxy-3-methoxyphenyl)thiazolidine), **d**, and **e** have been evaluated for their thromboxane A2 (TxA2) receptor antagonistic activity [164–166]. Pharmacologically thromboxane synthatase has a key role in the platelet aggregation and TxA2 is its potent stimulator [167]. The antagonists of TxA2 have an important place in the treatment of various circulatory disorders [168]. Also, these compounds are known to compete with the TxA2 for the same receptor site. Against this background some conformational mapping experiments between sulotroban and *o*-, *m*- and *p*-oxyacetic acid analogues of compound
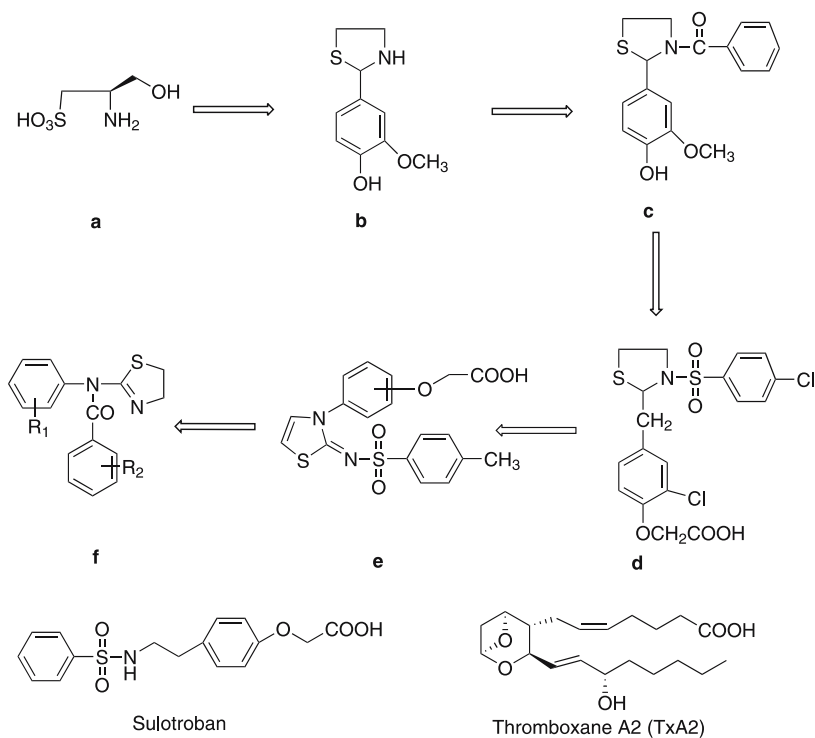
Fig. 24 *D*-Cysteinolic acid (**a**), sulotroban and thromboxane A2 (TxA2), in the development of different thiazoles (**b**–**f**) as TxA2 antagonists

e (Fig. 24) have been carried out to explore the spatial relationship between TxA2, sulotroban and the analogues of compound (e) (Fig. 24) [169]. Sulotroban (Fig. 24) is known to bind to the TxA2 receptor site in place of TxA2. For this study, in conformity with the active conformation of TxA2, the geometry of sulotroban has been considered in the form of a folded conformation [170]. This study has led Lacan et al. to suggest that the *m*-oxyacetic acid analogue of compound (e) maps the sulotroban structure space best
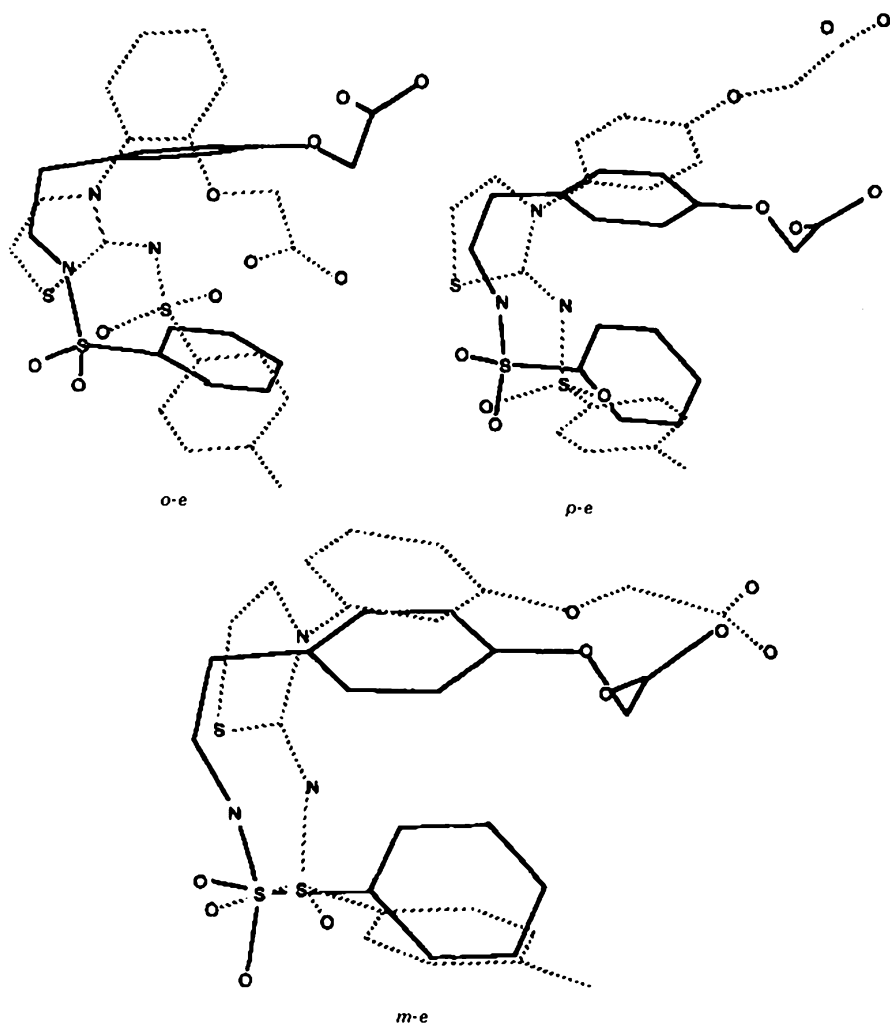
Fig. 25 Superimposition of selected minimum energy conformers of *o*-, *m*-, and *p*-phenoxy-acetic acid analogues of dihydrothiazoles (*o*-**e**, *p*-**e**, and *m*-**e**, shown in *dotted lines*) on the folded conformation of sulotroban (shown in *solid lines*) (Reprinted with permission from [169], Copyright 1999 Elsevier Paris.)

(Fig. 25) [169, 171]. This has signified the importance of the spatial disposition of the functional groups of these thiazolidines in deciding their TxA2 antagonistic activity.

Some 2-disubstituted amino-4,5-dihydrothiazoles (compound **f**, Fig. 24) have been reported to show in vivo antithrombotic activity. A QSAR study of these thiazoles (compound **f**, Fig. 24, Table 15) with the physicochemical parameters namely Hammett's sigma (σ) constant, dipole moment (μ) and Swain and Lupton's polarity ($\mathcal{F}$) constants of R_1 and R_2 substituent groups

Table 15   2-(*N*-aryl-*N*-aroyl)amino-4,5-dihydrothiazole derivatives in modeling the antithrombotic activity (comp. **f**, Fig. 23) [172]

No.	R_1	R_2	$\log(P/100 - P)$ [a]		
			obsd	cald [b]	cald [c]
1	2-CF$_3$	H	− 0.37	− 0.37	− 0.35
2	4-F	H	− 0.22	− 0.36	− 0.34
3	2,5(OMe)$_2$	H	− 0.37	− 0.33	− 0.32
4	2-Cl,6-Me	H	− 0.37	− 0.37	− 0.36
5	2-Me	H	− 0.60	− 0.50	− 0.46
6	2-CF$_3$	4-OMe	− 0.37	− 0.25	− 0.26
7	2-Me	4-OMe	− 0.37	− 0.38	− 0.36
8	2,5(OMe)$_2$	4-OMe	− 0.18	− 0.21	− 0.22
9	4-F	4-OMe	− 0.18	− 0.29	− 0.24
10	2-Cl,6-Me	2-Me	− 0.48	− 0.39	− 0.39
11	2-CF$_3$	2-Me	− 0.22	− 0.39	− 0.38
12	4-F	2-Me	− 0.37	− 0.37	− 0.37
13	4-OMe	2-Me	− 0.48	− 0.43	− 0.41
14	4-Et	4-Cl	− 0.18	− 0.14	− 0.34
15	2-Cl,6-Me	4-Cl	− 0.30	− 0.17	− 0.24
16	4-F	4-Cl	− 0.30	− 0.19	− 0.22
17	2-Me	2-Br	− 0.37	− 0.30	− 0.34
18	H	2-Br	− 0.18	− 0.29	− 0.33
19	2-Cl,6-Me	2-Br	− 0.22	− 0.18	− 0.24
20	2,5(OMe)$_2$	4-NO$_2$	− 0.12	− 0.03	− 0.01
21	4-NO$_2$	4-NO$_2$	0.00	0.02	0.03
22	4-F	4-NO$_2$	− 0.18	− 0.06	− 0.03
23	2-Me	4-NO$_2$	− 0.14	− 0.20	− 0.15
24	2-OMe	4-NO$_2$	0.00	− 0.11	− 0.08
25	4-Cl,3-NO$_2$	4-NO$_2$	0.26	0.14	0.13

[a] P is percent protection offered, in mice, to thrombotic challenge in comparison to inodmethacin
[b]   Eq. 25
[c]   Eq. 26

has resulted in the following equations [172].

$$\log(P/100 - P) = 0.301(0.076)\mathcal{F}R_1 + 0.447(0.072)\mathcal{F}R_2 - 0.485$$
$$n = 25, \quad r = 0.855, \quad s = 0.097, \quad F = 29.88 \tag{25}$$

$$\log(P/100 - P) = 0.254(0.079)\mathcal{F}R_1 - 0.074(0.012)\mu R_2 - 0.449$$
$$n = 25, \quad r = 0.850, \quad s = 0.099, \quad F = 28.56 \,. \tag{26}$$

On the basis of these results it has been suggested that electronic factors—Hammett's sigma (σ) constant, dipole moment (μ) and Swain and Lupton's polarity ($\mathcal{F}$)—are crucial for the antithrombotic activity of these compounds. Interestingly, in all the active compounds presented in Fig. 24 the arrangement of substituents around the thiazole skeleton is different from one another. This has further widened the scope of this skeleton in the exploration of potential platelet aggregation inhibitors and thromboxane A2 receptor antagonist.

3.3
Anti-infective Agents

3.3.1
Anti-HIV Agents

Thiazolidines are also known to selectively intercept the biochemical processes of the pathogenic organisms such as bacteria, virus, and fungi, in the host species. Thiazolidines introduction into the HIV/AIDS (Human Immunodeficiency Virus/Acquired Immune Deficiency Syndrome) therapy is due to 1-aryl-1H,3H-thiazolo[3,4-a]benzimidazole (TBZ) analogues (Fig. 26). Barreca et al. have modified the TBZ by opening its "B" ring to explore the thiazolidines namely 2-(2,6-dihalo phenyl)-3-(substituted pyridin-2-yl)-thiazolidin-4-ones (Table 16) as potential anti-HIV-1 RT agents [173].

In HIV type 1, the activity of all these compounds is due to inhibition of a key viral enzyme, reverse transcriptase (RT), necessary for the catalytic transformation of single-stranded viral RNA into the double-stranded linear DNA for incorporation into the host cell chromosomes [174]. The inhibitors of HIV-1 RT fall into two main classes. The first are termed nucleoside reverse transcriptase inhibitors (NRTIs). They mimic normal substrates of RT but lack the 3-$'$OH group required for DNA chain elongation, and cause premature termination of the growing viral DNA strand [175]. The second are termed non-nucleoside RT inhibitors (NNRTIs) and thiazolidine analogues belong to this class. They bind allosterically to a hydrophobic pocket close to the active site and achieve highly selective suppression of HIV-1 replication with little cytotoxicity to the host cells [176, 177]. Because of this considerable research efforts have been focused on the synthesis and structure-activity relationships of large numbers of different compounds as NNRTIs [178]. The
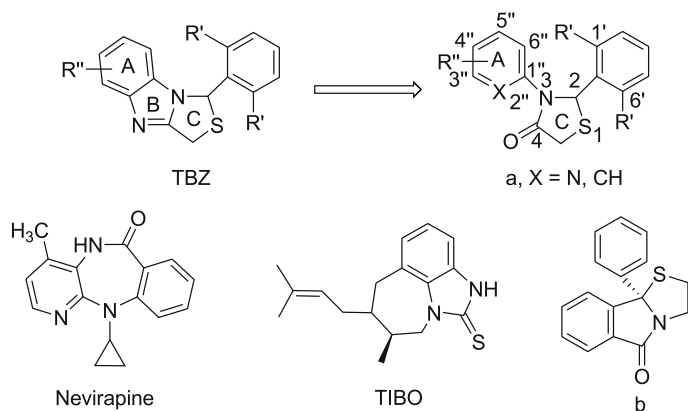
Fig. 26 Structures of TBZ, nevirapine, TIBO, (S)-(–)9b-phenyl-2,3-dihydrothiazolo[2,3-3]isoindol-5-(9bH)-one (**b**) and thiazolidin-4-ones associated with HIV-1 RT inhibitory activity

X-ray crystallographic studies of diverse NNRTIs/RT complexes have indicated that the NNRTIs, irrespective of their structure class, uniformly assume a "butterfly-like" shape in the receptor (Fig. 27) [179].

Barreca et al.'s modeling studies with 2-(2,6-dihalo phenyl)-3-(substituted pyridin-2-yl)-thiazolidin-4-ones (Fig. 26, Table 16) [173] in the GRID and AutoDock [180] programs in conjunction with nevirapine (Fig. 26) have suggested that (a) the binding mode of these thiazolidine analogues is similar to that of TBZ and other NNRTIs [173]; and (b) the aliphatic and aromatic binding regions of nevirapine match with the 2,3-diaryl moieties of thiazolidin-4-ones scaffold.

The QSAR of these compounds has been analyzed with the CP-MLR [51] procedure with physicochemical substituent constants [41] and several indicator parameters signifying their sub-structural features [181]. In this, the HIV-1 RT inhibitory activity of the compounds listed in Table 16 has been found to be correlated with the $CLOGP$, Swain and Lupton's resonance constant of the $4''$ position substituent ($\mathcal{R}_{4''}$) and some indicator parameters as shown.

$$-\log EC_{50} = 0.415(0.135)CLOGP - 1.414(0.136)I_{4''} + 5.377$$
$$n = 23, \quad r = 0.921, \quad Q^2 = 0.792, \quad s = 0.310, \quad F = 55.83 \tag{27}$$

$$-\log EC_{50} = 0.404(0.145)I_{2,3} - 1.327(0.141)I_{4''} + 6.668$$
$$n = 23, \quad r = 0.916, \quad Q^2 = 0.787, \quad s = 0.319, \quad F = 52.04 \tag{28}$$

$$-\log EC_{50} = 0.439(0.141)CLOGP + 9.141(0.925)\mathcal{R}_{4''} + 5.280$$
$$n = 23, \quad r = 0.914, \quad Q^2 = 0.775, \quad s = 0.323, \quad F = 50.67. \tag{29}$$

Table 16 2-(2,6-Dihalophenyl)-3-(substituted pyridin-2-yl)-thiazolidin-4-ones analogues in modeling the HIV-1 RT inhibitory activity (comp. **a**, X = N, Fig. 26) [181]

No.	R''				R'		$-\log EC_{50}$ [a]	
	$6''$	$3''$	$5''$	$4''$	$2'$	$6'$	obsd	cald [b]
1	H	H	H	H	Cl	Cl	6.75	6.89
2	H	H	H	H	Cl	F	6.55	6.70
3	H	H	H	H	F	F	6.07	6.53
4	H	H	H	Cl	Cl	Cl	5.75	5.77
5	H	H	H	Cl	Cl	F	5.67	5.56
6	H	H	H	Cl	F	F	5.14	5.41
7	H	H	H	Br	Cl	Cl	5.82	5.83
8	H	H	H	Br	Cl	F	5.91	5.64
9	H	H	H	Br	F	F	5.31	5.47
10	H	Br	H	H	Cl	Cl	6.56	7.24
11	H	Br	H	H	Cl	F	7.19	7.06
12	H	Br	H	H	F	F	7.52	6.88
13	Me	H	H	H	Cl	Cl	–	
14 [c]	Me	H	H	H	F	F	4.27	
15	H	H	Me	H	Cl	Cl	6.83	7.12
16	H	H	Me	H	Cl	F	7.00	6.94
17	H	H	Me	H	F	F	6.60	6.76
18	H	H	H	Me	Cl	Cl	5.85	5.71
19	H	H	H	Me	F	F	5.29	5.34
20	H	Me	H	H	Cl	Cl	7.36	7.12
21	H	Me	H	H	Cl	F	7.27	6.93
22	H	Me	H	H	F	F	7.08	6.76
23	H	Me	Me	H	Cl	Cl	7.04	7.35
24	H	Me	Me	H	Cl	F	7.38	7.17
25	H	Me	Me	H	F	F	7.23	6.99

[a] 50% Inhibitory concentration against cytopathic effect of HIV-1 in MT-4 cells
[b] Eq. 27
[c] Not included in the analysis

In these equations the indicator variable $I_{4''}$ has been defined for the $4''$-substituent of the 3-(pyridin-2-yl) moiety (zero for hydrogen and one otherwise) of thiazolidinones (Fig. 26). Also, in these compounds the HIV-1 RT inhibitory activity has been linked to their ability to assume a butterfly-like shape in the receptor. Collectively, the substituents of 2- and 3-aryl moieties of these compounds promote this molecular shape. In this connection, the indicator parameter $I_{2,3}$ has been introduced to address the collective steric features of the 2- and 3-aryl moieties of these compounds. In this, $I_{2,3}$ has been defined to take a value of "one" if any one substituent at $2'$- or $6'$- of the 2-phenyl moiety or at the $3''$- or $5''$- positions of the 3-(pyridin-2yl) moiety is larger than hydrogen and "zero" otherwise. These equations, while favor-
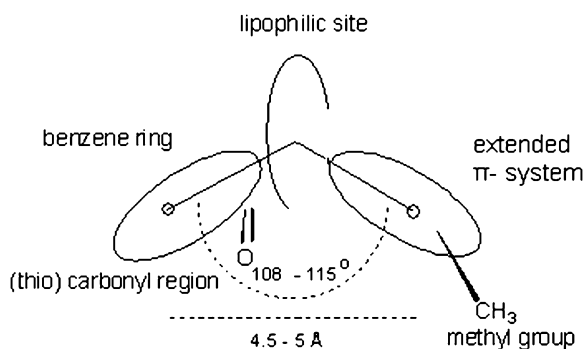
Fig. 27 The "butterfly like model" derived from the common 3D superimposition of 4,5,6,7-tetrahydro-5-methylimidazo[4,5,1-jk][1,4]benzodiazepin-2(1H)-ones (**TIBO**), Nevirapine and (S)-(–)9b-phenyl-2,3-dihydrothiazolo[2,3-3]isoindol-5-(9bH)-one (compound **b**, Fig. 25) (Reprinted with permission from [179]. Copyright 1993 American Chemical Society)

ing hydrophobic compounds, have clearly suggested that an unsubstituted 4″-position or a 4″-position substituent with a positive resonance contribution would be preferred for the HIV-1 RT inhibitory activity. The positive regression coefficient of $I_{2,3}$ has suggested the preference for substitution at one or more positions of the 2′, 6′ of 2-phenyl and/or 3″, 5″ positions of the 3-(pyridin-2yl) moiety, hence favoring the butterfly-like or an out of plane arrangement for the 2- and 3-aryl moieties. In these compounds a dual role has been assigned to the 3″-, 5″-position substituents of the 3-(pyridin-2yl) moiety (Fig. 26) in terms of providing a driving force to move the 3-pyridyl moiety to an out of plane arrangement with respect to the thiazolidinone nucleus and to fulfil hydrophobic and steric requirements at the receptor sites. The following regression equations have been derived to explain the HIV-1 RT inhibitory activity of 2-(2,6-dihalophenyl)-3-(substituted phenyl)-thiazolidin-4-ones (Fig. 26, Table 17) alone (Eq. 30) and in combination with 2-(2,6-dihalophenyl)-3-(substituted pyridin-2-yl)-thiazolidin-4-ones (Fig. 26 Table 16) (Eqs. 31 and 32) [181].

$$- \log EC_{50} = 0.454(0.100)\pi_{(2'+6')} + 0.168(0.060)MR_{3''}$$
$$- 0.014(0.005)(MR_{3''})^2 - 0.948(0.192)\mathcal{F}_{3''}$$
$$- 0.942(0.212)\mathcal{R}_{(3''+5'')} + 5.655$$

$$n = 28, \quad r = 0.867, \quad Q^2 = 0.620, \quad s = 0.247, \quad F = 13.38 \tag{30}$$

$$- \log EC_{50} = 0.356(0.080)ClogP - 0.732(0.259)\mathcal{R}_{(3''+5'')}$$
$$- 1.306(0.145)I_{4''} + 0.866(0.116)I_{2''} + 4.615$$

$$n = 51, \quad r = 0.861, \quad Q^2 = 0.695, \quad s = 0.319, \quad F = 33.12 \tag{31}$$

Table 17 2-(2,6-Dihalophenyl)-3-(substituted phenyl)-thiazolidin-4-ones analogues in modeling the HIV-1 RT inhibitory activity (comp. **a**, X = CH, Fig. 26) [181]

No.	R''		R'		$-\log EC_{50}$ [a]	
	3'	5'	2'	6'	obsd	cald[b]
26	H	H	Cl	Cl	6.40	6.46
27	H	H	F	F	5.64	5.94
28	Br	H	Cl	Cl	6.21	6.40
29	Br	H	Cl	F	6.19	6.14
30	Br	H	F	F	5.88	5.88
31	Cl	H	Cl	Cl	6.51	6.54
32	Cl	H	Cl	F	6.21	6.28
33	Cl	H	F	F	6.69	6.02
34	Me	H	Cl	Cl	7.09	6.95
35	Me	H	Cl	F	6.67	6.69
36	Me	H	F	F	6.16	6.43
37	Et	H	Cl	Cl	6.81	6.88
38	Et	H	Cl	F	6.67	6.34
39	Et	H	F	F	6.11	6.08
40	MeO	H	Cl	Cl	6.71	6.74
41	MeO	H	Cl	F	6.52	6.71
42 [c]	MeO	H	F	F	4.93	5.65
43	NO_2	H	Cl	Cl	6.14	5.95
44	NO_2	H	Cl	F	5.88	5.71
45	NO_2	H	F	F	5.26	5.45
46	Cl	Cl	Cl	Cl	6.55	6.65
47	Cl	Cl	Cl	F	6.50	6.42
48	Cl	Cl	F	F	6.01	6.17
49	F	F	Cl	Cl	6.89	7.02
50	F	F	Cl	F	6.61	6.42
51	F	F	F	F	6.27	6.16
52	Me	Me	Cl	Cl	6.72	6.72
53	Me	Me	Cl	F	7.06	6.81
54	Me	Me	F	F	6.62	6.55

[a] 50% Inhibitory concentration against cytopathic effect of HIV-1 in MT-4 cells
[b] Eq. 30
[c] Not included in the analysis

$$-\log EC_{50} = 0.363(0.081)ClogP - 0.738(0.264)\mathcal{R}_{(3''+5'')}$$
$$+ 8.424(0.960)\mathcal{R}_{4''} + 0.883(0.118)I_{2''} + 4.585$$
$$n = 51, \quad r = 0.856, \quad Q^2 = 0.684, \quad s = 0.325, \quad F = 31.69 . \tag{32}$$

All these regression equations suggested that the hydrophobic compounds provide better inhibitory activity. Moreover, they have displayed the influence

of polar/inductive effects of the $3''$- and $5''$-position substituents on the activity. The positive regression coefficient of $I_{2''}$ ["one" for 3-(pyridine-2-yl) and "zero" for 3-phenyl] in Eqs. 31 and 32 has suggested the advantage of 3-pyridyls over 3-phenyls for better inhibition of HIV-1 RT. A better blend of polarity, electronic, and hydrophobic features in 3-pyridyls, compared to the corresponding phenyl analogue, has been attributed as one reason for these compounds' improved activity. Furthermore, in the PLS analysis of the total compounds shown in Tables 16 and 17, the descriptor $I_{2''}$ has emerged as the single largest contributing descriptor and thereby suggested the importance of the 3-(pyridine-2-yl) moiety when compared to the 3-phenyl moiety in HIV-1 RT inhibition. This has further suggested that the varying centers of this molecule have almost uniform influence on the activity [181].

In addition to the physicochemical domain, the topological features of selected HIV-1 RT inhibitors, 2-(2,6-dihalophenyl)-3-(substituted pyridin-2-yl)-thiazolidin-4-ones (Fig. 26, Table 16), have been analyzed [182] with the empirical, constitutional, and graph theoretical descriptors from the DRAGON software package [47]. This study has resulted in the identification of several influential descriptors to model the inhibitory activity and the equations shown below represent some models stemming from these descriptors.

$$- \log EC_{50} = - 1.874(0.228)AECC - 300.003(30.650)PW3 + 126.245$$
$$n = 24, \quad r = 0.941, \quad Q^2 = 0.855, \quad s = 0.308, \quad F = 80.89 \tag{33}$$

$$- \log EC_{50} = - 263.490(24.496)JGI4 + 8.236(0.923)GGI7 + 21.831$$
$$n = 24, \quad r = 0.944, \quad Q^2 = 0.859, \quad s = 0.301, \quad F = 85.39 \tag{34}$$

$$- \log EC_{50} = 4.462(1.314)MATS3v - 1.037(0.103)GATS8e + 9.191$$
$$n = 24, \quad r = 0.931, \quad Q^2 = 0.824, \quad s = 0.331, \quad F = 68.59 . \tag{35}$$

Equation 33 with AECC (the average eccentricity of the topological graph) and PW3 (Randic's molecular shape descriptor representing the path/walk-3 ratio) represents a model from the simple topological descriptors, Eq. 34 with JGI4 (mean topological charge index of order 4) and GGI7 (topological charge index of order 7) represents a model from the Galvez topological charge descriptors, and Eq. 35 with MATS3v (Moran autocorrelation lag three weighed by atomic volumes) and GATS8e (Geary autocorrelation lag eight weighed by electronegativity) represents a model from the 2D autocorrelation descriptors of the compounds. These equations have prompted us to suggest that less extended or compact saturated structural templates would be better for the activity. Also, the participation of Galvez topological charge descriptors have indicated the importance of fourth and seventh eigenvalues of the polynomial of the corrected adjacency matrix of the compounds' charge indices. The 2D autocorrelation descriptors have suggested the role of three and eight centered structural fragments of the compounds in the activity information. In

terms of predictivity these equations have fared better than those involving physicochemical descriptors alone [182]. However, the topological models are more complex in nature when compared to physicochemical descriptors.

Roy and Leonard [183] have also presented QSAR models for the HIV-1 RT inhibitory activity of the thiazolidinones listed in Tables 16 and 17 along with some more similar analogues (Table 18) [184–187] using the hydrophobicity and molar refractivity, quantum chemical and topological and indicator parameters as descriptors. In this, the 3-pyridyls/phenyls (Tables 16 and 17) and 3-(pyrimidin-2-yls) (Table 18) [186] have become part of the dataset. Additionally, four compounds with the thiazolidin-4-thione nucleus have been included in the dataset. In Fujita-Ban [188] and mixed (Hansch and Fujita-Ban) approaches 7 to 17 descriptor models have been discovered for the cytopathicity effect (EC_{50}) and cytotoxic effect (CC_{50}) of the compounds. The following equations show the minimum descriptor models for each activity from this study.

$$-\log EC_{50} = 0.307(0.090)S_{sssC} - 0.079(0.056)S\_aasC$$
$$+ 0.837(0.291)\pi_{3''} - 1.363(0.355)E6 + 2.729(1.074)E10$$
$$- 1.293(0.389)E18 + 6.663(4.395)D1 - 1.339(0.732)I_{N_Z}$$
$$- 0.490(0.203)N_{Me_{RR1}} - 0.501(0.508)I_{MeO_{R3}}$$
$$- 1.847(0.708)I_{Me_{R4}} - 1.171(0.700)I_{Me_{R6}}$$
$$- 2.103(0.435)I_{Me_{R7}} - 19.634(13.581)$$
$$n = 66, \quad r = 0.911, \quad Q^2 = 0.504, \quad s = 0.334, \quad F = 19.60 \tag{36}$$

$$-\log CC_{50} = 0.051(0.048)S\_ssssC - 0.035(0.028)S\_ssO$$
$$+ 0.066(0.044)S\_sBr + 0.788(0.676)\pi_{2'+6'}$$
$$- 0.360(0.379)\pi^2_{2'+6'} + 0.320(0.339)I_{N-W}$$
$$- 0.253(0.114)I_{N-X} - 0.332(0.126)N_{Me-2'6'}$$
$$- 0.362(0.339)I_{Cl-R4'} + 1.144$$
$$n = 83, \quad r = 0.809, \quad Q^2 = 0.544, \quad s = 0.230, \quad F = 13.6 . \tag{37}$$

In terms of the common structural components, Roy and Leonard's [183] observations have been in good agreement with the previous QSAR and modeling studies [181, 182]. Additionally, they have suggested that the thiazolidin-4-one nucleus is a preferred one when compared to thaizolidin-4-thione for the activity. Also, it has been noted that a methyl group at the 5- and 3'-positions is detrimental to the activity, and both the 3-(pyridin-2-yl) and 3-(pyrimidin-2-yl) moieties are preferred for HIV-1 RT inhibitory activity.

In a follow-up of our modeling studies on thiazolidine-based HIV-1 RT inhibitors, we have synthesized some thiazolidin-4-ones, metathiazanones for this activity. The QSAR studies of these compounds with physicochemical and quantum chemical descriptors have highlighted the importance of PMIZ

Table 18 2,3-Disubstituted-thiazolidin-4-ones in modeling the HIV-1 RT inhibitory activity (comp. a, Fig. 26) [183] [a]

| No. | R'' | | | | | R' | | $\log EC_{50}$ [b] | | $-\log EC_{50}$ [c] | |
	2''	3''	4''	5''	6''	2'	6'	obsd	cald [d]	obsd	cald [e]
1	H	Me	H	H	H	Me	Me	–	–	1.44	1.19
2	Cl	Me	H	H	H	F	CF_3	–	–	1.49	1.52
3	Me	Me	H	H	H	Cl	F	2.83	3.25	1.39	1.75
4	H	Me	H	H	H	MeO	MeO	2.72	2.45	0.68	0.54
5	H	H	H	H	H	F	F	–	–	1.45	1.61
6	H	H	H	H	H	Cl	Cl	–	–	1.51	1.70
7 [f]	H	Me	H	H	H	F	MeO	2.94	2.67	0.84	1.13
8	Cl	H	H	Me	H	F	CF_3	2.67	2.42	1.03	0.89
9	H	H	H	Me	H	MeO	MeO	2.48	2.72	0.60	0.53
10	H	Me	H	H	H	Me	Me	2.81	2.49	0.55	0.69
11	Cl	Me	H	H	H	F	CF_3	2.52	2.84	0.92	0.91
12	Me	Me	H	H	H	Cl	F	4.30	3.75	1.42	1.35
13	H	Me	H	H	H	MeO	MeO	2.87	3.16	0.62	0.49
14	H	Br	H	H	H	Me	Me	2.20	2.69	0.57	0.92
15 [f]	H	Br	H	H	H	F	MeO	4.47	3.62	1.00	0.80
16	Cl	Br	H	H	H	F	CF_3	3.18	2.93	1.06	1.13
17	Me	Br	H	H	H	Cl	F	3.46	3.91	1.68	1.52
18	H	Me	H	Me	H	Me	Me	2.36	2.38	–	–
19	H	Me	H	Me	H	F	MeO	3.70	3.39	–	–
20	Cl	Me	H	Me	H	F	CF_3	2.23	2.76	0.79	0.90
21	Me	Me	H	Me	H	Cl	F	3.63	3.67	1.45	1.35
22	H	Me	H	Me	H	MeO	MeO	2.95	3.14	0.51	0.71
23	H	Me	H	H	H	F	F	2.19	2.60	1.41	1.31
24	H	Br	H	H	H	F	F	3.24	2.81	1.51	1.51
25 [f]	H	H	H	Me	H	F	MeO	3.06	3.11	–	–
26 [f]	H	Me	H	H	H	F	MeO	3.54	3.46	0.78	1.70
27	H	Br	H	H	H	F	MeO	2.67	2.42	1.03	0.891
28 [f]	H	H	H	H	Cl	F	F	–	–	1.53	1.36
29 [f]	H	H	H	Me	H	Cl	F	–	–	1.47	1.22
30 [f]	H	H	H	H	Me	F	F	–	–	0.70	1.03
31	H	Me	H	H	H	F	F	2.47	2.14	1.58	1.03

[a] Compounds shown are additional to those listed in Tables 16 and 17; comp. 1–7, 3-phenyls; comp. 8–30, 3-(pyridin-2-yl); comp. 31–35, 3-(pyridin-2-yl) with methyl at C5 of thiazolidine-4-one; comp. 36–38, 3-(pyridin-3-yl); comp. 39 and 40, 3-(pyridin-4-yl); comp. 41–49, 3-(pyrimidin-2-yl)
[b] 50% Inhibitory concentration against cytopathic effect of HIV-1 in MT-4 cells
[c] Concentration required to reduce 50% viability of MT-4 cells
[d] Eq. 36
[e] Eq. 37
[f] Test set compound

Table 18 (continued)

No.	R'' 2''	3''	4''	5''	6''	R' 2'	6'	log EC$_{50}$ [b] obsd	cald [d]	– log EC$_{50}$ [c] obsd	cald [e]
32	H	Me	H	H	H	Cl	Cl	2.42	2.62	1.05	1.35
33	H	Me	H	Me	H	F	F	2.51	2.83	1.45	1.35
34	H	Me	H	H	H	Cl	Cl	2.88	2.68	0.85	1.28
35 [f]	H	Me	H	Me	H	F	F	2.69	1.46	1.43	1.04
36	H	H	H	–	H	F	F	1.02	1.02	–	–
37	H	H	H	–	H	Cl	Cl	–	–	1.63	1.45
38 [f]	H	H	H	–	H	Cl	Cl	–	–	1.63	1.45
39	H	H	H	H	–	Cl	Cl	–	–	2.00	1.93
40	H	H	H	H	–	F	F	–	–	1.47	1.54
41	H	Me	–	H	H	F	F	3.41	3.57	–	–
42	H	Me	–	H	H	Me	Me	2.47	2.29	0.71	0.47
43	H	Me	–	H	H	F	MeO	3.27	3.46	0.50	0.76
44	Cl	Me	–	H	H	F	CF$_3$	3.04	2.70	0.72	0.67
45	Me	Me	–	H	H	Cl	F	3.11	3.50	0.81	1.16
46 [f]	H	Me	–	H	H	MeO	MeO	3.04	3.07	0.64	0.34
47	H	Me	–	Me	H	Cl	Cl	4.23	4.07	1.36	1.12
48	H	Me	–	H	H	Cl	Cl	3.55	3.18	1.61	1.49
49	H	Me	–	Me	H	F	F	2.19	2.58	1.35	1.21

[a] Compounds shown are additional to those listed in Tables 16 and 17; comp. 1–7, 3-phenyls; comp. 8–30, 3-(pyridin-2-yl); comp. 31–35, 3-(pyridin-2-yl) with methyl at C5 of thiazolidine-4-one; comp. 36–38, 3-(pyridin-3-yl); comp. 39 and 40, 3-(pyridin-4-yl); comp. 41–49, 3-(pyrimidin-2-yl)
[b] 50% Inhibitory concentration against cytopathic effect of HIV-1 in MT-4 cells
[c] Concentration required to reduce 50% viability of MT-4 cells
[d] Eq. 36
[e] Eq. 37
[f] Test set compound

(moment of inertia Z-component), $\log P_{(o/w)}$ and MNDO$_{dipole}$ in the HIV-1 RT inhibitory activity (comp. **a** and **b** Fig. 28, Table 19; comp. **c** Fig. 28, Table 20) [189, 190]. In these models, Eq. 38 has been derived for thiazolidin-4-ones, metathiazanones (Table 19) and Eq. 39 has been derived for thiazolidin-4-ones with the furfuryl moiety in place of pyridyl at N3 (Table 20).

$$– \log EC_{50} = – 0.0018(0.0003)PMIZ + 10.702$$
$$n = 5, \quad r = 0.950, \quad Q^2 = 0.573, \quad s = 0.297, \quad F = 27.91 \tag{38}$$

$$– \log EC_{50} = 1.479(0.206) \log P_{(o/w)} + 0.649(0.114)\text{MNDO\_dipole} – 1.191$$
$$n = 15, \quad r = 0.920, \quad Q^2 = 0.742, \quad s = 0.501, \quad F = 33.60. \tag{39}$$
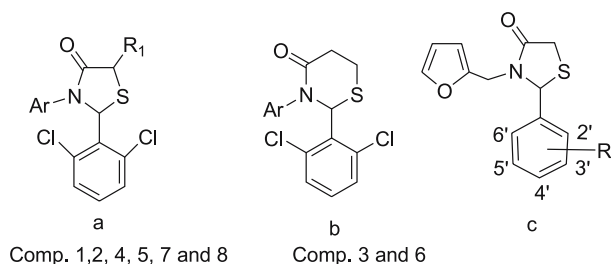
Fig. 28 Thiazolidin-4-ones and related analogues explored for HIV-1 RT inhibitory activity

Table 19 Physicochemical properties and HIV-1RT inhibitory activity of thiazolidin-4-one and metathiazanone derivatives (comp. **a** and **b**, Fig. 28) [189]

No.	Ar	R	PMIZ	$-\log EC_{50}$ [a] obsd	cald [b]
1	pyridin-2-yl	Me	2550.89	–	6.09
2	pyridin-3-yl methyl	H	3200.88	4.81	4.92
3	pyridin-3-yl methyl	H	3284.88	5.18	4.77
4	pyridin-3-yl methyl	Me	3307.00	4.56	4.73
5	furan-2-yl methyl	H	2273.00	6.69	6.60
6	furan-2-yl methyl	H	2894.60	5.25	5.47
7	furan-2-yl methyl	Me	2963.52	–	5.35
8	pyridin-2-yl	H	2573.53	–	6.05

[a] 50% Inhibitory concentration against cytopathic effect of HIV-1 in MT-4 cells
[b] Eq. 38

In this study thiazolidin-4-ones have been found to retain the activity even with the introduction of a furfuryl moiety in place of pyridyl at N3. This has expanded the nature and scope of the chemical space around the thiazolidin-4-one nucleus (comp. **c**, Fig. 28, Table 20) [190].

3.3.2
Antifungal Agents

The antifungal activity of azoles, the emergence of opportunistic fungal infections due to AIDS, and economic considerations of agro and food industry has generated considerable momentum to discover and explore other prototypes for the chemotherapy of fungal diseases. In this context, some thiazolidines, thiazoles, and thiadiazoles have been found to display antifungal activity against different human and plant pathogenic fungi.

Table 20 Physicochemical properties and HIV-1RT inhibitory activity of thiazolidin-4-one derivatives (comp. **c** Fig. 28) [190]

No.	R					Log $P_{(o/w)}$	MNDO _dipole	$-\log EC_{50}$ [a] obsd	cald [b]
	2'	3'	4'	5'	6'				
1	Cl	H	H	H	Cl	3.49	3.17	6.69	6.02
2	F	H	H	H	F	2.61	3.76	5.54	5.10
3	Cl	H	H	H	F	3.33	4.46	6.24	6.63
4	H	H	Cl	H	H	2.90	1.78	4.06	4.25
5	Cl	H	H	H	H	2.90	3.38	5.19	5.28
6	H	Cl	H	Cl	H	3.60	0.78	4.07	4.64
7	OMe	H	H	H	H	2.26	3.15	3.94	4.19
8	H	H	OMe	H	H	2.26	3.22	3.77	4.24
9	OMe	H	OMe	OMe	H	2.00	2.42	3.28	3.33
10	H	OMe	OMe	OMe	H	1.75	2.84	3.15	3.24
11	OMe	H	OMe	H	OMe	2.24	0.01	4.86	4.85
12	Me	H	H	H	H	2.60	2.21	4.54	4.09
13	Me	H	H	H	Me	2.90	2.21	5.11	4.53
14	F	F	F	F	F	3.06	1.04	4.33	4.01
15	1-Naphthyl					3.53	2.47	5.26	5.62

[a] 50% Inhibitory concentration against cytopathic effect of HIV-1 in MT-4 cells
[b] Eq. 39

In an exploratory study, some 2,3,4-substituted thiazolidines (Fig. 29; Table 21) have been discovered to show a broad spectrum in vitro antifungal activity against human pathogenic fungi namely *Candida albicans* (CA), *Cryptococcus neoformans* (CN), *Tricophyton mentagrophyte* (TM), and *Aspergillus fumigatus* (AF) [191]. The antifungal activities of these compounds have been analyzed in 2D- and 3D-QSAR studies to map the activity and to identify the common pharmacophore for the design of broad spectrum antifungals. The Apex-3D module of InsightII [69] has been put to use in the 3D-QSAR analysis. The following 3D-QSAR equations have emerged from molecular superimposition patterns based on three-biophoric sites of these compounds for their activity against the fungal strains CN, TM, and AF, respectively (Fig. 30).

$$
\begin{aligned}
-\log \text{MIC(CN)} = \ & 0.013(0.002)\text{TREF} - 0.427(0.079)\text{I}R_m \\
& + 4.475(1.593)\pi_a(\text{ss1}) + 0.099(0.041)\text{REF}_a(\text{ss2}) \\
& - 0.095(0.026)\text{REF}_a(\text{ss3}) - 0.102(0.037)\text{REF}_a(\text{ss4}) \\
& + 0.356(0.090)\text{I-Ring(ss5)} - 0.026
\end{aligned}
$$

$$ n = 50, \quad r = 0.808, \quad s = 0.197, \quad F = 11.26 \tag{40} $$
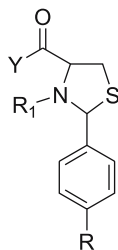
Fig. 29 General structure of 2,3,4-substituted thiazolidines associated with antifungal activity

$$-\log \text{MIC(TM)} = 0.005(0.001)\text{TREF} - 0.485(0.115)\pi_a(\text{ss1})$$
$$- 0.058(0.015)\text{REF}_a(\text{ss2}) - 0.027(0.012)\text{REF}_a(\text{ss3})$$
$$- 0.064(0.016)\text{REF}_a(\text{ss4}) + 0.080(0.027)\text{REF}_a(\text{ss5})$$
$$+ 0.452$$
$$n = 53, \quad r = 0.805, \quad s = 0.145, \quad F = 14.11 \tag{41}$$

$$-\log \text{MIC(AF)} = -0.419(0.135)\text{HA}(\text{ss1}) - 0.261(0.138)\text{HA}(\text{ss2})$$
$$- 0.362(0.090)\text{HA}(\text{ss3}) + 0.420(0.141)\text{HD}(\text{ss4})$$
$$+ 2.594(0.522)\pi_a(\text{ss5}) - 0.313(0.150)\pi_a(\text{ss6})$$
$$+ 0.130(0.034)\text{REF}_a(\text{ss7}) + 1.086$$
$$n = 36, \quad r = 0.841, \quad s = 0.119, \quad F = 9.63 . \tag{42}$$

In development of these equations, for the 3D-molecular superimpositions, the carbonyl oxygen in the vicinity of C4, S1, N3, the oxygen of t-butyloxycarbonyl or the benzoyl group attached to N3 and/or the C2-phenyl moiety of thiazolidines have provided the biophoric sites (Fig. 30). The parameters of these equations represent global attributes of the compounds (global parameters—TREF, total refractivity; IR_m, the nature of the meta-substituent of the C2-phenyl moiety) and/or conformational dependent attributes from the molecular superimposition pattern (secondary sites or ss; descriptors identified with suffix "ss"). In 3D-QSAR studies, all the secondary sites are local to each equation. They are conformation sensitive and location specific in the 3D-structure space. In these equations π_a, REF_a, I-Ring, HA and HD addressed the hydrophobicity, refractivity, aromatic ring indicator, H-acceptor and H-donor properties, respectively, of atoms or groups (secondary sites) at the predefined locations in the 3D space of corresponding models (Fig. 30). These equations have led to the suggestion that AF is sensitive to the structural and conformational features of the compounds. Figure 31 provides a composite 2D-representation of the biophoric and secondary sites pattern of the thiazolidines 3D-equations (Fig. 30; Eqs. 40 to 42).
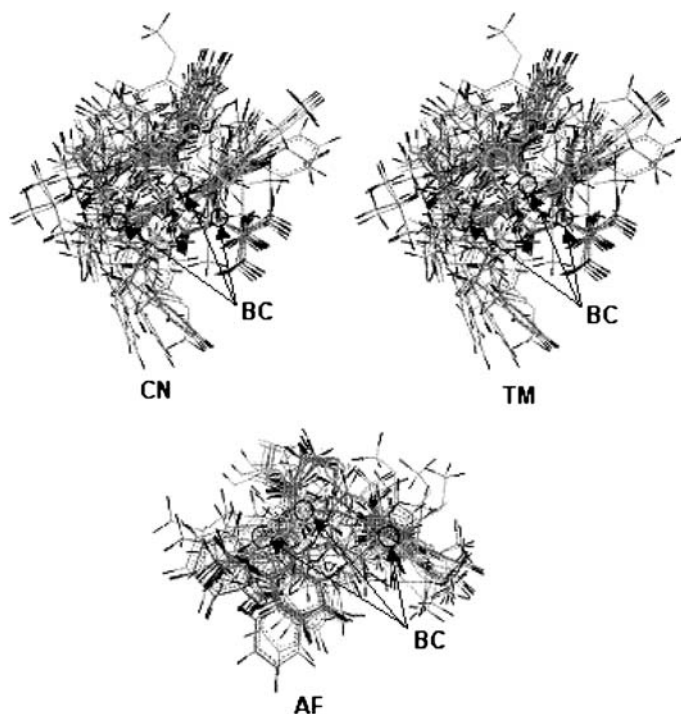
Fig. 30 Apex3D QSAR models of thiazolidines (Table 21) for their activity against *Cryptococcus neoformans* (CN) (Eq. 40), *Tricophyton mentagrophyte* (TM) (Eq. 41), and *Aspergillus fumigatus* (AF) (Eq. 42). In the molecular superimposition, *circles identified with arrows* represent the locations of the biophoric centers (BC)

A fundamental difference between 3D- and a 2D-QSAR equation is the non-existence of conformational dependent secondary sites in the latter. Hence, a direct transposition of 3D- and 2D-models is not always possible but the global properties of the chemical structures, if relevant to the activity, may show their presence in both of them. Moreover, in a broader perspective, all 2D-QSAR parameters—physicochemical as well as structural—can be considered as one or the other form of global descriptors. In light of this, to bridge the 2D- and 3D-features the following 2D-QSAR equations have been derived for the antifungal activity of 2,3,4-substituted thiazolidines (Table 21).

$$-\log \mathrm{MIC(CN)} = 0.011(0.003)MRR_2 + 0.751(0.162)\mathrm{Vw}R_1$$
$$- 0.335(0.061)\mathrm{I}R_m + 0.706$$
$$n = 41, \quad r = 0.800, \quad s = 0.187, \quad F = 21.86 \tag{43}$$

Table 21 Physicochemical properties and antifungal activity of 2,3,4-substituted thiazolidines (Fig. 29) [191]

No.	R^a	R_1^b	TREF	FR_p	σR_p	VwR_1	MRR_2	$-\log MIC^c$ CN obsd	TM obsd	cald^d	AF obsd	cald^e	CA obsd	cald^f
1	H	H	55.6	0.00	0.00	0.02	0.00	0.62	0.62	0.74	I		I^g	
2	Cl	H	60.4	0.41	0.23	0.02	0.00	I	0.69	0.75	I		I	
3	F	H	55.8	0.43	0.06	0.02	0.00	0.74	0.74	0.72	I		I	
4	OH	H	57.3	0.29	−0.37	0.02	0.00	I	I		I		I	
5	OMe	H	62.0	0.26	−0.27	0.02	0.00	I	I		I		I	
6	$	H	68.5	0.00	0.00	0.02	0.00	I	I		I		I	
7	£	H	75.0	0.26	−0.27	0.02	0.00	I	0.78	0.82	I		I	
8	H	¥	80.2	0.00	0.00	0.90	0.00	1.39	0.79	0.72	1.09	1.09	0.49	0.50
9	Cl	¥	85.0	0.41	0.23	0.90	0.00	1.44	0.84	0.75	0.84	0.82	0.54	0.54
10	F	¥	80.4	0.43	0.06	0.90	0.00	0.82	0.82	0.72	I		0.51	0.52
11	OH	¥	81.9	0.29	−0.37	0.90	0.00	0.81	0.81	0.73	I		0.51	0.52
12	OMe	¥	86.6	0.26	−0.27	0.90	0.00	1.43	0.53	0.79	0.83	0.83	0.53	0.53
13	$	¥	93.1	0.00	0.00	0.90	0.00	0.87	1.17	0.89	I		0.57	0.56
14	£	¥	99.5	0.26	−0.27	0.90	0.00	0.83	0.83	0.82	I		0.53	0.53
15	H	§	84.9	0.00	0.00	0.78	0.00	1.40	0.80	0.58	1.10	1.12	0.50	0.51
16	Cl	§	89.7	0.41	0.23	0.78	0.00	1.14	0.84	0.89	0.84	0.82	0.54	0.54

^{a} $, £ Correspond to 2,5-dimethoxy and 3,4,5-trimethoxy, respectively

^{b} ¥, § Correspond to CO_2-t-Bu and COPh, respectively

^{c} Minimum inhibitory concentration in NCCLS protocol

^{d} Eq. 41

^{e} Eq. 42

^{f} Eq. 46

^{g} Inactive under test conditions

Table 21 (continued)

No.	R^a	$R_1{}^b$	TREF	FR_p	σR_p	VwR_1	MRR_2	$-\log MIC^c$ CN obsd	TM obsd	cald^d	AF obsd	cald^e	CA obsd	cald^f
17	F	§	85.1	0.43	0.06	0.78	0.00	0.82	0.82	0.86	I		0.52	0.52
18	OMe	§	91.4	0.26	-0.27	0.78	0.00	1.44	0.54	0.67	0.84	0.87	0.54	0.54
19	$	§	97.8	0.00	0.00	0.78	0.00	1.17	0.57	0.70	1.17	1.15	0.57	0.57
20	£	§	104.3	0.26	-0.27	0.78	0.00	0.91	0.91	0.96	I		0.60	0.60
21	H	¥	97.5	0.00	0.00	0.90	1.03	1.18	0.88	0.92	1.18	1.08	0.58	0.58
22	H	§	102.3	0.00	0.00	0.78	1.03	1.19	0.58	0.45	0.88	0.92	0.58	0.58
23	Cl	¥	102.3	0.41	0.23	0.90	1.03	1.52	0.92	0.95	0.92	1.10	0.62	0.61
24	Cl	§	107.1	0.41	0.23	0.78	1.03	1.22	0.92	1.10	0.92	1.06	0.62	0.62
25	F	¥	97.7	0.43	0.06	0.90	1.03	I	0.90	0.92	I		0.60	0.59
26	F	§	102.5	0.43	0.06	0.78	1.03	1.51	0.60	0.53	0.90	1.07	0.60	0.60
27	OMe	¥	104.0	0.26	-0.27	0.90	1.03	1.52	0.91	0.95	0.91	1.10	0.61	0.61
28	OMe	§	108.7	0.26	-0.27	0.78	1.03	1.52	0.92	0.98	1.22	0.91	0.62	0.61
29	$	¥	110.5	0.00	0.00	0.90	1.03	0.94	0.94	0.98	I		0.64	0.64
30	$	§	115.2	0.00	0.00	0.78	1.03	0.95	1.55	1.16	I		0.65	0.64
31	£	¥	116.9	0.26	-0.27	0.90	1.03	0.97	1.27	1.00	I		0.67	0.67
32	£	§	121.7	0.26	-0.27	0.78	1.03	0.98	0.98	1.18	I		0.68	0.67

[a] $, £ Correspond to 2,5-dimethoxy and 3,4,5-trimethoxy, respectively

[b] ¥, § Correspond to CO_2-t-Bu and COPh, respectively

[c] Minimum inhibitory concentration in NCCLS protocol

[d] Eq. 41

[e] Eq. 42

[f] Eq. 46

[g] Inactive under test conditions

Table 21 (continued)

No.	R^a	$R_1{}^b$	TREF	FR_p	σR_p	VwR_1	MRR_2	$-\log MIC^c$ CN obsd	TM obsd	cald^d	AF obsd	cald^e	CA obsd	cald^f
33	H	¥	122.2	0.00	0.00	0.90	25.36	1.56	0.96	1.04	0.96	1.09	0.66	0.66
34	H	§	126.9	0.00	0.00	0.78	25.36	1.26	0.96	1.07	0.96	1.09	0.66	0.66
35	Cl	¥	127.0	0.41	0.23	0.90	25.36	0.99	0.99	1.07	0.99	1.09	I	
36	Cl	§	131.7	0.41	0.23	0.78	25.36	0.99	1.00	1.09	1.00	1.09	0.69	0.69
37	F	¥	122.4	0.43	0.06	0.90	25.36	1.28	0.98	1.03	1.28	1.07	0.68	0.67
38	F	§	127.1	0.43	0.06	0.78	25.36	1.88	0.98	1.05	1.28	1.07	0.68	0.68
39	Me	¥	128.6	0.26	−0.27	0.90	25.36	1.89	0.99	0.96	1.29	1.07	0.69	0.69
40	OMe	§	133.4	0.26	−0.27	0.78	25.36	1.29	1.29	1.08	1.29	1.07	0.69	0.69
41	$	¥	135.1	0.00	0.00	0.90	25.36	1.31	1.01	1.11	1.01	1.09	0.71	0.72
42	$	§	139.8	0.00	0.00	0.78	25.36	1.62	1.02	1.09	1.02	0.98	0.72	0.72
43	£	¥	141.5	0.26	−0.27	0.90	25.36	1.34	1.04	1.02	1.04	1.09	0.74	0.75
44	£	§	146.3	0.26	−0.27	0.78	25.36	1.34	1.04	1.17	1.04	1.09	0.74	0.76
45	H	¥	111.2	0.00	0.00	0.90	14.96	1.53	0.93	0.99	0.93	0.93	0.62	0.62
46	H	§	116.0	0.00	0.00	0.78	14.96	0.93	0.63	0.77	0.93	0.91	0.63	0.62
47	Cl	¥	116.0	0.41	0.23	0.90	14.96	1.86	0.66	0.93	1.26	1.08	0.66	0.66

[a] $, £ Correspond to 2,5-dimethoxy and 3,4,5-trimethoxy, respectively
[b] ¥, § Correspond to CO_2-t-Bu and COPh, respectively
[c] Minimum inhibitory concentration in NCCLS protocol
[d] Eq. 41
[e] Eq. 42
[f] Eq. 46
[g] Inactive under test conditions

Table 21 (continued)

No.	R^a	$R_1{}^b$	TREF	FR_p	σR_p	VwR_1	MRR_2	$-\log \text{MIC}^c$ CN obsd	TM obsd	cald^d	AF obsd	cald^e	CA obsd	cald^f
48	Cl	§	120.8	0.41	0.23	0.78	14.96	0.96	0.95	0.74	0.66	0.65	0.66	0.66
49	F	¥	111.4	0.43	0.06	0.90	14.96	1.55	0.94	0.88	0.94	1.09	0.64	0.64
50	F	§	116.2	0.43	0.06	0.78	14.96	1.25	0.65	0.77	0.65	0.65	0.65	0.64
51	OMe	¥	117.7	0.26	-0.27	0.90	14.96	0.96	0.96	1.02	0.66	0.68	0.66	0.65
52	OMe	§	122.4	0.26	-0.27	0.78	14.96	0.96	0.98	0.88	0.66	0.65	0.66	0.66
53	$	¥	124.1	0.00	0.00	0.90	14.96	0.98	0.98	1.05	I		0.68	0.68
54	$	§	128.9	0.00	0.00	0.78	14.96	0.99	0.99	1.09	I		0.69	0.69
55	£	¥	130.6	0.26	-0.27	0.90	14.96	1.31	0.71	0.87	1.31	1.89	0.71	0.71
56	£	§	135.3	0.26	-0.27	0.78	14.96	1.31	1.01	0.79	1.31	1.32	0.71	0.72

[a] $, £ Correspond to 2,5-dimethoxy and 3,4,5-trimethoxy, respectively
[b] ¥, § Correspond to CO_2-t-Bu and COPh, respectively
[c] Minimum inhibitory concentration in NCCLS protocol
[d] Eq. 41
[e] Eq. 42
[f] Eq. 46
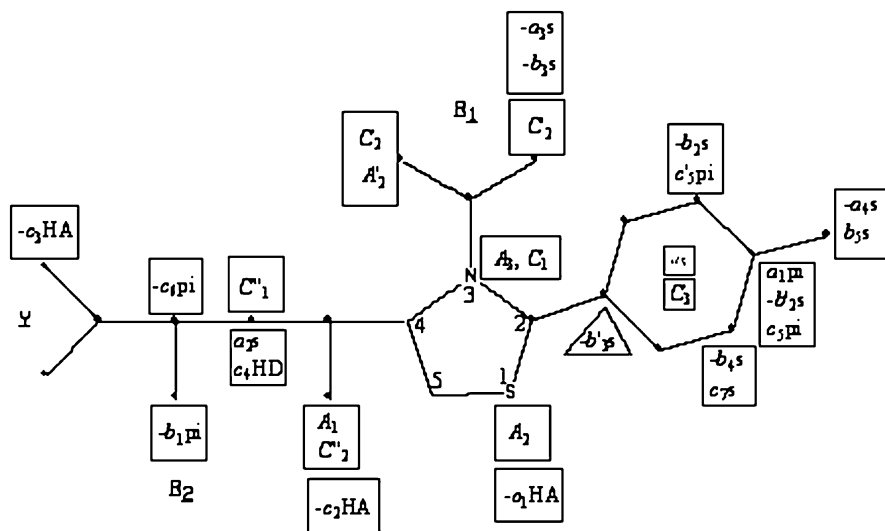[g] Inactive under test conditions

Fig. 31 A composite representation of the thiazolidines' superimposition pattern corresponding to Eqs. 40–42 in 2D-structure space. Annotations in italic capital letters A and B stand for the most probable locations of biophoric centers of Eq. 40 (also Eq. 41) and Eq. 42, respectively, and the italic small case a, b and c stand for secondary site locations of Eqs. 40, 41, and 42, respectively. The subscripts of annotations represent the i th center/site. The most probable atoms for biophoric centers: A_1 is O, A_2 is O or S, A_3 is N, C_1 is N, C_2 is O, and C_3 is ring center. Biophore distances: $A_1 - A_2$ is 4.7415 Å (sd, 0.1831), $A_2 - A_3$ is 2.4872 Å (sd, 0.1657), $A_1 - A_3$ is 3.5598 Å (sd, 0.1635), $C_1 - C_2$ is 2.2790 Å (sd, 0.0279), $C_2 - C_3$ is 5.7242 Å (sd, 0.3156), and $C_1 - C_3$ is 3.9253 Å (sd, 0.1330). The suffixes pi(π), s, HA, or HD, of a, b, and c indicate the nature of the secondary site, as hydrophobic, steric, hydrogen acceptor or hydrogen donor, respectively. The prefixed negative sign, if any, of a, b, and c indicates the sign of the i th site coefficient in the regression equation. A prime sign on any annotation (lower or upper case) indicates the alternative location of the corresponding site (Reprinted with permission from [191]. Copyright 2003 Wiley)

(excluded compounds: **12, 13, 19, 43, 44, 54, 56, 59** and **60**)

$$- \log \mathrm{MIC(TM)} = 0.005(0.0007)\mathrm{TREF} + 0.217(0.098)\mathrm{FR}_p + 0.280$$
$$n = 47, \quad r = 0.734, \quad s = 0.113, \quad F = 25.74 \tag{44}$$

(excluded compounds: **15, 34, 38, 55, 58** and **63**)

$$- \log \mathrm{MIC(AF)} = - 0.039(0.009)\mathrm{MRR}_2 + 0.002(0.0004)\mathrm{MRR}_2^2$$
$$- 2.357(1.074)\mathrm{FR}_p + 6.048(2.787)\mathrm{FR}_p^2$$
$$- 0.620(0.300)\sigma R_p + 0.971$$
$$n = 30, \quad r = 0.777, \quad s = 0.124, \quad F = 7.29 \tag{45}$$

(excluded compounds: **21, 29, 36, 55, 63**, and **64**)

In deriving these equations several compounds have been excluded from the dataset. In 2D-QSAR, the descriptors TREF, IR_m, MRR_2, VwR_1, FR_p, and σR_p have been found to be the parameters of choice to explain the antifungal activity of the compounds with TREF and IR_m as common variables for both 3D- and 2D-equations. With the identification of the 2D-parameters in the 3D-region, that is R_2 to the C4 region, R_1 to the N3 region, and R_p to the C2-phenyl moiety, the 2D and 3D-studies have been integrated to diagnose the activity of the compounds.

The thiazolidines' (Table 21) activity against CA has been found to be distributed in a very narrow range. Also, no 3D-molecular/conformational preferences of these compounds have been noticed in deciding this antifungal activity (Eqs. 46 and 47).

$$- \log \mathrm{MIC(CA)} = 0.179 + 0.001(0.00001)\mathrm{MW}$$
$$n = 48, \quad r = 0.997, \quad s = 0.005, \quad F = 7689.85 \tag{46}$$

$$- \log \mathrm{MIC(CA)} = 0.210 + 0.004(0.00001)\mathrm{TREF}$$
$$n = 48, \quad r = 0.976, \quad s = 0.015, \quad F = 934.85 \,. \tag{47}$$

These equations have indicated a strong correlation between the CA inhibitory activity and global properties namely, molecular weight (MW) and total refractivity (TREF), of these compounds. This exploration has elucidated the potential of the thiazolidines as antifungal agents. Some 1 : 1 adducts of triphenyltin chloride and 2,3-disubstituted thiazolidin-4-ones have been evaluated, in vitro, against the plant pathogenic fungus, Dutch elm, *Ceratocystis ulmi* [192]. However, attempts to obtain structure-activity correlations between the activity and the descriptors of triphenyltin chloride and thiazolidin-4-one adduct have been reported to be unsuccessful [192].

Zou et al. [193] have explored the QSAR of the antifungal profile of 5-[1-aryl-1,4-dihydro-6-methylpyridazin-4-one-3-yl]-2-arylamino-1,3,4-thiadiazoles (Fig. 32, Table 22) in terms of the sum of the physicochemical properties of all the substituent groups namely, hydrophobic effects ($\sum \pi$), meta- and para- Hammett's sigma constants ($\sum \sigma$), steric effects ($\sum$Es), and the inductive effects ($\sum$F).

These compounds have been tested in vivo against wheat leaf rust, *Puccinia recondite*, at a fixed dose of 0.001 M. The following equation represents the best QSAR model for the antifungal activity ($D = \log[a/(100 - a)] - \log$ Mw; where, a is the percentage inhibition and Mw is the molecular weight of the tested compound) of these compounds.

$$D = 2.802(0.450) \sum \pi - 3.275(0.534) \sum \sigma + 0.995(0.214) \sum \mathrm{Es}$$
$$- 0.936(0.21) \sum \mathrm{F} - 2.844$$
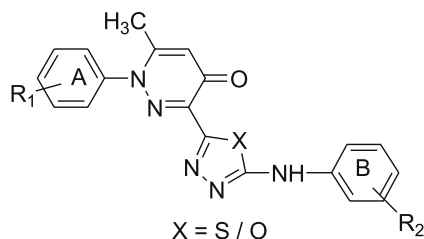$$n = 16, \quad r = 0.902, \quad s = 0.281, \quad F = 11.96 \,. \tag{48}$$

Fig. 32 General structure of 5-[1-aryl-1,4-dihydro-6-methylpyridazin-4-one-3-yl]-2-arylamino-1,3,4-thiadiazoles and oxadiazoles associated with antifungal activity

Table 22 Physicochemical properties and fungicidal activity of pyridazinonethiadiazoles (Fig. 32) [193]

	R_1	R_2	$\sum \sigma$	$\sum F$	$\sum \pi$	$\sum Es$	D^a obsd	cald^b
1	2-Cl	3-CF$_3$	0.66	0.79	1.59	− 1.21	− 2.30	− 2.49
2	2-Cl	2-F	0.29	0.07	0.85	− 1.43	− 3.57	− 2.90
3	2-Cl	H	0.23	0.41	0.71	− 0.97	− 3.16	− 2.96
4	H	2-F	0.06	− 0.34	0.14	− 0.46	− 2.58	− 2.79
5	H	3-CF$_3$	0.43	0.38	0.88	− 0.24	− 2.46	− 2.38
6	2,6-Cl$_2$	3-CF$_3$	0.89	1.19	2.30	− 2.18	− 2.70	− 2.60
7	2,6-Cl$_2$	2-F	0.52	0.47	1.56	− 2.40	− 3.01	− 3.00
8	4-Cl	3-CF$_3$	0.66	0.79	1.59	− 1.21	− 2.44	− 2.49
9	4-Cl	2-F	0.29	0.07	0.85	− 1.43	− 2.67	− 2.90
10	2,4,5-Cl$_3$	2-F	0.75	0.41	2.27	− 3.37	− 2.50	− 2.68
11	2,4,5-Cl$_3$	3-CF$_3$	1.12	0.89	3.01	− 3.15	− 2.36	− 2.04
12	2,4-di-Me	3-CF$_3$	0.09	1.61	2.00	− 2.72	− 1.69	− 1.75
13	2,4-di-Me	2-F	− 0.28	0.30	1.26	− 2.94	− 1.66	− 1.60
14	2,4-Cl$_2$	2-F	0.52	− 0.42	1.56	− 2.40	− 2.05	− 2.17
15	2,4-Cl$_2$	3-CF$_3$	0.89	0.48	2.30	− 2.18	− 1.74	− 1.93
16	2,4-Cl$_2$	H	0.46	1.20	1.42	− 1.94	− 3.23	− 3.42

^{a} $D = \log[a/(100 − a)] − \log Mw$; where, a is the percentage inhibition and Mw is the molecular weight of test compound
^{b} Eq. 48

On the basis of this equation Zou et al. have concluded that hydrophobic compounds with inductively electron-donating ortho substituents would be favorable for the activity [193]. In continuation of this, Zou and coworkers have carried out CoMFA-based 3D-QSAR analysis of these compounds together with 5-[1-aryl-1,4-dihydro-6-methylpyridazin-4-one-3-yl]-2-arylamino-1,3,4-oxadiazoles [194]. Here also the antifungal activity of these compounds has been found to be well explained by their steric and electrostatic properties. In addition to this, it has confirmed the bioisosterism
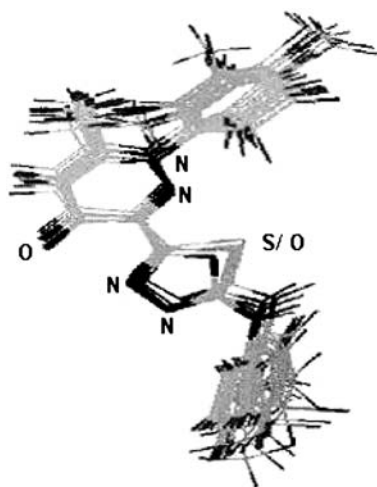
Fig. 33 Alignment and superposition models of 5-[1-aryl-1,4-dihydro-6-methylpyridazin-4-one-3-yl]-2-arylamino-1,3,4-thiadiazoles and corresponding oxadiazoles in CoMFA. (Reprinted with permission from [194]. Copyright 2002 American Chemical Society)

between the 1,3,4-thiadiazole and 1,3,4-oxadiazole analogues in expressing the antifungal activity (Fig. 33)

3.3.3
Octopamine Agonists (OA)

Several scaffolds closely related to thiazolindines have been reported to possess octopamine (OA) agonist/antagonist activity mediated through the adenylate cyclase. The OA is associated with the altered levels of cyclic AMP in the nerve tissue of insects, e.g., the migratory locust, *Locusta migratoria* L [195–199]. This has prompted the investigation of these heterocycles as safe and selective pesticides [200, 201]. Against this background Hirashima et al. investigated the QSAR of octopaminergic agonistic activity of 2-(arylimino)thiazolidine derivatives (Fig. 34, Table 23) [202] with different physicochemical parameters such as total hydrophobicity ($\sum \pi$), molar re-
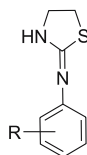

Fig. 34 General structure of 2-(arylimino)thiazolidines associated with octopaminergic agonistic activity

Table 23 Physicochemical properties and octopamine agonist activity of 2-(arylimino)thi-azolodines (Fig. 34) [203]

No.	X	$\sum \pi$	σ_P	Es^m	$\log V_{max}$ [a] obsd	cald [b]
1	H	0.00	0.00	0.00	0.92	0.78
2	3-Cl	0.87	0.00	− 0.97	0.54	0.75
3	3-NO$_2$	0.23	0.00	− 2.52	0.28	0.17
4	4-F	0.12	0.06	0.00	0.75	0.83
5	4-Me	0.50	− 0.17	0.00	0.88	0.89
6	4-CN	− 0.21	0.66	0.00	0.92	0.84
7	4-EtO	0.48	− 0.24	0.00	0.69	0.87
8	2,4-Cl$_2$	1.34	0.23	0.00	1.25	1.17
9	2,4-F$_2$	0.22	0.06	0.00	0.60	0.85
10	2-Br,4-Me	1.12	− 0.17	0.00	0.89	1.05
11	2-NO$_2$, 4-Me	0.36	− 0.17	0.00	0.56	0.85
12	2-NO$_2$, 4-OMe	0.10	− 0.27	0.00	0.65	0.71
13	2-Me,4-Br	1.32	0.32	0.00	1.61	1.18
14	2-Me,4-Cl	1.16	0.23	0.00	1.49	1.13
15	2-Me,4-F	− 0.11	0.06	0.00	1.15	0.77
16	2-Me,4-I	0.01	0.18	0.00	1.38	0.82
17	2-Me,4-NO2	0.61	0.78	0.00	1.21	1.08
18	2,4-Me$_2$	0.81	− 0.17	0.00	1.02	0.97
19	2,4-(MeO)$_2$	− 0.31	− 0.27	0.00	0.53	0.66
20	2-Et, 4-Br	1.78	0.23	0.00	1.49	1.29
21	2,5-Cl$_2$	1.36	0.00	− 0.97	0.89	0.88
22	2-Cl,5-CF$_3$	1.70	0.00	− 2.40	0.66	0.59
23	2,5-F$_2$	0.43	0.00	− 0.46	1.08	0.77
24	2-Me,5-Cl	1.18	0.00	− 0.97	1.03	0.83
25	2-MeO,5-Cl	0.52	0.00	− 0.97	0.49	0.66
26	2,5-(MeO)$_2$	− 0.21	0.00	− 0.55	0.34	0.58
27	2-Cl,6-Me	0.80	0.00	0.00	0.95	0.99
28	2,6-F$_2$	0.20	0.00	0.00	0.56	0.84
29	2,6-iPr$_2$	2.30	0.00	0.00	1.38	1.39
30	3-Cl,4-Me	1.37	− 0.17	− 0.97	0.53	0.85
31	3-NO$_2$,4-Cl	1.08	0.23	− 2.52	0.56	0.44
32	3-CF$_3$,4-Cl	2.06	0.23	− 2.40	0.86	0.72
33	3,4-(MeO)$_2$	0.18	− 0.27	− 0.55	0.49	0.64
34	3,5-Cl$_2$	1.74	0.00	− 0.97	0.89	0.98
35	3,5-(Me)$_2$	1.08	0.00	− 1.24	0.57	0.74
36	3,5-(CF$_3$)$_2$	2.42	0.00	− 2.40	0.94	0.78

[a] V_{max} is the maximal efficacy of the compound against adenylate cyclase in thoracic nerve cord of *Periplantea americana* L. relative to 1 mM of octopamine
[b] Eq. 49

Table 23 (continued)

No.	X	$\sum \pi$	σ_P	Es^m	$\log V_{max}$ [a] obsd	cald [b]
37	3,5-(MeO)$_2$	0.28	0.00	– 0.55	0.60	0.71
38	2,3,4-Cl$_3$	2.21	0.23	– 0.97	0.93	1.14
39	2,4,5-Cl$_3$	2.21	2.23	– 0.97	1.13	1.49
40	2,3,5,6-F$_4$	0.86	0.00	– 0.46	1.06	0.89
41	2,3,4,5,6-F$_5$	0.98	0.06	– 0.46	0.73	0.93

[a] V_{max} is the maximal efficacy of the compound against adenylate cyclase in thoracic nerve cord of *Periplantea americana* L. relative to 1 mM of octopamine
[b] Eq. 49

fraction (MR), electronic effect sigma meta constant (σ_m), steric (Es), steric meta (Es^m), Swain and Lupton's polarity ($\mathcal{F}$) and resonance constants ($\mathcal{R}$). In these compounds the relative maximal efficacy of the compounds, log V_{max} has been shown to be correlated with the parameters $\sum \pi$, σ_P and Es^m (Eq. 49) [203].

$$\log V_{max} = 0.784(0.055) + 0.261(0.055) \sum \pi + 0.173(0.095)\sigma_P$$
$$+ 0.266(0.050)Es^m$$
$$n = 41, \quad r = 0.744, \quad s = 0.229, \quad F = 15.26 . \tag{49}$$

On the basis of this model, it has been concluded that more hydrophobic compounds having *ortho* and *para* substituents with an electron-withdrawing property and less bulky *meta*-position substituents would lead to better activity. In these compounds octopamine agonistic activity in terms of K_a, the concentration of the agonist necessary for half-maximal activation of adenylate cyclase, and its log V_{max} are mutually correlated. This has prompted us to suggest that the larger the V_{max} value, the greater would be the activity of the compounds [202].

In 2-(substituted benzylamino)-2-thiazolines (Fig. 35, Table 24) [204, 205] the octopamine agonist activity (log V_{max}) has been reported to be correlated with the parameters σ_m and Es^m as shown [206].

$$\log V_{max} = 0.663(0.125)\sigma_m + 0.118(0.036)Es^m + 1.414$$
$$n = 17, \quad r = 0.855, \quad s = 0.048, \quad F = 19.11 . \tag{50}$$

In these compounds the *meta* substituent's electronic and steric effect have been found to be important for the OA agonistic activity. Similar to the compounds of Table 24, for 2-(substituted benzylamino)-2-thiazolines (Fig. 35, Table 24) also less bulky *meta*-substituents have been reported as favorable for the activity. The positive regression coefficient of σ_m has suggested more
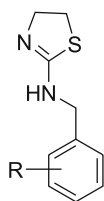
Fig. 35 General structure of 2-(substituted benzylamino)-2-thiazolines associated with octopaminergic agonistic activity

Table 24 Physicochemical properties and octopamine agonist activity of 2-(substituted benzylamino)-2-thiazolines series (Fig. 35) [206]

No.	R	σ_m	Es^m	$\log V_{max}$ [a] obsd	cald [b]
1	H	0.00	0.00	1.32	1.41
2	2-Br	0.00	0.00	1.44	1.41
3	2-Cl	0.00	0.00	1.39	1.41
4	2-F	0.00	0.00	1.46	1.41
5	2-Me	0.00	0.00	1.48	1.41
6	2-CF$_3$	0.00	0.00	1.36	1.41
7	3-F	0.34	– 0.46	1.61	1.58
8	3-CF$_3$	0.43	– 2.40	1.42	1.42
9	4-Cl	0.00	0.00	1.35	1.41
10	4-Me	0.00	0.00	1.41	1.41
11	4-OMe	0.00	0.00	1.45	1.41
12	2,3-Cl$_2$	0.23	– 0.97	1.46	1.45
13	2,4-F$_2$	0.00	0.00	1.38	1.41
14	2-F,4-Cl	0.00	0.00	1.46	1.41
15	2,5-Cl$_2$	0.23	– 0.97	1.45	1.45
16	2,5-F$_2$	0.06	– 0.46	1.43	1.40
17	3,5-Cl$_2$	0.74	– 1.94	1.66	1.68

[a] V_{max} is the maximal efficacy of the compound against adenylate cyclase in thoracic nerve cord of *Periplantea americana* L. relative to 1 mM of octopamine
[b] Eq. 50

electron-withdrawing substituents at this position. However, in these compounds, the K_a and V_{max} are negatively correlated. This has been attributed to the phenyl substituents of these compounds [206].

Thiazolidines and related compounds have also been indicated for their pheromone production inhibitory activity in female moths, *Helvicoverpra armigera*. Pheromone production is a chemical signaling pathway related to the octopaminergic receptor in moths for controlling their reproductive be-
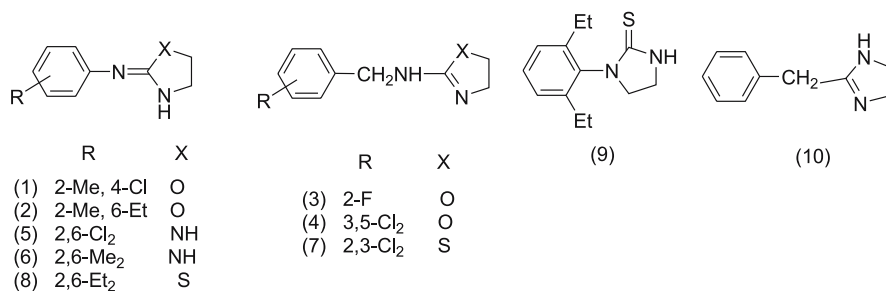
Fig. 36 Different thiazoles and oxazoles associated with octopaminergic agonistic activity

Table 25 Physicochemical properties and octopamine agonist activity of thiazolidine derivatives (Fig. 36) [215, 216]

No.	LowEne	SXZF	JX	R	pK_i [a] obsd	cald [b]	cald [c]	cald [d]	cald [e]
1	8.85	0.69	2.18	55.60	8.21	8.20	7.95	8.02	8.32
2	63.71	0.87	2.30	60.40	5.21	5.23	5.36	5.15	5.45
3	49.98	0.78	1.86	50.80	4.00	3.99	3.95	3.82	3.96
4	– 5.69	0.88	1.89	60.20	7.16	7.19	7.16	7.22	7.17
5	52.65	0.71	2.25	57.30	8.05	8.00	8.01	8.01	7.78
6	37.67	0.80	2.29	57.80	8.41	8.43	8.84	8.46	8.29
7	73.53	0.69	1.92	66.60	4.11	4.11	4.31	4.22	3.95
8	88.28	0.67	2.33	71.50	7.21	7.25	6.89	7.22	7.11
9	106.18	0.78	2.41	74.00	5.27	5.24	5.22	5.42	5.34
10	13.91	0.86	2.00	49.10	7.11	7.11	7.06	7.19	7.38

[a] K_i is the concentration of octopamine agonist necessary for half-maximal inhibition of pheromone biosynthesis activating neuropeptide (PBAN) binding at 1 p mol/intersegment
[b] Eq. 51 [215]
[c] Eq. 52 [216]
[d] Eq. 53 [216]
[e] Eq. 54 [216]

havior [207–212]. For a set of ten compounds (Fig. 36, Table 25) [213, 214] Hirashima and co-workers have identified the following 3D-QSAR model in GFA to explain their OA agonistic activity (K_i) (Eq. 51) [215].

$$pKi = -0.082 \text{LowEne} - 14.819 \text{SXZF} + 8.818 \text{JX}$$
$$+ 0.004(\text{MR} - 57.7808)^2 + 3.085$$
$$n = 10, \quad r = 1.000, \quad F = 5681.367 .$$
$$(51)$$

In this equation LowEne is the energy of the most stable conformation, SXZF is the fraction of area of molecular shadow in the XZ plane over the area of

the enclosing rectangle, JX is a topological parameter from Balaban's shape indices, and MR is the molecular refractivity. Hirashima and co-workers have interpreted this equation to suggest that compounds with positive JX, negative or smaller LowEne and SXZF would result in improved activity [215]. In continuation of this study they have analyzed these compounds using molecular shape analysis (MSA), molecular field analysis (MFA) and receptor surface model (RSM) [216]. In MSA a significant equation for the activity of these compounds has been discovered with information content (IC), radius of gyration (RG), and common overlap steric volume (COVS) (Eq. 52). Models from MFA have involved the potentials of the 3D-grid points generated from the atomic coordinates of the contributing models. The MFA model identified for these compounds has laid emphasis on the proton probes corresponding to lattice points H+/372, H+/298 and the methyl probe corresponding to lattice point CH3/164 (Eq. 53). The RSM analysis has highlighted the associated steric, physicochemical, and electronic properties of the grid of a hypothetical receptor site of the compounds. The RSM equation (Eq. 54) of these compounds has emerged from the electrostatic interaction energy (ELE) at grid points 137 (ELE/137) and 546 (ELE/546) and van der Waals interaction energy at point 780 (VDW/780).

$$pKi = -0.960(IC)^2 - 6.579RG - 0.055(152.765 - COSV)^2 + 39.1401$$
$$n = 10, \quad r = 0.0992, \quad F = 119.50 \tag{52}$$

$$pKi = -0.003(H+/372)^2 + 0.063(H+/298) + 0.025CH_3/164 + 7.209$$
$$n = 10, \quad r = 0.997, \quad F = 407.92 \tag{53}$$

$$pKi = 2.763ELE/137 - 1.529x(ELE/546)^2 - 0.061VDW/780 + 8.214$$
$$n = 10, \quad r = 0.994, \quad F = 184.36 . \tag{54}$$

These equations have highlighted the steric, physicochemical, and electronic requirements at the specified grid locations of the compounds and the pseudo receptor [216].

3.3.4
Trehalase Inhibitors

Also, thiazolidine derivatives have been reported to control an insect's energy metabolism through the inhibition of trehalase, an enzyme involved in the energy functions, especially in the insect-flight [217, 218]. The affinity of trehazolin (**a**) for this enzyme has motivated workers to explore 2-aryl-iminothiazolidine/oxazolidine derivatives (comp. **b**, Fig. 37, Table 26) as its inhibitors [219].

The QSAR of the trehalase inhibitory activity (pIC50) of these compounds has been investigated with dipole moment (D), lipophilicity [V_1/V_2, where V_1
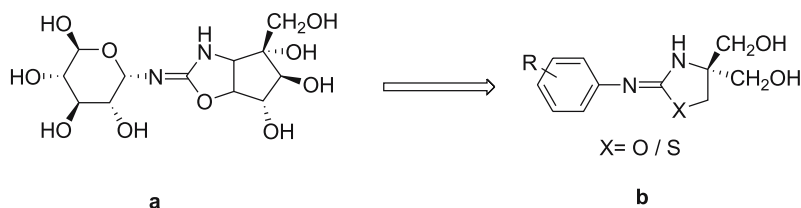
Fig. 37 Structures of trehazolin (**a**) and 2-aryliminothiazolidines/oxazolidines (**b**) associated with trehalase inhibitory activity

Table 26 Physicochemical properties and trehalase inhibitory activities of 2-arylimino-thiazolidine/oxazolidine derivatives (comp. **b**, Fig. 37) [219]

No.	R	X	d_2 (Å)^2	V_1/V_2	D	pIC$_{50}$ [a] obsd	cald [b]
1	2-F	O	4.55	3.21	0.19	4.21	4.05
2	2-F	S	4.55	3.62	0.16	3.08	2.97
3	4-F	O	4.55	2.97	0.15	3.58	3.62
4	4-F	S	4.55	3.28	0.18	3.24	2.77
5	2,4-F$_2$	O	4.55	3.14	0.16	3.05	3.53
6	2,4-F$_2$	S	4.55	3.55	0.16	2.21	2.48
7	3-Cl, 4-F	O	5.09	3.35	0.14	4.45	4.50
8	3-Cl, 4-F	S	5.10	3.70	0.14	3.62	3.60
9	2,3,4-F$_3$	O	4.77	3.38	0.16	4.07	3.81
10	2,3,4-F$_3$	S	4.77	3.63	0.15	3.15	3.34

[a] Percent inhibition = $[1 - A/B] \times 100$, where A and B are the molarity of glucose solution with and without test compound
[b] Eq. 55

and V_2 correspond to the non-polar surface area and polar surface area (Å^2) of the water solvation shell, respectively] and length (d_2).

$$pIC_{50} = 0.376(0.124)D + 3.174(0.624)d_2 - 2.071(0.529)V_1/V_2 - 5.109$$
$$n = 10, \quad r = 0.830, \quad s = 0.335, \quad F = 9.79 . \tag{55}$$

On the basis of this model, it has been concluded that polar compounds with higher d$_2$ values would be better for the activity. Moreover, it has been suggested that hydrophilic compounds would lead to improved inhibitory activity.

4
Concluding Remarks

The present review has addressed two issues namely, applications of QSAR in rational drug design and more importantly the review has highlighted the potential of the thiazolidine ring system as a biologically privileged scaffold. Over the years there has been substantial progress in QSAR methodologies from the classical to high-dimensional modeling studies leading to more realistic prediction of physicochemical properties as well as the biological activities of compounds under investigation. Through the examples cited in this review we have tried to emphasize that by rational design, biological activity inherent to the chemical entities can be accentuated culminating in therapeutically useful molecules. The studies on neuropeptide Y5 receptor (NPY5R) antagonists as antiobesity agents has clearly illustrated how the modeling studies can be focused in the design of novel and highly active compounds for the identified target. In this case, highly active NPY5R antagonists with a thiazole scaffold have been designed using modeling studies starting from totally unrelated chemical entities [130, 131]. QSAR study of the antihistaminic (H_1) activity of substituted thiazoles and benzthiazole derivatives [111, 112] using the logP and normal and reversed phase thin layer chromatographic (TLC) parameters generated through impregnating the TLC plates with the amino acids of the receptor domain provided insight into the nature and requirements of receptor domain vis-à-vis the compounds under investigation. Also, it provided a handle to deal with the much larger problems of receptor domain with simple yet reliable tools. This study has opened up a novel way of generating the receptor-directed interaction information in terms of amino acids of the active site. One can also adapt this kind of procedure for the study of other receptors. Another interesting example discussed in this review involves a simple classification of antiulcer activity of 4-substituted-2-guanidino thiazoles with topological indices namely Wiener's and molecular connectivity indices [117]. These approaches are very useful and quick for the screening of large databases. The QSAR and modeling results of thiazolidin-4-ones as HIV-1 RT inhibitors from different groups have shown consistency from different perspectives and provided scope to expand the substitution around the thiazolidinone moiety by the introduction of furfuryl in place of pyridyl at N3 [173, 181–183, 189, 190]. Through these and other examples we have tried to highlight the prospects of this heterocyclic system as well as QSAR and modeling studies in lead identification, development, and optimization in the drug discovery program.

References

1. Abraham DJ (2003) Burgers Medicinal Chemistry and Drug Discovery, 6th edn. Wiley, New Jersey
2. Frühbeis H, Klein R, Wallmeier H (1987) Angew Chem Int Ed 26:403
3. Livingstone D (1995) Data Analysis for Chemists: Applications to QSAR and Chemical Product Design. Oxford University Press, New York
4. Negwer M (1994) Organic-Chemical Drugs and Their Synonyms, 7th edn. Akademie Verlag, VCH Publishers, New York
5. Koch P, Perrotti E (1974) Tetrahedron Lett 15:2899
6. Cook AH, Heilbron I (1949) In: The chemistry of penicillin, chap 25. Princeton University Press, Princeton, p 921
7. Metzger JV (1984) Comprehensive heterocyclic chemistry: The Structure, Reactions, Synthesis and Uses of Heterocyclic compounds. In: Katrizky AR, Rees CW, Potts KT (eds) Thiazoles and their benzo derivatives. Pergamon Press, New York, p 235
8. Pesek J, Frost J (1975) Tetrahedron 31:907
9. Brich A, Harris S (1930) Biochem J 24:1080
10. Schubert J (1935) Biochem J 111:671
11. Kallen RG (1971) J Am Chem Soc 93:6236
12. Wystouch A, Lisowski M, Pedyczak A, Siemion IZ (1992) Tetrahedron Assym 3:1401
13. Patek M, Darke B, Lebel M (1995) Tetrahedron Lett 36:2227
14. Pesek JJ, Frost JH (1975) Tetrahedron 31:907
15. Dains FB, Krober OA (1939) J Am Chem Soc 61:1830
16. Damico JJ, Harman MH (1955) J Am Chem Soc 77:476
17. Bon V, Tisler M (1962) J Org Chem 27:2878
18. Rao RP (1961) J Indian Chem Soc 38:784
19. Bhargava PN, Chaurasia MR (1969) J Pharm Sci 58:896
20. Chaubey VN, Singh H (1970) Bull Chem Soc Jpn 43:2233
21. Wilson FJ, Burns R (1922) J Chem Soc 121:870
22. Bougault J, Cattelain E, Chabrier P, Quevauviller A (1949) Bull Soc Chim Fr 16:433
23. Surrey AR, Cutler RA (1954) J Am Chem Soc 76:578
24. Srivastava SK, Srivastava SL, Srivastava SD (2000) J Indian Chem Soc 77:104
25. Shrama RC, Kumar D (2000) J Indian Chem Soc 77:492
26. Baraldi PG, Simoni D, Moroder F, Manferdini S, Mucchi L, Vecchia FD (1982) J Heterocycl Chem 19:557
27. Srivastava T, Haq W, Katti SB (2002) Tetrahedron 58:7619
28. Rawal RK, Srivastava T, Haq W, Katti SB (2004) J Chem Res 368
29. Holmes C, Chinn JP, Look GC, Gordon EM, Gallop MA (1995) J Org Chem 60:7328
30. Popp FD, Rajopadhye M (1987) J Heterocycl Chem 24:261
31. Brown FC, Jones RS, Kent M (1963) Can J Chem 41:817
32. Liu H, Li Z, Anthonsen T (2000) Molecules 5:1055
33. Kato T, Ozaki T, Tamura K, Suzuki Y, Akima M, Ohi N (1999) J Med Chem 42:3134
34. Troutman HD, Long LM (1948) J Am Chem Soc 70:3436
35. Surrey AR (1948) J Am Chem Soc 70:4262
36. Omar MT, EI-Khamry AE, Sherif FA (1981) J Heterocycl Chem 18:633
37. Brown FC (1961) Chem Rev 61:463
38. Danila G (1978) Rev Chim (Bucharest) 29:820 Chem Abstr (1979) 90:72086p
39. Danila G (1978) Rev Chim (Bucharest) 29:1152 Chem Abstr (1979) 90:152037p
40. Singh SP, Parmar SS, Raman K, Stenberg VI (1981) Chem Rev 81:175

41. Hansch C, Leo A (1979) Substituent Constants for Correlation Analysis in Chemistry and Biology. Wiley-Interscience, New York
42. Stewart JJP (2004) J Mol Mode 10:155
43. CS Chem3D Ultra Cambridge Soft Corporation, Cambridge, USA
44. Katritzky AR, Lobnov V, Karelson M (1994) CODESSA (Comprehensive Descriptors for Structural and Statistical Analysis). University of Florida, Gainesville, FL, http://www.codessa-pro.com
45. Katritzky AR, Perumal S, Petrukhin R, Kleinpeter E (2001) J Chem Inf Comput Sci 41:569
46. Liu SS, Yin CS, Li ZL, Cai SX (2001) J Chem Inf Comput Sci 41:321
47. Todeschini R, Consonni V, Mauri A, Pavan M (2003) DRAGON software version 3.0. http://disat.unimib.it/chm/Dragon.htm
48. Wold S, Ruhe A, Wold H, Dunn WJ (1984) J Sci Stat Comput 5:135
49. Rogers D, Hopfinger AJ (1994) J Chem Inf Comput Sci 34:854
50. Cerius^2 Version 4.8 (2002) Life science modeling and simulation software. Accelrys, San Diego, USA
    http://www.accelrys.com/products/cerius2/
51. Prabhakar YS (2003) QSAR Comb Sci 22:583
52. Liu SS, Liu HL, Yin CS, Wang LS (2003) J Chem Inf Comput Sci 43:964
53. Gasteiger J, Zupan J (1993) Angew Chem Intl Ed Engl 32:503
54. Manallack DT, Ellis DD, Livingstone DJ (1994) J Med Chem 37:3758
55. Kövesdi I, Dominguez-Rodriguez MF, Ôrfi L, Náray-Szabó G, Varró A, Gy Papp J, Mátyus P (1999) Med Res Rev 19:249
56. Cramer RD, Patterson DE, Bunce JD (1998) J Am Chem Soc 110:5959
57. Klebe G, Abraham U, Meitzner T (1994) J Med Chem 37:4130
58. Hopfinger AJ (1980) J Am Chem Soc 102:7196
59. Tokarski JS, Hopfinger AJ (1994) J Med Chem 37:3639
60. Hopfinger AJ, Tokarsi JS (1997) In: Charifson PS (ed) Practical applications of computer-aided drug design. Marcel Dekker Inc, New York, p 105
61. Hahn M (1995) J Med Chem 38:2080
62. Hahn M, Rogers D (1995) J Med Chem 38:2091
63. Golender VE, Vorpogel ER (1993) Computer Assisted-Pharmacophore Identification. In: Kubinyi H (ed) 3D-QSAR in Drug Design: Theory, Methods and Application. ESCOM Science Publishers, Leiden, Netherlands, p 137
64. Rational Drug Design Software Catalyst, Accelrys, San Diego, CA
    http://www.accelrys.com/products/catalyst/
65. Cox B, Denyer JC, Binnie A (2000) Prog Med Chem 37:83
66. Walters WP, Stahl MT, Murcko MA (1998) Drug Discovery Today 3:160
67. Morris GM, Goodsell DS, Halliday RS, Huey R, Hart WE, Belew RK, Olson AJ (1988) J Comput Chem 19:1639
68. AutoDock: Automated docking of flexible ligands to macrimolecules
    http://www.scripps.edu/mb/olson/doc/autodock
69. Insight II, version 2.3.0, Biosym Technologies Inc, 9685, Scranton Road, San Diego, CA, USA, 1993
70. SYBYL 6.9 Tripos Inc., St. Louis, MO, USA
71. MOE: The Molecular Operating Environment, Chemical Computing Group Inc. Quebec, Canada. http://www.chemcomp.com
72. Klose N, Niedbolla K, Schwazrtz K, Bottcher I (1983) Arch Pharm 1983:316
73. Satsangi RK, Zaidi SM, Misra VS (1983) Pharmazie 38:341

74. Pignatello R, Mazzone S, Panico AM, Mazzone G, Penissi G, Castano R, Matera M, Blandino G (1991) Eur J Med Chem 26:929
75. Hadjipavlou-Litina D, Geronikaki A, Sotiropoulou E (1993) Res Commun Chem Pathol Pharmacol 79:355
76. Geronikaki A, Hadjipavlou-Litina D (1993) Pharmazie 48:948
77. Garg R, Kurup A, Mekapati SB, Hansch C (2003) Chem Rev 103:703
78. Fleischmann R, Iqbal I, Slobodin G (2002) Expert Opin Pharmacother 10:1501
79. Naito Y, Goto T, Akahoshi F, Ono S, Yoshitomi H, Okada T, Sugiyama N, Abe S, Hanada S, Hirata M, Watanabe M, Fukaya C, Yokoyama K, Fujita T (1991) Chem Pharm Bull 39:2323
80. Naito Y, Yamaura Y, Inoue Y, Fukaya C, Yokoyama K, Nakagawa Y, Fujita T (1992) Eur J Med Chem 27:645
81. Verloop A, Hoogenstraaten W, Tipkar J (1976) In: Ariens EJ (ed) Drug Design, vol. VII. Academic Press, New York, pp 165-207
82. Liu SS, Cui SH, Shi YY, Wang LS (2002) Internet Electron J Mol Des 1:610
83. Liu SS, Yin CS, Shi YY, Cai SX, Li ZL (2001) Chin J Chem 19:751
84. Liu SS, Liu LH, Shi YY, Wang LS (2002) Internet Electron J Mol Des 1:310 http://www.biochempress.com
85. Vigorita MG, Ottanà R, Monforte F, Maccari R, Monforte MT, Trovato A, Taviano MF, Miceli N, De Luca G, Alcaro S, Ortuso F (2003) Bioorg Med Chem 11:999
86. Pettipher ER, Higgs GA, Henderson B (1986) Proc Natl Acad Sci USA 83:874
87. Panico AM, Geronikaki A, Mgonzo R, Cardile V, Gentile B, Doytchinova I (2003) Bioorg Med Chem 11:2983
88. McInnes IB, Leung PB, Field M, Huang FP, Sturrock RD, Kinninm J (1996) J Exp Med 184:1519
89. Misra R, Stephan S, Chander CL (1999) Inflamm Res 48:119
90. De Nanteuil G, Portevin B, Benoist A (2001) Il Farmaco 56:107
91. Litina DH, Geronikaki A, Mgonzo R, Doytchinova I (1999) Drug Develop Res 48:53
92. Ellis GA, Blake DR (1993) Ann Rheum Dis 52:241
93. van Muijlwijk-Koezen JE, Timmerman H, Vollinga RC, von Drabbe F, Kunzel J, de Groote M, Visser S, IJzerman AP (2001) J Med Chem 44:739
94. van Tilburg EW, van der Klein PAM, de Groote M, Beukers MW, IJzerman AP (2001) Bioorg Med Chem Lett 11:2017
95. Jung KY, Kim SK, Gao ZG, Gross AS, Melman N, Jacobson KA, Kim YC (2004) Bioorg Med Chem 12:613
96. Fan M, Qin W, Mustafa SJ (2003) Am J Physiol Lung Cell Mol Physiol 284:L1012
97. Ezeamuzie CI (2001) Biochem Pharmacol 61:1551
98. Avila MY, Stone RA, Civan MM (2002) Invest Ophthalmol Vis Sci 43:3021
99. Mubagwa K, Flameng W (2001) Cardiovasc Res 52:25
100. Liang BT, Jacobson KA (1998) Proc Natl Acad Sci USA 95:6995
101. Tracey WR, Magee W, Masamune H, Kennedy SP, Knight DR, Buchholz RA, Hill R (1997) J Cardiovasc Res 33:410
102. von Lubitz DKJE (1999) Eur J Pharmacol 371:85
103. Bhattacharya P, Leonard JT, Roy K (2005) Bioorg Med Chem 13:1159
104. Bhattacharya P, Leonard JT, Roy K (2005) J Mol Model 11:516
105. Borghini A, Pietra D, Domenichellia P, Bianucci AM (2005) Bioorg Med Chem 13:5330
106. Naruto S, Motoc I, Marshall GR (1985) Eur J Med Chem 20:529
107. Borea PA, Bertolasi V, Gilli G (1986) Arzneim Forsch 36:895

108. Diurno MV, Mazzoni O, Piscopo E, Caliganao A, Giordano F, Bolognese A (1992) J Med Chem 35:2910
109. Singh P, Ojha TN, Shrama RC, Tiwari S (1994) Indian J Pharm Sci 57:162
110. Agrawal VK, Sachan S, Khadikar PV (2000) Acta Pharma 50:281
111. Brzezinska E, Koska G, Walczynski K (2003) J Chromatogr A 1007:145
112. Brzezinska E, Koska G, Klimczak A (2003) J Chromatogr A 1007:157
113. Walczynski K, Timmerman H, Zuiderveld OP, Zhang MQ, Glinka R (1999) Il Farmaco 54:533
114. Walczynski K, Guryn R, Zuiderveld OP, Zhang MQ, Timmerman H (1999) Il Farmaco 54:684
115. Walczynski K, Guryn R, Zuiderveld OP, Zhang MQ and Timmerman H (2000) Il Farmaco 55:569
116. La Mattina JL, McCarthy PA, Reiter LA, Holt WF, Yeh LA (1990) J Med Chem 39:543
117. Goel A, Madan AK (1995) J Chem Inf Comput Sci 35:504
118. Wiener H (1947) J Am Chem Soc 69:2636
119. Randić M (1965) J Am Chem Soc 97:6609
120. Borges EG, Takahata Y (2002) J Mol Struct (Theochem) 580:263
121. Mizoule J, Meldrum B, Martine M, Croucher M, Ollat C, Uzan A, Legvand JJ, Gueremy C, LeFur G (1995) Neuropharmacology 24:767
122. Benoit E, Escande D (1991) Pflugers Arch 419:603
123. Hays SJ, Rice MJ, Ortwine DF, Johnson G, Schwarz RD, Boyd DK Copeland LF, Vartanian MG, Boxer PA (1994) J Pharma Sci 83:1425
124. Mathvink RJ, Barritta AM, Candelore MR, Cascieri MA, Deng L, Tota L, Strader CD, Wyvratt MJ, Fisher MH, Weber AE (1999) Bioorg Med Chem Lett 9:1869
125. Mathvink RJ, Tolman JS, Chitty D, Candelore MR, Cascieri MA, Colwell LF, Deng L Jr, Feeney WP, Forrest MJ, Hom GJ, MacIntyre DE, Tota L, Wyvratt MJ, Fisher MH, Weber AE (2000) Bioorg Med Chem Lett 10:1971
126. Nisoli E, Tonello C, Carruba MO (2003) Curr Med Chem Central Nervous Syst Agents 3:257
127. Naylor EM, Parmee ER, Colandrea VJ, Perkins L, Brockunier L, Candelore MR, Cascieri MA, Colwell LF, Deng L, Feeney WP, Forrest MJ, Hom GJ, MacIntyre DE, Strader CD, Tota L, Wang PR, Wyvratt MJ, Fisher MH, Weber AE (1999) Bioorg Med Chem Lett 9:755
128. Shih TL, Candelore MR, Cascieri MA, Chiu SHL, Colwell LF, Deng L, Feeney WP, Forrest MJ, Hom GJ, MacIntyre DE, Miller RR, Stearns RA, Strader CD, Tota L, Wyvratt MJ, Fisher MH, Weber AE (1999) Bioorg Med Chem Lett 9:1251
129. Hanumantharao P, Sambasivarao SV, Soni LK, Gupta AK, Kaskhedikar SG (2005) Bioorg Med Chem 15:3167
130. Guba W, Neidhart W, Nettekoven M (2005) Bioorg Med Chem Lett 15:1599
131. Nettekoven M, Guba W, Neidhart W, Mattei P, Pflieger P, Roche O, Taylor S (2005) Bioorg Med Chem Lett 15:3446
132. Criscione L, Rigollier P, Batzl-Hartmann C, Rueger H, Stricker-Krongrad A, Wyss P, Brunner L, Whitebread S, Yamaguchi Y, Gerald C, Heurich RO, Walker MW, Chiesi M, Schilling W, Hofbauer KG, Levens N (1998) J Clin Invest 102:2136
133. Fukami T, Okamoto O, Fukuroda T, Kanatani A, Ihara M (1998) PCT Int Appl WO 9840356 (Banyu Pharmaceutical Co Ltd, Japan) 78
134. Norman MH, Chen N, Han N, Liu L, Hurt CR, Fotsch CH, Jenkins TJ, Moreno OA (1999) PCT Int Appl WO9940091 (Amgen Inc, USA) 469
135. Breu V, Dautzenberg F, Guerry P, Nettekoven MH, Pieger P (2002) PCT Int Appl WO2002020488 (F. Hoffmann-La Roche, Switzerland) 62

136. Iwaoka M, Takemoto S, Tomoda S (2002) J Am Chem Soc 124:10613
137. Mangelsdorf DJ, Evans RM (1995) Cell 83:841
138. Sohda T, Mizuno K, Tawada H, Sugiyama Y, Fujita T, Kawamastu Y (1982) Chem Pharm Bull 30:3563
139. Sohda T, Mizuno K, Imamiya E, Sugiyama Y, Fujita T, Kawamastu Y (1982) Chem Pharm Bull 30:3580
140. Hulin B, McCarthy PA, Gibbs EM (1996) Curr Pharm Des 2:85
141. Sohda T, Momose Y, Meguro K, Kawamastu Y, Sugiyama Y, Ikeda H (1990) Arzneim Forsch 40:37
142. Sohda T, Mizuno K, Momose Y, Ikeda H, Fujita T, Meguro K (1992) J Med Chem 35:2617
143. Yoshioka T, Fujita T, Kanai T, Aizawa Y, Kurumada T, Hasegawa K, Horikoshi H (1989) J Med Chem 32:421
144. Hulin B, Clark DA, Goldstein SW, McDermott RE, Dambek PJ, Kappeler WH, Lamphere CH, Lewis DM, Rizzi JP (1992) J Med Chem 35:1853
145. Parks DJ, Tomkinson NCO, Villeneuve MS, Blanchard SG, Willson TM (1998) Bioorg Med Chem Lett 8:3657
146. Sohda T, Mizuno K, Kawamastu Y (1984) Chem Pharm Bull 32:4460
147. Weatherman RV, Fletterick RJ, Scanlan TS (1999) Annu Rev Biochem 68:559
148. Nolte RT, Wisely GB, Westin S, Cobb JE, Lambert MH, Kurokawa R, Rosenfeld MG, Willson TM, Glass CK, Milburn MV (1998) Nature 395:137
149. Uppenberg J, Svensson C, Jaki M, Bertilsson G, Jendeberg L, Berkenstam A (1998) J Biol Chem 273:31108
150. Yanagisawa H, Takamura M, Yamada E, Fujita S, Fujiwara T, Yachi M, Isobe A, Hagisawa Y (2000) Bioorg Med Chem Lett 10:373
151. Iwata Y, Miyamoto S, Takamura M, Yanagisawa H, Kasuya A (2001) J Mol Grap Model 19:536
152. Murakami K, Tobe K, Ide T, Monchizuki T, Ohashi M, Akanuma Y, Yazaki Y, Kadowaki T (1998) Diabetes 47:1841
153. Desai RC, Han W, Metzger EJ, Bergman JP, Gratale DF, MacNaul KL, Berger JP, Doebber TW, Leung K, Moller DE, Heck JV, Sahoo SP (2003) Bioorg Med Chem Lett 13:2795
154. Desai RC, Gratale DF, Han W, Koyama H, Metzger EJ, Lombardo VK, MacNaul KL, Doebber TW, Berger JP, Leung K, Franklin R, Moller DE, Heck JV, Sahoo SP (2003) Bioorg Med Chem Lett 13:3541
155. Khanna S, Sobhia ME, Bharatam PV (2005) J Med Chem 48:3015
156. Xu HE, Lambert MH, Montana VG, Plunket KD, Moore LB, Collins JL, Oplinger JA, Kliewer SA, Gampe Jr RT, Mckee DD, Moore LB, Willson TM (2001) Proc Natl Acad Sci USA 98:13919
157. Terashima H, Hama K, Yamamoto R, Tsuboshima M, Kikkawa R, Hatanaka I, Shigeta Y (1984) J Pharmacol Exp Ther 229:226
158. Chung SSM, Ho ESM, Lam KSL, Chung SK (2003) J Am Soc Nephrol 14:233
159. Kador PF (1988) Med Res Rev 8:325
160. Fresneau P, Cussac M, Morand J, Szymonski B, Tranqui D, Leclerc G (1998) J Med Chem 41:4706
161. Wilson DK, Bohren KM, Gabbay KH, Quiocho FA (1993) Proc Natl Acad Sci USA 90:9847
162. Mimura T, Kohama Y, Kuwahara S, Yamamoto K, Komiyama Y, Satake M, Chiba Y, Miyashita K, Tanaka T, Imanishi T, Iwata C (1988) Chem Pharm Bull 36:1110

163. Sataka M, Chiba Y, Kohama Y, Yamamoto K, Okabe M, Mimura T, Imanishi T, Iwata C (1989) Experientia 45:1110
164. Sato M, Kawashima Y, Goto J, Yamane Y, Chiba Y, Jinno S, Satake M, Imanishi T, Iwata C (1994) Chem Phram Bull 42:521
165. Ezumi K, Yamakawa M, Narisada M (1990) J Med Chem 33:1117
166. Patscheke H, Stegmeier K (1984) Thromb Res 33:277
167. Arita H, Nakano T, Hanasaki K (1989) Prog Lipid Res 28:273
168. Coleman RA, Sheldrick RLG (1989) Br J Pharmacol 96:688
169. Lacan F, Verache-Lembege M, Vercauteren J, Leger JM, Masereel B, Donge JM, Nuhrich A (1999) Eur J Med Chem 34:311
170. Ezumi K, Yamakawa M, Narisada M (1990) J Med Chem 33:1117
171. Fukumoto S, Shiraishi M, Terashita ZI, Ashida Y, Inada Y (1992) J Med Chem 35:2202
172. Saxena AK, Pandey SK, Seth P, Singh MP, Dikshit M, Carpy A (2001) Bioorg Med Chem 9:2025
173. Barreca ML, Balzarini J, Chimirri A, De Clercq E, De Luca L, Holtje HD, Holtje M, Monforte AM, Monforte P, Pannecouqe C, Rao A, Zapalla M (2002) J Med Chem 45:5410
174. Jonckheere AJ, De Clercq E (2000) Med Res Rev 20:129
175. Tantillo JPC, Ding A, Jacobomolina RG, Nanni PL, Boyer SH, Hunghes R, Pawels K, Anderis PAJ, Arnold E (1994) J Mol Biol 243:369
176. De Clercq E (1993) Med Res Rev 13:229
177. Hajos G, Riedi S, Monar J, Szabo D (2000) Drugs Fut 25:47
178. Garg R, Gupta SP, Gao H, Babu MS, Debnath AK, Hansch C (1999) Chem Rev 99:3525
179. Schaefer W, Friebe WG, Leinert M, Merttens A, Poll T, Von der Saal W, Zilch H, Nuber H, Ziegler ML (1993) J Med Chem 36:726
180. Morris GM, Goodsell DS, Halliday RS, Huey R, Hart WE, Belew RK, Olson AJ (1998) J Comput Chem 19:1639
181. Prabhakar YS, Solomon VR, Rawal RK, Gupta MK, Katti SB (2004) QSAR Comb Sci 23:234
182. Prabhakar YS, Rawal RK, Gupta MK, Solomon VR, Katti SB (2005) Comb Chem High T Scr 8:431
183. Roy K, Leonard T (2005) QSAR Comb Sci 24:279
184. Rao A, Balzarini J, Carbone A, Chimirri A, De Clercq E, Monforte AM, Monforte P, Pannecouqe C, Zapalla M (2004) Il Farmaco 59:33
185. Barreca ML, Chimirri A, De Clercq E, De Luca L, Monforte AM, Monforte P, Rao A, Zapalla M (2003) Il Farmaco 58:259
186. Rao A, Carbone A, Chimirri A, De Clercq E, Monforte AM, Monforte P, Pannecouque C, Zappala M (2003) Il Farmaco 58:115
187. Barreca ML, Chimirri A, De Luca L, Monforte AM, Monforte P, Rao A, Zapalla M, Balzarini J, De Clercq E, Pannecouqe C (2001) Bioorg Med Chem Lett 11:1793
188. Fujita T, Ban T (1971) J Med Chem 14:148
189. Rawal RK, Solomon VR, Prabhakar YS, Katti SB (2005) Comb Chem High T Scr 8:439
190. Rawal RK, Prabhakar YS, Katti SB (2005) Bioorg Med Chem 13:6771
191. Prabhakar YS, Jain P, Khan ZK, Haq W, Katti SB (2003) QSAR Comb Sci 22:456
192. Eng G, Whalen D, Musingarimi P, Tierney J, De Rosa M (1998) Appl Organomet Chem 12:25
193. Zou XJ, Jin GY, Zhang ZX (2002) J Agric Food Chem 50:1451
194. Zou XJ, Lai LH, Jin GY, Zhang ZX (2002) J Agric Food Chem 50:3757

195. Roeder T, Nathanson JA (1993) Neurochem Res 18:921
196. Roeder T, Gewecke M (1990) Biochem Pharmol 39:1793
197. Roeder T (1992) Life Sci 50:21
198. Roeder T (1995) Br J Pharmacol 114:210
199. Roeder T (1990) Eur J Pharmacol 191:221
200. Jennings KR, Kuhn DG, Kukel CF, Trotto SH, Whiteney WK (1988) Pestic Biochem Physiol 30:190
201. Ismail SMM, Baines RA, Downer RGH, Dekeyser MA (1996) Pestic Sci 46:163
202. Hirashima A, Yoshii Y, Eto M (1992) Pestic Biochem Physiol 44:101
203. Hirashima A, Tomita J, Pan C, Taniguchi E, Eto M (1997) Bioorg Med Chem 5:2121
204. Hirashima A, Yoshii Y, Eto M (1992) Biosci Biotech Biochem 56:1062
205. Hirashima A, Yoshii Y, Eto M (1994) Biosci Biotech Biochem 58:1206
206. Pan C, Hirashima A, Tomita J, Kuwano E, Taniguchi E, Eto M (1997) J Sci Biol Chem 1: www.netsci-journal.com/97v1/97013/index.htm
207. Raina AK (1993) Ann Rev Entomol 38:320
208. Ma PWK, Roelofs W (1995) Insect Biochem Molec Biol 25:467
209. Fabrias G, Barrot M, Camps F (1995) Insect Biochem Molec Biol 25:655
210. Zhu J, Millar J, Loefstedt C (1995) Archs Insect Biochem Physiol 30:41
211. Jurenka RA (1996) Arch Insect Biochem Physiol 33:245
212. Rafaeli A, Gileadi C (1997) Invertebr Neurosci 3:223
213. Hirashima A, Pan C, Katafuchi Y, Taniguchi E, Eto M (1996) J Pestic Sci 21:419
214. Hirashima A, Shinkai K, Kuwano E, Taniguchi E, Eto M (1998) Biosci Biotech Biochem 62:1179
215. Rafaeli A, Gileadi C, Hirashima A (1999) Pestic Biochem Physio 65:194
216. Hirashima A, Morimoto M, Kuwano E, Eto M (1999) Bioorg Med Chem 7:2621
217. Clifford KH (1980) Eur J Biochem 106:337
218. Sacktor BS, Wormser-Shavit E (1966) J Biol Chem 241:634
219. Qian X, Liu Z, Li Z, Song G (2001) J Agric Food Chem 19:5279